CONTROL AND SYNTHESIS OF CERIUM OXIDE NANOPARTICLES FOR MEDICAL APPLICATIONS

IGNACIO SALVO IBÁÑEZ
UNIVERSITAT AUTONOMA BARCELONA
TESIS DOCTORAL 2018

UAB

Universitat Autònoma de Barcelona

Vall d'Hebron
Institut de Recerca
VHIR

PhD Thesis

CONTROL AND SYNTHESIS OF

CERIUM OXIDE NANOPARTICLES

FOR MEDICAL APPLICATIONS

Ignacio Salvo Ibáñez

Doctorado ciencia de materiales

Director y tutor: *Víctor F. Puntes*

Institut de Recerca de Vall d´Hebron (VHIR)

Universidad Autónoma de Barcelona

Bellaterra 2018

Facultad de ciencias de la Universidad Autónoma de Barcelona.

Departamento de Química.

Programa de doctorado en ciencia de materiales.

"Control and synthesis of cerium oxide nanoparticles for medical applications"

Memoria presentada para optar al grado de Doctor:

Ignacio Salvo Ibáñez

Tesis realizada bajo la supervisión del profesor y a la vez tutor, Víctor Franco Puntes del grupo farmacodinámica y diseño de nanopartículas del Institut de Recerca de Vall d´Hebron (VHIR).

INDEX

ABSTRACT

Cerium oxide nanoparticles (CeO$_2$ NPs) are one of the most promising materials for future applications in medicine because of their interesting properties at nanoscale. CeO$_2$ NPs have special attention due to their catalytic properties as antioxidant agent, being able to scavenge reactive oxygen species (ROS) such as H$_2$O$_2$, OH$^{\cdot}$, O$_2^{-}$. These free radicals when they are in excess generate alterations in metabolism, producing effects such as neurodegenerative diseases, hepatic damage, retinal illnesses and, of course, inflammation. Necessity to have a properly agent for facing oxidative stress make CeO$_2$ NPs interesting from medical point of view.

However, CeO$_2$ NPs also have the ability to act as oxidant elements in some cases. This fact is due to their high capacity to buffer electrons thanks to their unfilled 4f electronic structure, being reduced or oxidized in accordance with surroundings.

In literature there is much controversy about mechanism of action and catalytic activity of cerium oxide nanoparticles in biological systems, apart from their toxicity too. For that reason, a suitable synthesis of this material is necessary and studying their mechanism of reaction is also required to understand characteristics of these nanomaterials which will be essential for their future applications.

Characteristics of nanoceria produced have to be evaluated before their utilization because type of synthesis is responsible for properties of final product. In addition, it is also indispensable study activity of CeO$_2$ NPs in biological media for being able to predict their behavior in those conditions.

In conclusion, synthesis of CeO$_2$ NPs will be responsible for characteristics of material so, studying and developing this process will be essential for taking the maximum advantage of their desired properties from cerium oxide nanoparticles for future medical applications.

CHAPTER 1:

INTRODUCTION

1.1 INTRODUCTION

Nanotechnology has been an emerging field in the last years. This fact is due to physical and chemical properties of materials change when their size is reduced to the nanoscale, getting even more reactive. This effect has allowed for development of new nanomaterials with applications in catalysis, sensing, fuel cells, energy storage, environmental monitoring, chemiresistors and medicine[1–3]. In fact, the increasing use of nanomaterials in consumer products that are exposed to the environment has led the necessity to understand their fate and transport. For this reason, an intensive research of nanoparticles behavior is necessary in each area of application.

From all kind of existing nanoparticles, metal oxide nanoparticles have had a great importance in several applications, mostly in medical field[2], thanks to their biocompatibility and stability. Properties of these nanomaterials are dependent of size and shape of the nanoparticle[4], which make them interesting and susceptible of modification according to their use.

Majority of applications in biotechnology which employ metal oxide nanoparticles are based on taking advantage of their physicochemical properties. Metal oxide nanoparticles present interesting characteristics which make them useful in medicine, such as magnetic properties[5] in case of iron oxide nanoparticles, antimicrobial effect[6,7] in case of zinc oxide nanoparticles, catalytic activity[8] in case of cerium oxide nanoparticles, vehicles for drugs and different biological substances[9] in case of silica nanoparticles and, even also as active substances[10]. It has been widely reported the use of magnetic iron oxide nanoparticles as magnetic resonance image (MRI) contrast agent and also in hyperthermia treatment[11,12]. In addition, ferumoxytol is a medical solution of this kind of nanoparticles which is injected in the blood stream for anemic chronic patients[13,14]. It is commonly known the utilization of titanium in implant technology because of their biocompatibiblity and stability. Consequently, studies about titanium oxide for improving prosthesis materials and taking advantage of their photocatalytic properties are described in literature[15]. Zinc is a known element involved in metabolism and their toxic properties for microorganisms have been paid

attention for medical applications[16]. Moreover, silica nanoparticles offer a wide diversity of possibilities to use them in medical field because of their chemical stability and their easily functionalization of surface. These characteristics made this type of material really interesting for drug delivery applications, improving transport and solubility of hydrophobic drugs such as camptothecin[17]. Additionally, it has been reported useful application of silica nanoparticles in osteoporosis treatment[18]. Better efficiency in medical application will be done if nanoparticles have good monodispersity and suitable size of nanoparticle although these requirements are not indispensable in other applications of metal oxide nanoparticles such as petrochemistry, for example.

In particular, cerium oxide nanoparticles are the most promising in the medical applications due to their catalytic activity as antioxidant[19] and their capacity of acting as catalyzer mimicking enzymes superoxide dismutase (SOD) and catalase, although there are some studies which disapprove the beneficial effects of ceria and they affirm that CeO_2 can be toxic because they may behave as pro-oxidant, causing oxidative stress for microorganisms and human health[20–23]. This antioxidant property depends on number of oxygen vacancies and crystal structure of nanoparticle[24]. Cerium oxide has the capacity to scavenge reactive oxygen species (ROS), H_2O_2, $OH^.$, O_2^-, causers of oxidative stress and inflammation. ROS are generated accidently in cellular respiratory process, reacting with proteins, lipids membrane or even genetic material due to its high instability and producing cell damage and, consequently inflammation. Normally, there are several existents enzymes which are responsible for reacting with those species such as superoxide dismutase, catalase, peroxidase and glutathione has antioxidant activity (GSH), allowing a correct balance in metabolism. However, when cellular stress conditions are given, a high production of these free radicals is triggered. This ability of ceria nanoparticles to react with free radicals could be benefited in treatments of diseases deriving from oxidative stress. This is the case of liver cirrhosis, age-related macular disease (AMD), neurodegenerative illnesses and some cardiovascular problems and even cancer among others[10,19,25,26].
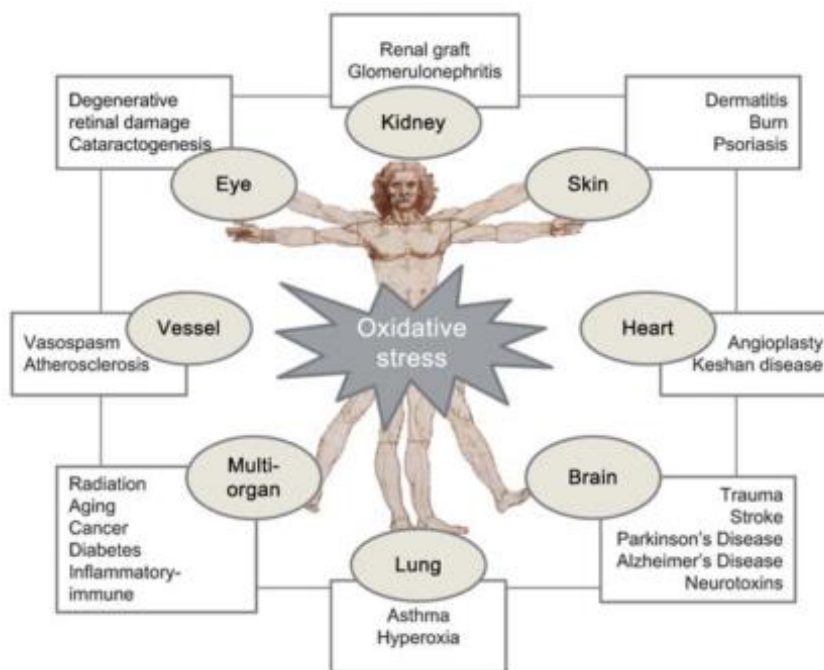
*Figure 1: Different diseases produced by oxidative stress, image taken from Celardo et al "Pharmacological potential of cerium oxide nanoparticles", Nanoscale, 3(4), 1411-1420, **2008.***

Due to potential of nanoceria as biomedical tool[8], a proper synthesis and intensive study of this nanomaterial have to be performed. Cafun et al[24] reported a relation between catalytic activity and primary size of CeO_2 NPs, viewing a major effect in nanoparticles of 3nm in comparison with 5 or 25nm, monitoring the decomposition of hydrogen peroxide by HERFD-XAS. So, small size of cerium oxide nanoparticles is preferable instead of big size of cerium oxide nanoparticles for medicine.

It has been reported many different kind of synthesis of cerium oxide nanoparticles in the literature but many of the products obtained differ from each other, presenting diverse characteristics. Also there are numerous reports viewing diverse effects of CeO_2 NPs in biological systems. There is much controversy in bibliography about this material concretely. In this thesis work is questioned the quality of the nanomaterials synthesized in literature. It is significant highlight the fact that properties of materials are dependent of their synthesis, apart from the fact that many of the described effects probably may be correlated with size and aggregation of nanoparticles elaborated. Aggregation is the main problem during synthesis and in most cases is

related with the negative effects of these nanomaterials. Additionally, most toxicity studies of nanoceria described have been done with powder state nanoparticles. The utilization of nanopowder is not recommended, especially in medicine. In these conditions, correct solubility of nanoparticles or good dispersion of them is not resulted in many occasions, causing aggregates of hundreds or even thousands nanometers in size, greater responsible for the observed nanotoxicity. Zhang et al[27] reported that neither ultrasound nor chemical dispersants are able to break up powder aggregates into primary monodispersed nanoparticles. Nowadays, it is still working in different ways to reduce aggregates in small agglomerates dispersible in water without affecting characteristics of product. As far as possible, aggregation ideally has to be avoided and stable colloidal nanoparticles should be considered, especially if medical field is their destination.

Thus, utilization of surfactants looks like good option if aggregation of nanoceria is not desired. In other applications, the nature of surfactant is not important but in medicine, there has to be in consideration biocompatibility of surfactant employed.

On the other hand, nanoparticles tend to be unstable in biological media. That is mainly because of ionic strength conditions and pH. Cerium oxide nanoparticles need to be conjugated with biocompatible coatings (polyethylene glycol, dextran) or different biomolecules (e.g. antibodies, proteins) when they are applied in medical fields. The no coating of nanoparticles in physiological media produce the phenomenon of aggregation and, consequently, properties of nanoparticles are negatively affected and, in addition, an immunologic response can be generated in biological systems. For this reason, nanoparticles have to be well dispersed and protected when they are applied for systems in-vivo.

So, the objective of this work consists in optimizing a suitable synthesis of monodisperse CeO_2 NPs, understanding their mechanism of reaction in order to be able to predict behavior of these nanomaterials and studying physicochemical characteristics of the product synthesized, being capable of maintaining the desired properties in biological media for being applied to medical field.

1.2 NON AQUEOUS SYNTHESIS OF CeO$_2$ NPs

In non-aqueous phase, organic solvents interacted with a metallic precursor to form metal oxide nanoparticles. Indeed, solvent usually is the provider of oxygen in cerium oxide synthesis. Synthesis in organic phase let to apply knowledge of organic chemistry for producing inorganic nanomaterials. The fact that solvent acts as reactant has the advantage of controlling better the hydrolysis rate of precursor, mixing, pH, and concentration of anions[28]. Moreover, morphology of cerium oxide nanoparticles synthesized depends on precursors and solvents employed. Thus, non-aqueous synthesis offers a good size and shape control of nanoparticle, few problems with aggregation and control of crystal growth even at low temperature. Normally, it is used in this kind of synthesis organic precursors such as alkoxides which can also be supplier for oxygen. Niederberger et al[29] described four different mechanism of formation for all kind of metal oxide nanoparticles in non-aqueous phase; (Eq.1) Combination of metal halide with metal alkoxide eliminating an alkyl halide, (Eq. 2) Condensation of two alkoxide precursor releasing ether organic molecule, (Eq. 3) Reaction of metal alkoxide with metal carboxylate eliminating ester organic molecule, (Eq. 4) Aldol condensation when ketones are used as solvents.
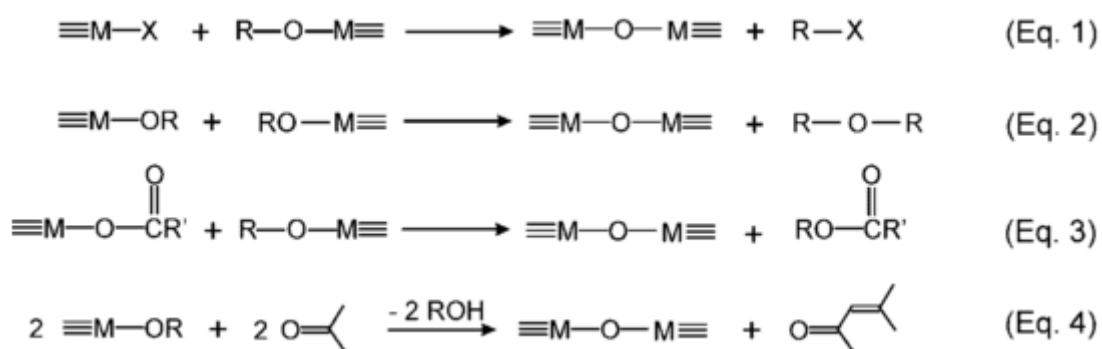
Figure 2: *Scheme explaining the four mechanisms about formation of different kind of metal oxide nanoparticles in non-aqueous synthesis, taken from Niederberger "Non-aqueous sol-gel routes to metal oxide nanoparticles", Accounts of Chemical Research, 40(9), 793-800, **2007**.*

Non-aqueous synthesis can be also made with help of surfactants and even with only solvent as reactant. Surfactants are substances which provide good colloidal stability avoiding aggregation. Surfactants stabilize nanoparticles by steric or electrostatic interactions. Thus, surfactants offer a good size and shape control about cerium oxide nanoparticles synthesized but their use in organic phase does not ensure that reaction happens by mechanisms described previously. In fact, use of surfactants may generate secondary reactions generating unexpected organic impurities, apart from limiting accessibility at the cerium oxide nanoparticle surface[30].

For the purpose to avoid those disadvantages, non-aqueous synthesis with solvent control is developed. In this type of reaction, there are only two components: cerium metallic precursor and solvent. Choice of solvent in this kind of synthesis is essential to determine size, shape and distribution size. So, products generated in these reactions are easily predicted and high purity is obtained in comparison with surfactant synthesis. However, solvent control synthesis offers less control of size and morphology in comparison with employment of surfactants, and formation of agglomerates in some cases[30].

1.3 AQUEOUS SYNTHESIS OF CeO₂ NPs

Water is used as media instead of organic solvents due to economic reasons, solubility of precursors and non-toxicity. The wide complexity of aqueous solutions because of water reactivity tends to affect size and morphology of nanoparticles when slight variations are done during process of synthesis. There are many different ways to produce cerium oxide nanoparticles in non-aqueous synthesis which can be also applied for aqueous phase. Sonochemical and hydrothermal methods are some examples of that. Aqueous sonochemical synthesis consists in applying high-intensity ultrasound for a solution of a cerium precursor, forming millions of micro-bubbles which generate high temperatures, high pressures and elevated cooling rates in the moment of their implosion[31]. These extreme conditions are able to form nanoparticles from inorganic salts. On the other hand, hydrothermal synthesis consists in submitting a cerium precursor dissolved in water to high temperatures and pressures. Size particle in hydrothermal method depends on subjected thermodynamic conditions and concentration of precursor used[32]. Other method employed to synthesize cerium oxide nanoparticles in aqueous phase consists in the sol-gel technique. This method basically creates an inorganic polymer from a cerium precursor by reaction of water with addition of a suitable reagent (acid or base for instance). This colloidal dispersion of nanoparticles is called sol and, after hydrolysis, condensation is produced, forming a solid gel in liquid phase. The liquid is removed to dry the gel and thermal treatment is done after that obtaining nanoparticles. According to the treatment of gel used, it forms a different variety of sizes and shapes of cerium oxide nanoparticles. Of course type of precursor employed, inorganic salt or alkoxide can also influence synthesis. As the same case as non-aqueous synthesis, use of surfactants are also very common in aqueous synthesis. In fact, microemulsion method of synthesis employs surfactants to separate two immiscible phases, oil and water. Surfactants in these special conditions generate microemulsions or micellas which works as tiny reactors for cerium oxide nanoparticles synthesis. Modification of surfactant concentration or type of surfactant in this class of synthesis allow for controlling size and morphology of CeO₂ NPs produced[33].

However, the most promising synthesis are soft-chemistry routes, in which good control from the molecular precursor to the final product is achieved, offering high purity and homogeneity, and low processing temperatures. Alkali precipitation method, for instance, is gaining interest because of its ease, cheap and low energy applied for the synthesis system. Precipitation method offers some advantages: it is simple and rapid reaction, easy control and size composition, and various possibilities to modify the particles surface state and overall homogeneity. Precipitation of salts (nitrates, sulphates, chlorides) under a fine control of pH by addition of ammonium hydroxide, sodium bicarbonate or sodium hydroxide solutions yields corresponding metal oxide nanoparticles. In this process, desired component is precipitated in hydroxide specie from the aqueous solution (Eq. 5). Then, step of dehydration is generated forming oxide specie (Eq. 6).

$$M^{n+} + nOH^- \leftrightarrow M(OH)_n \quad (Eq.~5)$$

$$M(OH)_n \leftrightarrow MO + H_2O \quad (Eq.~6)$$
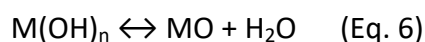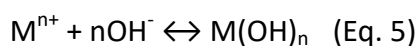
When there are two components in the system is called co-precipitation. For example, in the case of synthesis of iron oxide nanoparticles (Fe_3O_4), Fe^{2+} and Fe^{3+} species are precipitated at the same time.

Several steps can be identified: supersaturation, nucleation, crystal growth to form primary products and aggregation of primary nanoparticles[34]. Initial mixing in solution has a significant effect in phenomenon of precipitation. Good mixing results in homogeneous synthesis of nanoparticles, particularly in co-precipitation methods. Rate of stirring affects initially nucleation and also agglomeration but growth rate is not very influenced by this fact. Solution must to be supersaturated so that precipitation happens. Concentration of precursor, pH and temperature are parameters which affect supersaturation. High temperatures increase solubility and, on the contrary, high pH decrease solubility. For this reason, an addition of base is more suitable for precipitation methods of synthesis. Besides, supersaturation is needed to nucleation happens. Nucleation may proceed automatically through formation of $M(OH)_n$ specie. Nucleation starts with the formation of clusters

which are capable of growing spontaneously by the continuous addition of monomers until a critical size is reached. On the other hand, growth of nanoparticles is produced by adsorption of ions on surface of seeded particles.

This growth depends on concentration of ions, temperature and pH. Rates of growth and nucleation are independents. If nucleation rate is faster than growth, a narrow size distribution of small cerium oxide nanoparticles will be produced but if growth rate is faster than nucleation, then a narrow size distribution of large cerium oxide nanoparticles will be formed. Finally, agglomeration consists in electrostatic interactions among size primary nanoparticles on their own. This phenomenon is difficult to control and is very common in aqueous synthesis of metal oxide nanoparticles although many times these aggregates can be undo of several ways such as surfactants, ultrasounds or vigorous stirring.

Aggregation is responsible of many negative effects caused by cerium oxide nanoparticles so, it is indispensable to avoid this phenomenon if it is wanted to allocate CeO_2 NPs to medicine.

1.4 METHODOLOGIES DESCRIBED OF CeO₂ NPs

Synthesis of nanoparticles is one of the most important parts in the area of nanotechnology and it is still active. A suitable synthesis of materials at the nanoscale offers a high quality product with characteristics which are not present in big scale and they can be beneficial according to its application. In general, synthesis of any metal oxide nanoparticles is an attractive task because of their intrinsic properties. Intrinsic properties of these materials depend on size and morphology of the nanoparticle. For this reason, several types of synthesis have been described in the literature. Conditions of synthesis such as solvent, temperature, pressure or reactants affect to nanoparticles and a modification of them can lead to structural changes in the nanoparticle and, consequently in their characteristics. However, not all changes generated have to be positives for material. In fact, small variations tend to produce negative effects in most cases. For this reason, controlling synthesis of nanoparticles is the most significant step of working in nanoscience.

Synthesis of nanoparticles normally may be classified in non-aqueous and aqueous phase but not all kind of synthesis is valid for any future application. For instance, non-aqueous phase employs organic compounds and nanoparticles made by this route would not be so appropriated for medicine because of possibility of existing toxic traces used in this synthesis for biological organisms. Summarizing, synthesis method ideally has to be adapted according to the purpose where nanoparticles will be fated.

Then, the following table 1 summarizes the synthesis of CeO₂ NPs described in literature, with details of reactants, temperature, size nanoparticle, phase of synthesis and techniques employed:

Technique	Phase	Reactants	Temperature	Primary size CeO$_2$ NPs	References	Year
Hydrothermal	Aqueous	$((NH_4)_2Ce(NO_3)_6$	5h at 150-240ºC	6nm	Hirano et al[35]	2000
Sonochemical	Aqueous	$Ce(NO_3)_3$, TMAOH, AZO	Sonication 3h at 80ºC	3.3nm	Yin et al[36]	2002
Precipitation	Aqueous	$Ce(NO_3)_3$, HMT	Room temperature	3-12nm	Zhang et al[37]	2002
Precipitation	Non-Aqueous	$Ce(NO_3)_3$, NH_4OH, alcohol	Reaction at 50ºC/ Dried at 60ºC	<10nm	Chen et al[38]	2004
Microemulsion	Non-Aqueous	Phosphatidylcoline, NH_4OH, $Ce(NO_3)_3$	Room temperature	3.7nm	Tsai et al[39]	2007
Hydrothermal	Aqueous	$Ce(NO_3)_3$, NH_4OH	Reaction 110ºC/1h at 300ºC/ 24h at 120ºC	3-5nm	Patil et al[40]	2007
Precipitation	Aqueous	$Ce(NO_3)_3$, NH_4OH, PAA, dextrane	Room temperature	3-4nm	Asati et al[41]	2010
Sol-Gel	Aqueous	$Ce(NO_3)_3$, NH_4OH, urea	Sol dried at 100ºC 24h/Gel calcined 400-600ºC	7nm	Periyat et al[42]	2011
Solvothermal	Non-Aqueous	Ethanol, $Ce(NO_3)_3$	24h at 110-150ºC	9.5nm	Walton et al[43]	2011
Hydrothermal	Aqueous	HMT, CeN	2h at 100ºC/ 12h at 150ºC	5-10nm	Xue et al[44]	2011
Precipitation	Aqueous	$Ce(NO_3)_3$, ammonia	Calcination at 500ºC	5nm	Renuka et al[45]	2012
Precipitation	Aqueous	$Ce(NO_3)_3$, NH_4OH, ethylene glycol	14h at 50ºC/Calcination	16-22nm	De Marzi et al[21]	2013
Microemulsion	Non-Aqueous	AOT, H_2O_2, NH_4OH, $Ce(NO_3)_3$	Room temperature	3-5nm	Chaudhury et al[46]	2013
Sol-Gel	Non-Aqueous	$Ce(NO_3)_3$, etanol, TEA	Dissolution at 90ºC/2h at 270ºC/Calcination	6.5nm	Balavi et al[47]	2013
Microemulsion	Non-Aqueous	Octanol, ammonia, DEAO, $Ce(NO_3)_3$	Drying at 90ºC/Calcination	3.9nm	Balavi et al[47]	2013
Precipitation	Aqueous	$Ce(NO_3)_3$, ammonia	1h at 70ºC/24h at 0ºC/drying at 90ºC	10nm	Khadse et al[48]	2014
Hydrothermal	Aqueous	$Ce(NO_3)_3$, agarose	200-800ºC	20nm	Kargar et al[49]	2015

Table 1: List of different synthesis of CeO$_2$ NPs described.

As it is viewed in table 1, there are many ways to obtain cerium oxide nanoparticles. However, in this work it is tried to look for a synthesis which origins a product useful for medicine, with systems in-vivo as destination. As it is mentioned before, non-aqueous synthesis employs organic solvents or compounds which in most cases are toxic for living organisms. Preventing the use of toxic substances because of possibility of having few traces in the final product looks like reasonable. Consequently, in this thesis, an aqueous synthesis has been developed.

On the other hand, Karakoti et al[50] reported the effect of temperature during synthesis with the catalytic activity of synthesized CeO_2 NPs. They viewed a major pro-oxidative effect of nanoceria when high temperatures were used in comparison with synthesis at room temperature, which generated a major antioxidant capacity. In the following table (table 2) the correlation between temperature and catalytic activity of cerium oxide nanoparticles can be checked. As it apparently seems to be better working at room temperature, in this thesis work this requirement is chosen.

Once it is decided to work in aqueous phase and room temperature, the technique of synthesis has to be defined. Model of work employed by Zhang et al (viewed previously in table 1) easily fits with these desired conditions. So, consequently method of alkali precipitation is chosen.

It is important to say that in this thesis; Zhang´s work will be initially taken as reference, but modifications will be done in the protocol of synthesis described with the purpose of adjusting characteristics of CeO_2 NPs synthesized to our objective, their future application in the medical field.

Synthesis	Study	Response
High temperature	Inflammation in lungs by metal oxide nanoparticles	Pro-oxidative
	Oxidative stress of ceria nanoparticles in bronchial epithelial cells	Pro-oxidative
	Inflammatory response in mice treated with ceria nanoparticles by intratracheal instillation	Pro-oxidative
	Biodistribution and oxidative stress of commercial ceria nanomaterials	Pro-oxidative
	Toxicity of cerium oxide nanoparticles in human lung cancer cells	Pro-oxidative
	Ceria-nanoparticle-induced pulmonary inflammation in rats	Pro-oxidative
	Oxidative stress induced by ceria nanoparticles in BEAS-2B cells	Pro-oxidative
	Cerium oxide nanoparticles trigger neuronal survival	Anti-oxidative
	Cardioprotective effects of ceria nanoparticles	Anti-oxidative
	Comparison of toxicity of zinc oxide and ceria nanoparticles based on dissolution of metal ions	Anti-oxidative
	Screening nanoparticulate ceria as a diesel fuel additive	Neutral or both
	Hazard and risk assessment of ceria nanoparticles	Neutral or both
	Effect of ceria nanoparticles in vascular endothelial cells	Neutral or both
Heated in Solvent	Cytotoxicity of ceria nanoparticles for *E coli*	Neutral or both
	Nanoceria exhibits no detrimental effects on eye lens proteins	Neutral or both
	Interaction between ceria nanoparticles and 3T3 fibroblasts	Neutral or both
	DNA damage in human dermal fibroblasts by ceria nanoparticles	Pro-oxidative
	Brain distribution and toxicological evaluation of ceria nanoparticles	Neutral or both
	Adverse effects of ceria nanoparticles at environmentally relevant concentrations	Pro-oxidative
Room Temperature	Altered vascular reactivity and ischemia-reperfusion injury following ceria nanoparticle instillation	Pro-oxidative
	pH-dependent antioxidant activity of ceria nanoparticles	Anti-oxidative
	Yttria and ceria nanoparticles are neuroprotective	Anti-oxidative
	Ceria nanoparticles inhibit oxidative stress in H9c2 cardiomyocytes exposed to cigarette smoke	Anti-oxidative
	Combined cytotoxic and anti-invasive properties of redox-active nanoparticles in tumor–stroma interactions	Anti-oxidative
	Rare earth nanoparticles prevent retinal degeneration induced by intracellular peroxides	Anti-oxidative
	Protection from radiation-induced pneumonitis using cerium oxide nanoparticles	Anti-oxidative
	Auto-catalytic ceria nanoparticles offer neuroprotection to adult rat spinal cord neurons	Anti-oxidative
	Vacancy-engineered ceria nanostructures for protection from radiation-induced cellular damage	Anti-oxidative
	PEGylated nanoceria as radical scavenger with tunable redox chemistry	Anti-oxidative
	The role of cerium redox state in the SOD mimetic activity of nanoceria	Anti-oxidative
	Anti-inflammatory properties of cerium oxide nanoparticles	Anti-oxidative
	Rare earth oxides as nanoadditives in 3-D nanocomposite scaffolds for bone regeneration	Anti-oxidative
	Superoxide dismutase mimetic properties exhibited by vacancy-engineered ceria nanoparticles	Anti-oxidative
	Nanoceria inhibit the development and promote the regression of pathologic retinal neovascularization in the *Vldlr* knockout mouse	Anti-oxidative

Table 2: *Scheme which relates response of CeO$_2$ NPs with their temperature, taken from Karakoti et al, "Preparation and characterization challenges to understanding environmental and biological impacts of ceria nanoparticles", Surfaces and interface analysis, 44(8), 882-889,* **2012***.*

CHAPTER 2:

SYNTHESIS CeO_2 NANOPARTICLES BY ALKALI PRECIPITATION

2.1 INTRODUCTION

As it was mentioned in chapter 1, Zhang´s protocol is taken as reference to synthesize CeO$_2$ NPs but rapidly changes are done in the methodology of synthesis.

Firstly, reactant hexamethylenetetramine (HMT) used in synthesis of Zhang will be substituted by a base. This fact is due to toxicity of this reactant towards microorganisms. HMT act as a detergent, being able to destabilize cell membranes and, as consequence, producing cellular death. HMT in water solution is discomposed forming formaldehyde and ammonia with time, offering the basic media necessary to produce CeO$_2$ NPs. With the aim of avoiding HMT toxic traces in the final product, this precursor will be changed.

Consequently, tetramethylammonium hydroxide (TMAOH) will be used in reaction instead of HMT as base to cause alkali precipitation. TMAOH is chosen because it offers advantages which are not present in some bases such as ammonium hydroxide (NH$_4$OH) or sodium hydroxide (NaOH). Cation TMA$^+$ is capable of acting as electrostatic surfactant in better way in comparison with NH$_4^+$ cation thanks to their hydrocarbon chains so, consequently synthesized CeO$_2$ NPs are more stables. On the other hand, cation TMA$^+$ is less aggregating in comparison with cation Na$^+$. This phenomenon is due to their low value q/r relation (q is charge and r is ratio of molecule). Large counter-ions provide better stability at nanoparticles. A high q/r relation always tends to be related with high aggregating effect. Cation TMA$^+$ is bigger in size than sodium cation and both have same charge so, Na$^+$ lead to more aggregation.

Then, synthesis of CeO$_2$ NPs in this thesis work will consist in a cerium (III) salt (nitrate, chloride) as metallic precursor dissolved in water and subsequent addition of TMAOH to initiate reaction. Ce^{3+} in solution will be oxidized in basic media and later precipitation and formation of nanoceria will be produced. Quantity of TMAOH added will be responsible for yield of reaction. This point will be explained with more detail in section 2.2.7 xylenol-orange in studies of reaction.

Analysis of results obtained is shown in following section studies of reaction.

2.2 STUDIES OF REACTION

2.2.1 ULTRAVIOLET VISIBLE SPECTROSCOPY MONITORING

It is clearly recognized peak of Ce^{3+} at 253nm and peak of CeO_2 NPs ~290nm. There is an increase of peak CeO_2 since first minute until 75 minutes in both cases. After that, there is a reduction of absorbance because of aggregation which is produced. Phenomenon of aggregation tends to decrease peak and cause red-shift. This effect is higher according to grade of aggregation. It is also viewed no differences between different precursors.
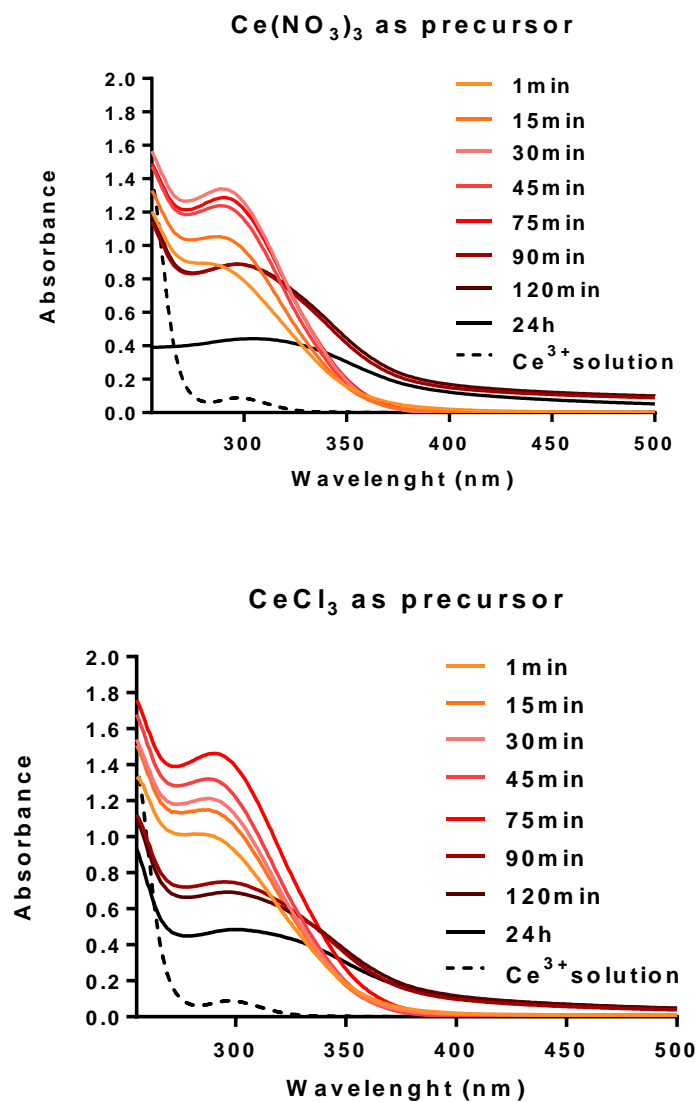
Figure 3: Evolution of reaction measured by Ultraviolet spectrophotometer for both precursors.

2.2.2 DYNAMIC LIGHT SCATTERING MONITORING

Dynamic light scattering (DLS) is a technique that can be used to determine the size distribution profile of small particles in suspension or polymers in solution. A laser is shot through a polarizer and into a sample. The scattered light is collected by a photomultiplier and the resulting image is projected onto a screen. All molecules in the solution are being hit with the light and all of the molecules diffract the light in all directions. The resulting set of speckle patterns are analyzed by an autocorrelator that compares the intensity of light at each spot over time. Consequently, signal analyzed is related with size of colloidal object. Thus, DLS is used to check size of cerium oxide nanoparticles in solution (hydrodynamic size) and presence of aggregates in the sample. Results are shown below in table 3 and figure 4. Values of table 3 are analysed by number distribution while graphics represented in figure 4 are obtained by intensity distribution.

	Ce(NO₃)₃ as precursor Hydrodynamic ratio (diameter)			CeCl₃ as precursor Hydrodynamic ratio (diameter)
1min	12.4±1.7nm		1min	12.8±0.2nm
15min	11.2±1.05nm		15min	10.2±0.6nm
30min	15.3±0.94nm		30min	9.3±0.44nm
45min	16.3±1.11nm		45min	10.4±0.64nm
75min	27.2±8.1nm		75min	10.3±0.66nm
90min	85.7±30nm		90min	25.5±3.3nm
120min	122.8±25nm		120min	168.6±57nm
24h	564.6±42nm		24h	656.6±482nm

Table 3: *Evolution of hydrodynamic size respect time for both precursors. Values obtained by Number distribution.*
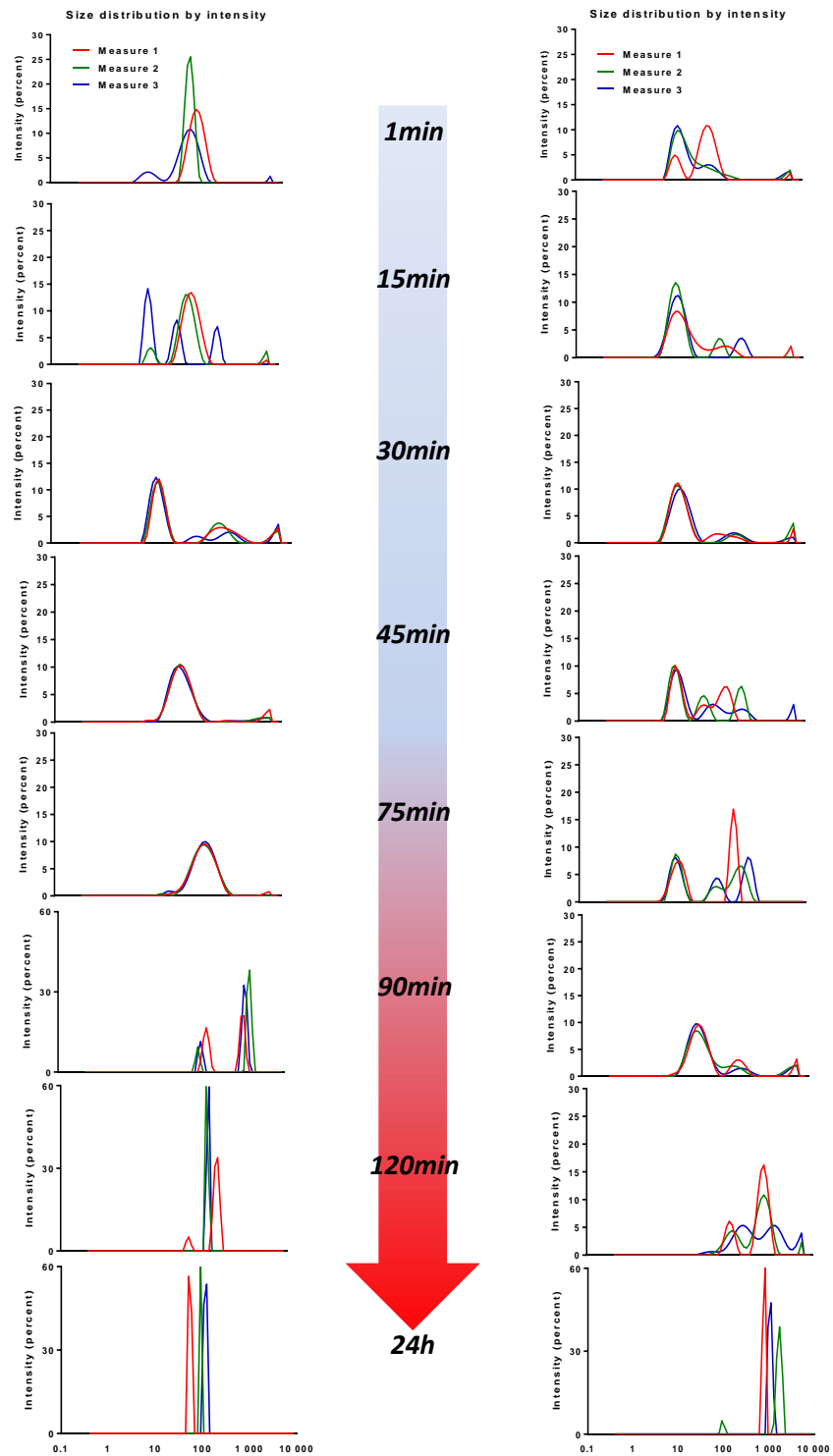
Figure 4: *Graphic representation of size distribution by intensity respect different times of reaction for both precursors. Each data shown is measured by triplicate.*

2.2.3 COLOUR EVOLUTION OF SYNTHESIS CeO₂ NPs

In the first moment of addition TMAOH, mix starts to be red. This colour is generated as consequence of oxidation process. Intensity of red colour is apparently related with quantity of Ce^{4+} formed in reaction. This red colour persists until 75 minutes and then, a white colour appears indicating formation of CeO_2 NPs aggregated. This effect is checked in both precursors.
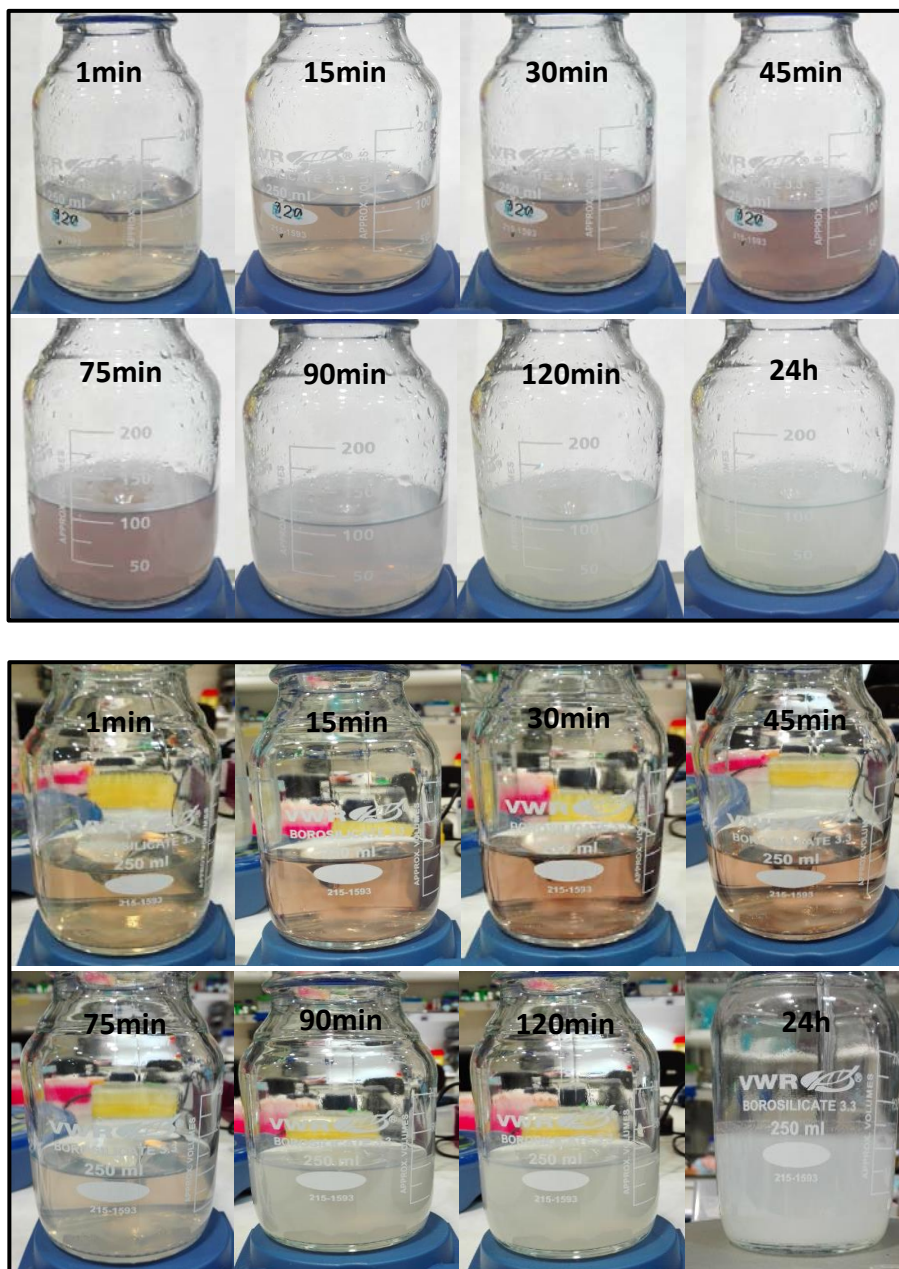
Figure 5: *In the top, colour evolution of synthesis CeO₂ NPs with Ce(NO₃)₃ as precursor. On the bottom, colour evolution of synthesis CeO₂ NPs with CeCl₃ as precursor.*

2.2.4 EVOLUTION pH REACTION

Initial pH 12 corresponds to base added. After addition, close to neutral pH is kept as consequence of combination between base and cerium precursor solution until approximately 40 minutes during the mix. Then, values of pH start to reduce until a slight acidic pH 5, where is practically constant the rest of the time. There is no much difference between both precursors.
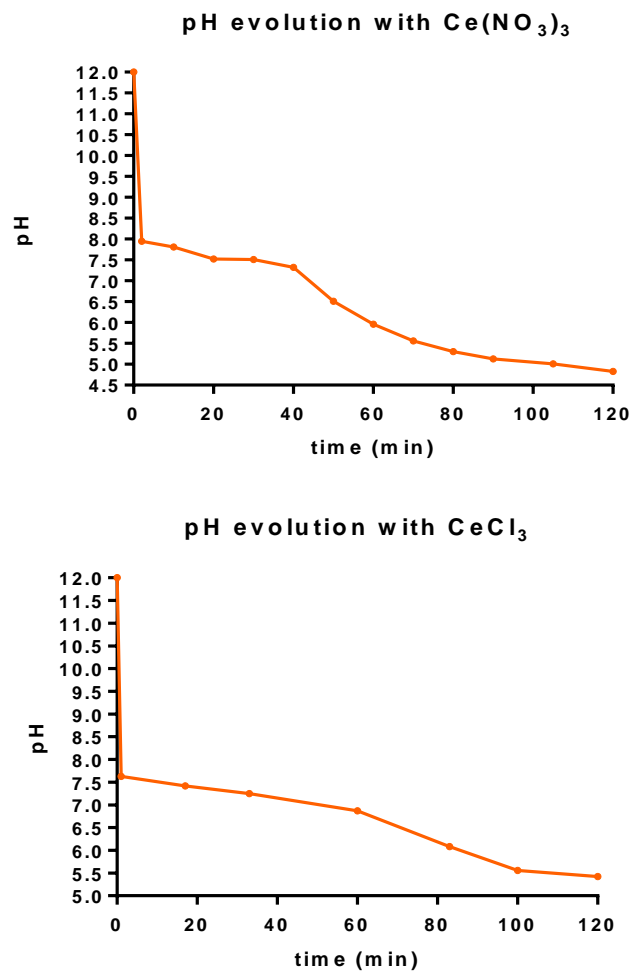
Figure 6: *Evolution of pH in reaction of synthesis with both precursors.*

2.2.5 TRANSMISSION ELECTRON MICROSCOPY (TEM)

Images TEM of CeO$_2$ NPs synthesized with both precursors were analysed. Same size is practically viewed for both cases, around 5 nanometres and crystalline structure was viewed by HR-TEM.
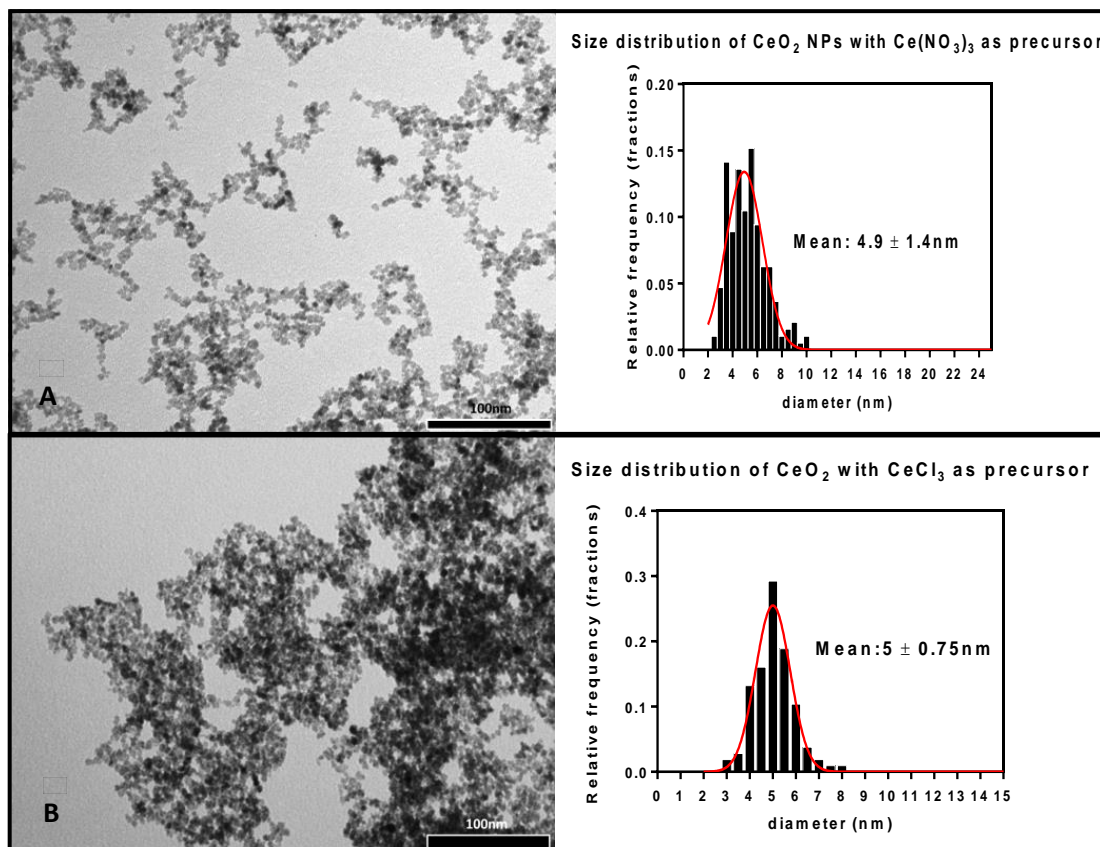
Figure 7: *Images TEM taken from Jeol 1010 80KV for both precursors (A-nitrate; B-chloride). Size distribution is calculated by ImageJ software.*
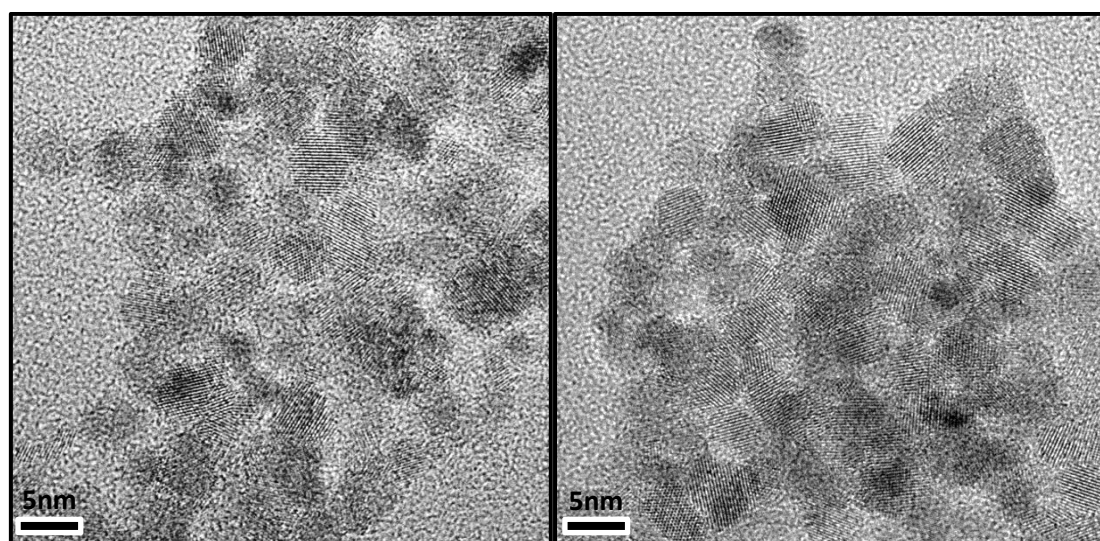
Figure 8: *Images HR-TEM taken from Tecnai F20 200KV, in which is viewed crystalline planes (crystalline structure) of synthesized CeO$_2$ nanoparticles.*

2.2.6 SYNTHESIS UNDER N$_2$ CONDITIONS

Synthesis of CeO$_2$ NPs is prepared under N$_2$ stream. Also, both solutions of cerium and base were previously deoxygenated with N$_2$ during 30 minutes before mixing. This experiment is done with the aim of understanding role of oxidation in the process of synthesis in which O$_2$ is apparently responsible. It is viewed no formation of nanoparticles when chloride is used as precursor while a peak of CeO$_2$ NPs is detected when nitrate is employed (see figure 9). This fact is due to weak oxidant property of nitrate, which is only detected at long times. Conclusions obtained in this experiment will be used to explain the mechanism of reaction in the following section.
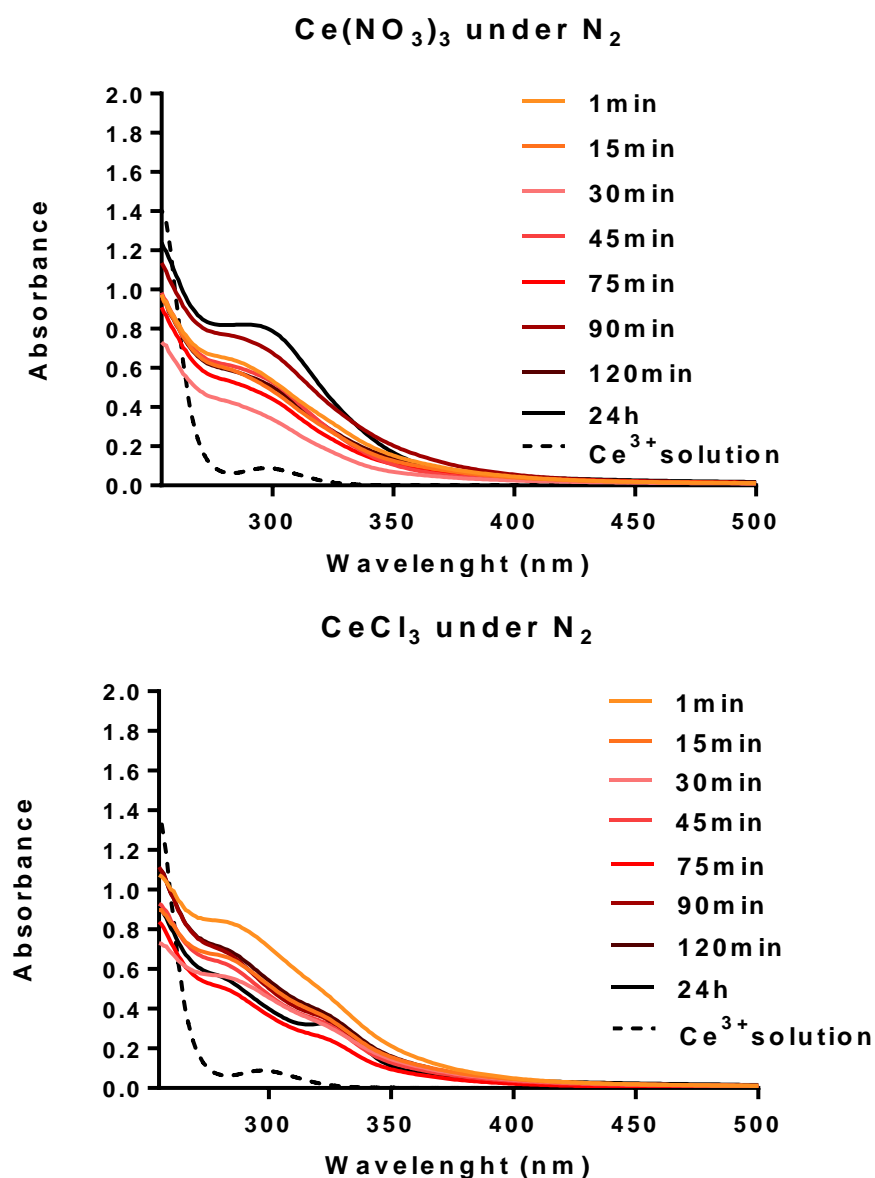
Figure 9: *Evolution of reaction under N$_2$ stream measured by UV spectrophotometer for both precursors*

.

2.2.7 XYLENOL-ORANGE

Xylenol-orange is a metallochromic indicator that forms a stoichiometric complex 1:1 with some rare earths elements in which cerium (III) is included. Ce^{3+} in solution mixed with xylenol-orange forms a colored product easily measurable at 576nm by spectrophotometer not only allowing qualitative detection but also quantitative analysis. This technique was described by Tonosaki et al[51] and their protocol is adapted in this thesis work with some modifications, allowing to detect from 0 until 40µg of Ce^{3+} in solution. This technique will be tremendously useful for finding out conversion of the synthesis according to base added and also to study evolution of cerium (III) during reaction. It can be viewed in figure 10 evolution of precursor during synthesis (stoichiometry Ce-base 1:1 is represented although the same evolution is tested at different stoichiometry). It can be checked diminution of Ce^{3+} concentration until 75 minutes of reaction and then, concentration is practically constant. Also it is viewed conversion of Ce^{3+} respect base added in the same figure (represented in function of stoichiometry, considering 1 for cerium in each point). It is clearly seen the higher concentration of base employed, the higher conversion rate in reaction.

Experimental method of xylenol-orange is described in section 8.3 Annex.
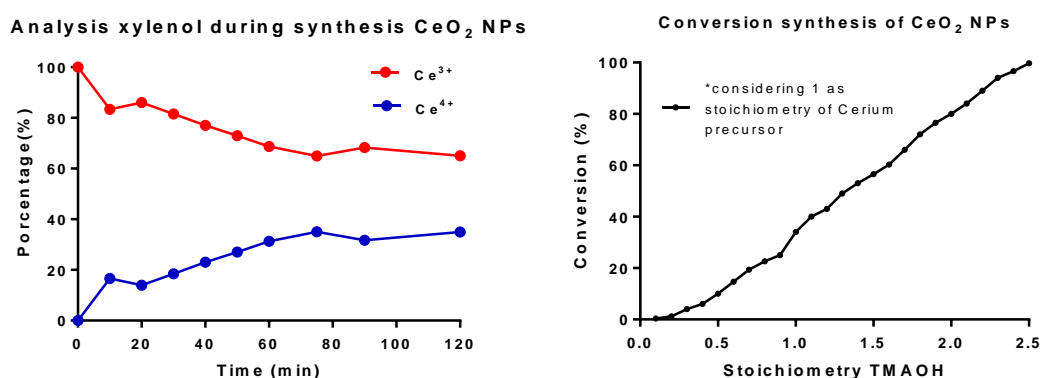
Figure 10: *In the left, it is viewed evolution of Ce^{3+} during reaction of synthesis. In the right, graphic which represents conversion of cerium respect concentration of base added in function of their stoichiometry, considering value 1 for cerium concentration.*

2.3 MECHANISM OF REACTION

2.3.1 INTRODUCTION

In this section, it is described a hypothesis of possible mechanism of reaction of the synthesis employed in this thesis. It is important to highlight that in this process of synthesis, oxidation is produce because precursor of Ce^{3+} is used. Zhou et al[52] reported a synthesis of CeO_2 NPs by oxidation of Ce^{3+} with hydrogen peroxide. However this process cannot be generated as it has been tested in this thesis in figure 11. In neutral or acidic pH, hydrogen peroxide is not capable of oxidizing Ce^{3+} but a yellow complex is formed[53]. Hayat described in his book *Stains and citochemical methods* (chapter 8, pages 102-103) this phenomenon, characterizing the yellow specie perhydroxide $Ce(OH)_2(OOH)$ when cerium (III) is reacted with H_2O_2, especially in cases where the H_2O_2 is in excess, forming an stable soluble complex that avoids Ce^{3+} oxidation. Hence, it can be concluded dissolved oxygen is the main source of oxidation. Nevertheless, oxygen only will be active in basic media.

Then, mechanism of reaction will be explained and it will be able to classify in 3 steps, easily distinguished viewing evolution of pH in reaction. Also, diagrams of Pourbaix for cerium will be resorted in order to understand and facilitate a major comprehension.
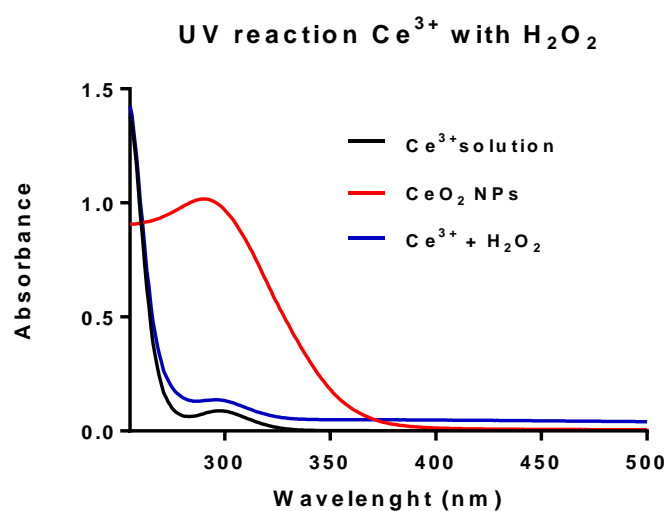
Figure 11: *UV spectrum in which is easily detectable no peak of CeO₂ NPs when H₂O₂ is used as reactant. In fact, is quiet similar to cerium precursor and there is no evolution in the peak for several days.*

2.3.2 STEP 1: HYDROXILATION OF PRECURSOR

All this set of reactions happens rapidly when the reaction begins. The basic solution initially is at pH 12 and the first drop of it which makes contact with cerium solution produces chemical insoluble specie $Ce(OH)_3$ (Figure 12,B). Because of vigorous stirring the mix is at pH 8 so, consequently $Ce(OH)_3$ is dissolved forming ionic species $Ce(OH)^{2+}$ or $Ce(OH)_2^{+}$(Figure 12,C). From this way, in solution there are hydroxylated soluble species of cerium.

In defect of base concentration this mechanism is done while in excess of base concentration it is not. At high concentration of ions OH^- do not allow to redissolve $Ce(OH)_3$ produced into soluble species. Thus, subsequent oxidation is resulted from an insoluble solid instead of soluble components, generating $Ce(OH)_4$ with rather amorphous structure. This effect is viewed in many precipitation methods described in bibliography (See table 1) in which base is always abundant. This fact is corrected submitting synthesized products at high temperatures, forming nanoparticles with crystalline structure at the end. But consequences of this last step consists in the collection of CeO_2 NPs in powder state and it was previously described the problem of working with that type of nanomaterials for medical applications.

So, it is recommendable in this kind of synthesis work with defect of base. According to diagram of Pourbaix, all quantity of base in which pH of synthesis is too high is not desirable for good quality collection of nanoceria.
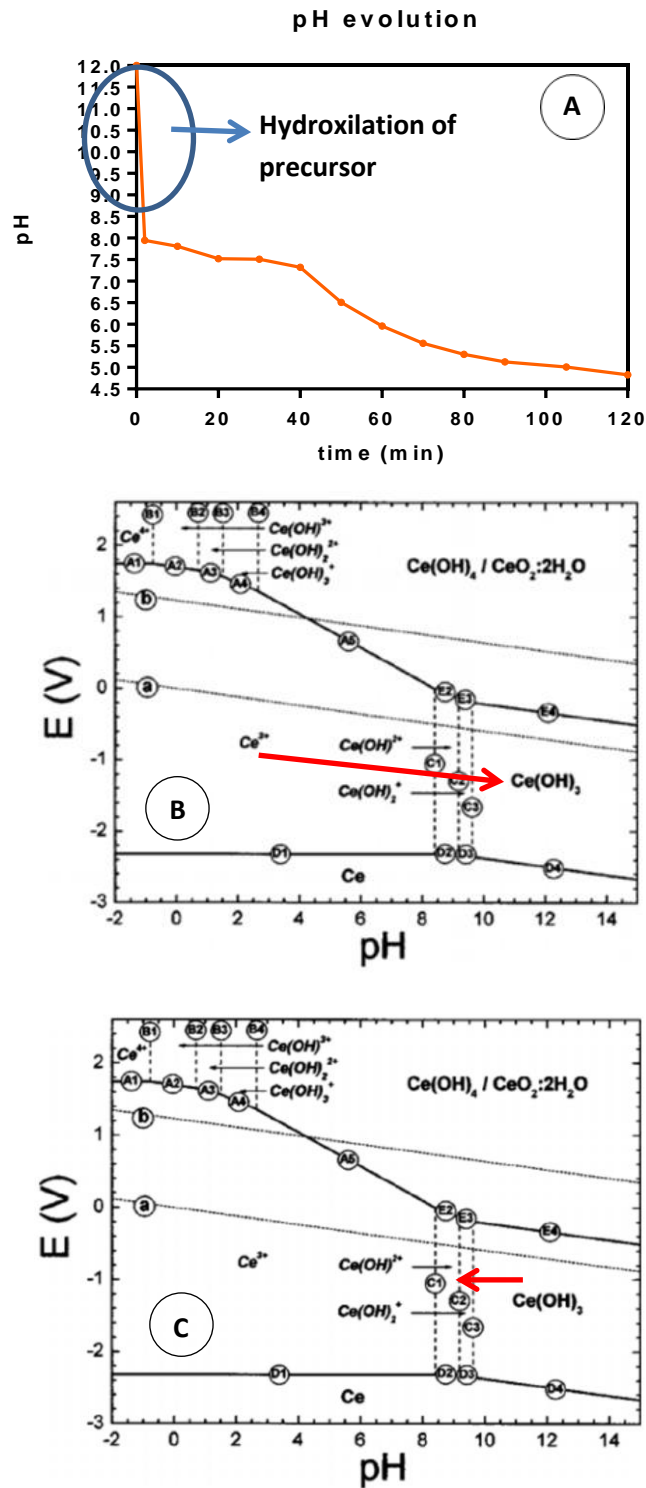
Figure 12: *A) Step of hydroxylation of precursor signaled in monitoring pH of reaction. B) Diagram of Pourbaix in which is represented formation of insoluble Ce(OH)₃ from Ce³⁺ as consequence of base addition. C) Diagram of Pourbaix in which is represented formation of soluble species Ce(OH)²⁺ and Ce(OH)₂⁺ from Ce(OH)₃ as consequence of pH in the mix.*

2.3.3 STEP 2: OXIDATION OF CERIUM

The following step to hydroxylation of cerium consists in oxidation. Soluble specie Ce(OH)$^{2+}$ and Ce(OH)$_2^+$ are susceptible of being oxidized by oxygen, contrarily to Ce^{3+}. Ce^{3+} is a stable ion in solution resistant to oxidation as described previously in 2.3.1 point of this thesis but their hydroxylated compounds are not. Dissolved oxygen is the mean responsible of this step, checking it fundamentally in earlier 2.2.6 section (experiments of synthesis under N$_2$ atmosphere where there is no presence of O$_2$). It was viewed no existence of CeO$_2$ NPs in synthesis under N$_2$ stream when CeCl$_3$ was used as precursor. In other words, there was only precipitation of white solid Ce(OH)$_3$ in absence of oxidant substances. Nevertheless, there was nanoceria in this same conditions when Ce(NO$_3$)$_3$ was used. This fact is because ion nitrate act as an oxidizing agent at long reaction times. So, it can be concluded dissolved O$_2$ becomes one more reactant of the process to be considered in this type of synthesis.

Therefore, species Ce(OH)$^{2+}$ and Ce(OH)$_2^+$ are oxidized in species Ce(OH)$^{3+}$, Ce(OH)$_2^{2+}$ or Ce(OH)$_3^+$ according to diagram of Pourbaix (Figure 13). Besides, there is possibility of these new soluble oxidized species is related with red colour viewed in the process of synthesis but there is still controversy in this point. Some authors attribute red colour to Ce^{3+} while others attribute it to Ce^{4+}. Chen et al[54] reported that red colour can be related with Ce(H$_2$O)$_x$(OH)$_y^{(4-y)+}$ compound. What seems certain is the red colour is not related with morphology of nanoparticles. Tang et al[55] reported the presence of that colour in synthesis of CeO$_2$ nanotubes.

Finally, it is viewed that reaction of oxidation is done practically at pH constant. It is truth that it is detected a variation since pH 8 until pH 7.5 (figure 13) but analyzing it as concentration of ions [H$^+$], variation is irrelevant. This fact is significance because it can be concluded both oxidation as formation of Ce(OH)$_4$ are not simultaneous processes.
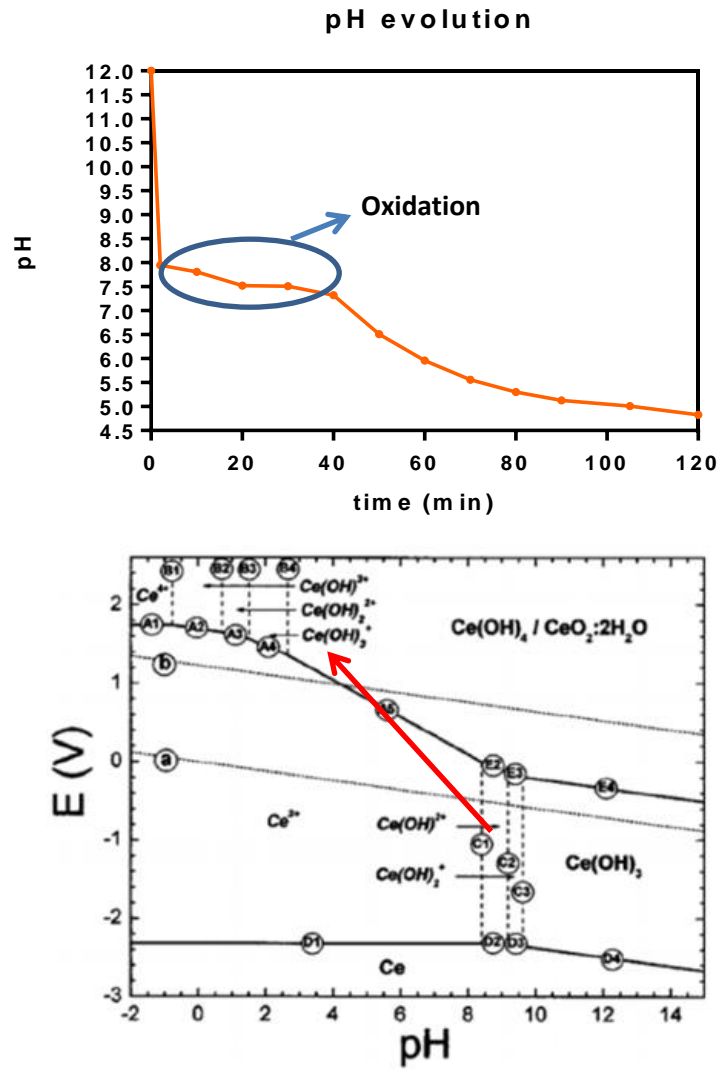
Figure 13: *In the top, step of oxidation signaled in monitoring pH of reaction. On the bottom, diagram of Pourbaix in which is represented formation of oxidized soluble species of Ce^{4+} from soluble species of Ce^{3+}.*

2.3.4 STEP 3: PRECIPITATION AND FORMATION OF CeO$_2$ NPs

Once Ce^{4+} was obtained, soluble oxidized species ($Ce(OH)^{3+}$, $Ce(OH)_2{}^{2+}$, $Ce(OH)_3{}^{+}$ or $Ce(H_2O)_x(OH)_y{}^{(4-y)+}$) are converted into CeO_2 owing to release of hydronium ions H_3O^+ (Eq. 7, figure 14), coinciding with decrease of pH detected during reaction of synthesis. This fact is also reported by Chen et al[56] and Hirano et al[57].

$$Ce(H_2O)_x(OH)_y{}^{(4-y)+} + H_2O \leftrightarrow CeO_2.nH_2O + H_3O^+ \text{ (Eq.7)}$$

$$CeO_2.2H_2O \leftrightarrow Ce(OH)_4 \text{ (Eq.8)}$$
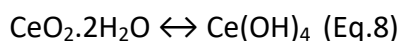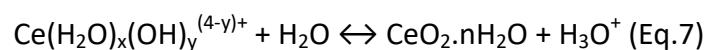
Acidification in mix of synthesis behaves as indicator of nanoparticles formation. There is no CeO$_2$ NPs until great variation in pH is measured. It is important highlight species cerium oxide and hydroxide are in equilibrium with water in solution (Eq.8). As it was described in this thesis, nanoceria synthesized by this method already have crystalline structure so, there is no necessity of heating final product. Indeed, it was already commented disadvantages and consequences of using high temperatures in previous sections of this work in synthesis of nanoparticles for medical applications.

However, all cerium oxide nanoparticles synthesized are aggregated. This fact is caused because of presence of conditions which affect negatively stabilization once final product is generated. These bad conditions are meanly the high ionic strength due to high concentration of ions in solution and the surface charge. Ionic strength seems not so critical factor in comparison with surface charge because there are still aggregates when concentration of precursors is reduced. So, with the aim of studying effect of surface charge in stabilization, measures of potential zeta as a function of pH are done. Analyzing isoelectric point or point zero charge (PZC) of nanoparticles synthesized will help to understand this phenomenon. It is viewed the instability area (general values accepted of potential zeta for dispersion of nanoparticles to be electrostatically stabilized are between +30/-30mV) at neutral pH, indicating destabilization of CeO$_2$ NPs in those conditions of pH, coinciding with evolution of reaction for this type of synthesis (Figure 14).

Consequently, it has to find a way to avoid this irreversible aggregation of CeO$_2$ NPs in the process of synthesis or it will be required utilization of surfactants.

pH evolution

Formation of CeO₂ NPs

Zeta potential vs pH

pI: pH=7
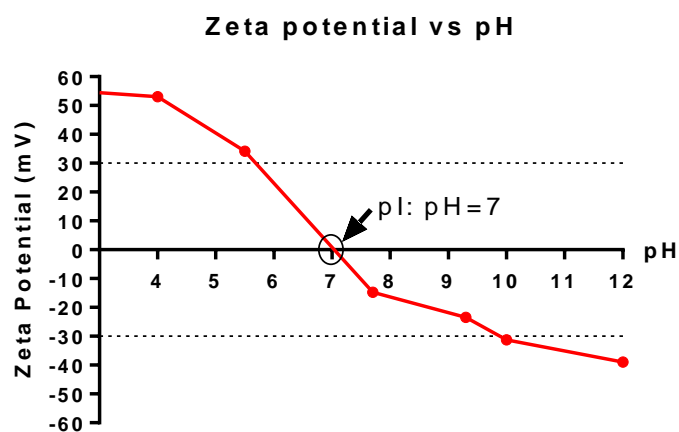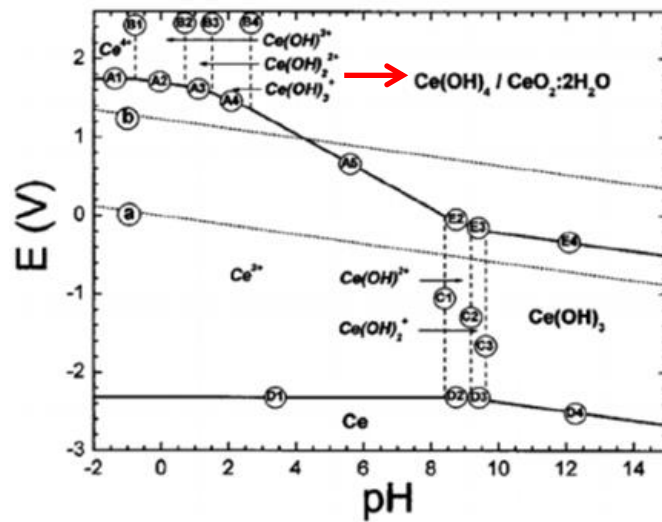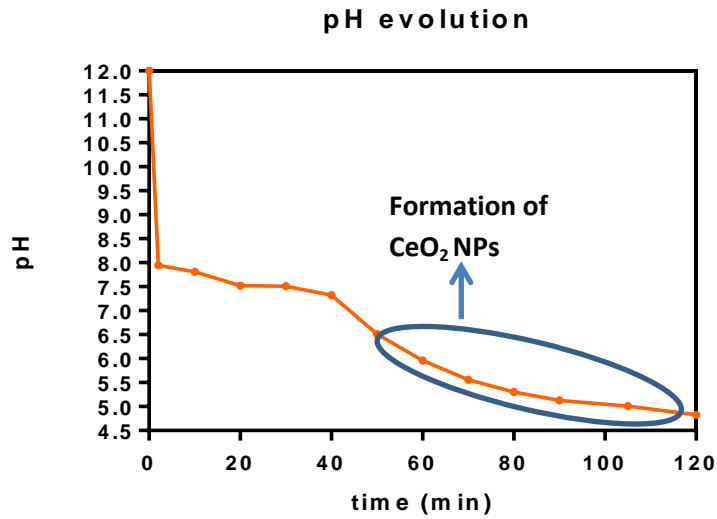
Figure 14: In the top, step of precipitation signaled in monitoring pH of reaction. In the middle, diagram of Pourbaix in which is represented formation of CeO₂ NPs from oxidized soluble species of Ce⁴⁺. On the bottom, representation of potential zeta respect pH, calculating PZC at pH 7 and area of instability between pH 5.5 and 10.

2.4 SYNTHESIS OF CeO₂ NAKED

Due to the fact that irreversible aggregation of CeO_2 NPs is obtained at long times in this type of synthesis, modifications are required. One option consists in stopping reaction at short times before aggregation happens in reaction. This is succeeded centrifuging solution in the middle of reaction, separating cerium components from solution and removing supernatant with high concentration of ions. Thus, aggregation is avoided and good monodispersed nanoceria is generated (Figure 15).

Method of synthesis is described in section 8.4 Annex of this thesis work. It is finally obtained CeO_2 NPs well dispersed with positive surface charge. Besides, final pH is slightly acidic, between 4 and 5.
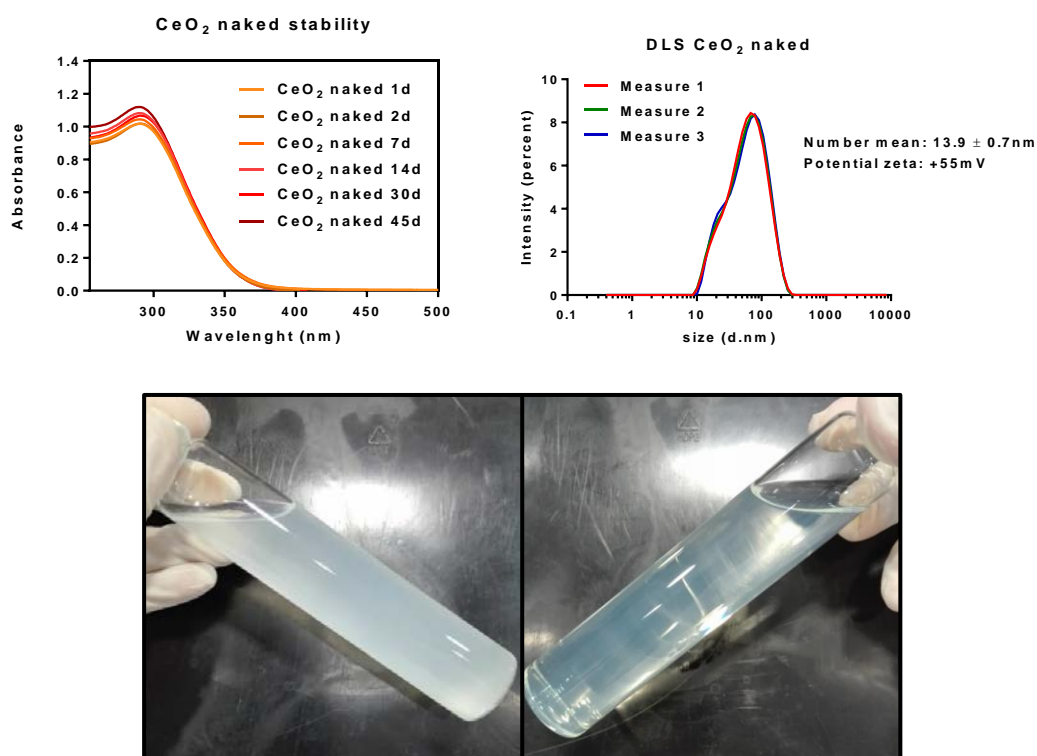
Figure 15: *In the top left, it is shown stability of CeO₂ naked by UV measures for several days. In the top right, it is shown DLS measures by intensity distribution of CeO₂ naked, presenting monodispersity and positive charge in their surface. On the bottom, pictures of CeO₂ aggregated (left) and CeO₂ naked (right) made by this method.*

2.5 DISCUSSION

Experiments done in this thesis work have allowed know much better this type of reaction of synthesis CeO$_2$ NPs. Results have shown both cerium nitrate and cerium chloride are useful for synthesis, viewing no much differences in UV, DLS, TEM and pH monitoring. Nevertheless, nitrate precursor seems to be more suitable precursor because this anion presents oxidant capacity (tested in synthesis under N$_2$ conditions). It has been viewed oxidation is the most important step in this reaction so, use of reactants which favors this effect looks like more appropriate.

At the same time, it has been analyzed important role of oxygen in reaction as oxidant. Anaerobic conditions have probed there is no formation of cerium oxide nanoparticle but cerium (III) hydroxide formation, unless another oxidant is present in reaction. Consequently, good ventilation and distribution of O$_2$ is required for suitable synthesis of CeO$_2$ NPs. Also, it has been checked only specie Ce(OH)$_x$ can be susceptible of being oxidized instead of Ce^{3+} which cannot in spite of some authors reported it.

On the other hand, possible reasonable mechanism of reaction has been developed in order to explain formation of cerium oxide nanoparticles with the aim of producing an optimized proper product for medical applications. It has been checked working in excess of base is not good option because subsequent oxidation in that conditions will form nanoparticles with amorphous structure instead of crystalline structure and interesting catalytic properties of cerium reside in the crystal. Contrarily, soluble species (viewed in diagram of Pourbaix) are generated at lower base concentrations and these species are oxidized meanly by dissolved oxygen, producing the precursors of nanoceria. These oxidized soluble species are possibly related with red colour visualized in solution during reaction. After that, formation of CeO$_2$ NPs is done by release of H$^+$ acidifying solution (condensation). It is significant highlight the fact that this last step and oxidation process are not simultaneous. In first place, oxidation is produced and later formation of nanoparticles is done. This effect can be checked by pH and xylenol-orange experiments. During oxidation step pH is practically constant while during formation of nanoparticles Ce^{3+} detected by xylenol is practically constant as well and pH is decreased as consequence of release H$^+$.

To know the mechanism of reaction will allow better final optimization of CeO_2 NPs synthesized subsequently.

Regarding the fact that oxide specie in water is in equilibrium with their hydroxide specie, as described in Eq. 8, there is no necessity of heating final product as other methods of synthesis described in table 1 because the product is already in solution. Dehydrate nanoparticles synthesized in order to dissolve it again when they are applied is an unnecessary process in this work.

Finally, it is checked formation of CeO_2 aggregates at the end of synthesis. This phenomenon of aggregation is easily detected viewing decrease in peaks of ultraviolet spectrum, increase in hydrodynamic sizes by DLS or visualizing white colour in the solution. This aggregation effect is done because there are no suitable conditions (the high ionic strength and neutral pH) when CeO_2 NPs are formed to be stable. Study of point zero charge (PZC) helps to understand this effect. To analyze surface charge at different pH allow verifying pH of instability for nanoparticles which coincide with conditions during formation of CeO_2 NPs during reaction.

As aggregation is not permitted for medical applications, modifications in synthesis had to be done with the objective of obtaining monodispersed nanoceria instead of aggregated product. Thanks to understanding and conclusions drawn from experiments, it was capable to create good proper synthesis of CeO_2 NPs (CeO_2 naked) that complied with our requirements.

CHAPTER 3:

SYNTHESIS CeO_2 NANOPARTICLES BY ALKALI PRECIPITATION WITH SURFACTANTS

3.1 INTRODUCTION

In this thesis work it is also studied this type of reaction with employment of surfactants. Biocompatibility of these compounds has to be considered if medicine is their destination. One possibly useful reactant for this task consists in polyvinylpyrrolidone (PVP), a water-soluble polymer which is biocompatible until 10KDa of molecular weight. PVP with molecular weight bigger than 10KDa can be harmful because of their accumulation in the body. Indeed, in the past this substance had been massively used to increase the oncotic pressure in cases of bleeding[58]. Besides, the solubility in water of this polymer makes it good option for this kind of synthesis. Koczkur et al[59] reported advantages of using PVP not only for synthesis of metal oxide nanoparticles but also for metal nanoparticles. PVP act as steric stabilizer being attached on nanoparticle surface, from this way interactions among nanoparticles are invalid.

On the other hand, it was viewed the behaviour of molecule citrate as surfactant[60]. This substance gives negative charge to nanoparticles offering electrostatic repulsion and preventing interactions among them. Moreover, the utilization of citrate (at low doses) as surfactant in nanoparticles for medical application is promising because of the own nature of material. Citrate is a compound which is produced as intermediary metabolite of Krebs cycle in mitochondria so; the idea of a substance generated by their own body could be a stabilizer of synthesized nanoparticles is quite attractive. Additionally, citrate is employed in food industry as preserving agent and antioxidant. This characteristic of citrate is pretty remarkable in order to stabilize cerium oxide nanoparticles because both materials share the same property of interest for medicine.

Consequently, synthesis of CeO₂ NPs with PVP and citrate are done in this work and it is explained in the following sections.

3.2 SYNTHESIS CeO$_2$ WITH PVP

3.2.1 INTRODUCTION

Due to the fact that surfactants offer wide stability, final product is subsequently difficult to purify. For that reason, modifications in concentrations of precursors are done with the aim of having high conversions of reaction to reduce presence of impurities. PVP does not have pH properties so, pH reaction is not altered and evolves in the same way explained in chapter 2.

Then, synthesis in presence of surfactant PVP is done. It is obtained CeO$_2$ NPs good dispersed with no surface charge. Procedure is explained in section 8.5 Annex.

Other alternative can be once CeO$_2$ naked NPs (see section 2.4) are synthesized, then this solution can be added on PVP solution. The results obtained by this route are the same in comparison with presence of PVP during synthesis, showing no differences. This is indeed a control to avoid aggregation and confirm mechanism.

3.2.2 STUDIES OF REACTION

3.2.2.1 UV SPECTROSCOPY MONITORING

It is shown no decrease of peak ~290nm in comparison with synthesis without surfactant, indicating stability and efficacy of PVP.
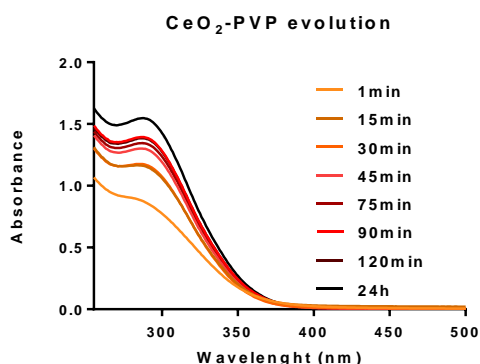
Figure 16: *UV monitoring of formation CeO$_2$ NPs with PVP during synthesis. Peaks visualized are independent of PVP concentration.*

3.2.2.2 DLS MONITORING

Small size of hydrodynamic size of nanoparticle is kept respect time and no aggregation was viewed. At the same time, x-ray diffraction is done in order to know chemical nature of synthesized material, coinciding with oxide specie (CeO_2).

	Hydrodynamic ratio (diameter)
1min	6.2±1.9nm
15min	3.9±0.2nm
30min	8.6±0.44nm
45min	9.5±0.34nm
75min	3.6±0.75nm
90min	9.4±0.65nm
120min	8.3±0.53nm
24h	15.7±0.6nm

Table 4: *It is shown values of hydrodynamic size respect time by Number distribution.*

X-ray diffraction
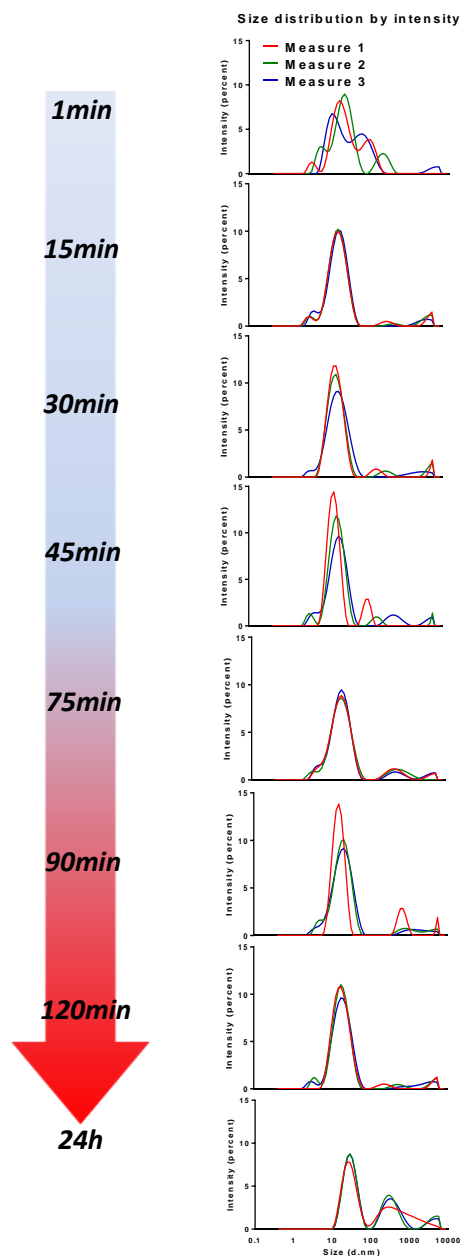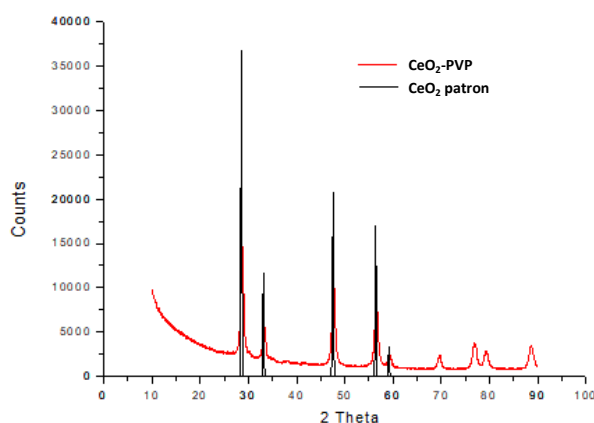
Figure 17: *In the right, scheme presenting evolution of hydrodynamic size of nanoparticle by intensity distribution. In the left, X-ray diffraction showing product synthesized is really CeO₂.*

3.2.2.3 IMAGES TEM

There is no change in size of nanoparticles when PVP is used as surfactant.
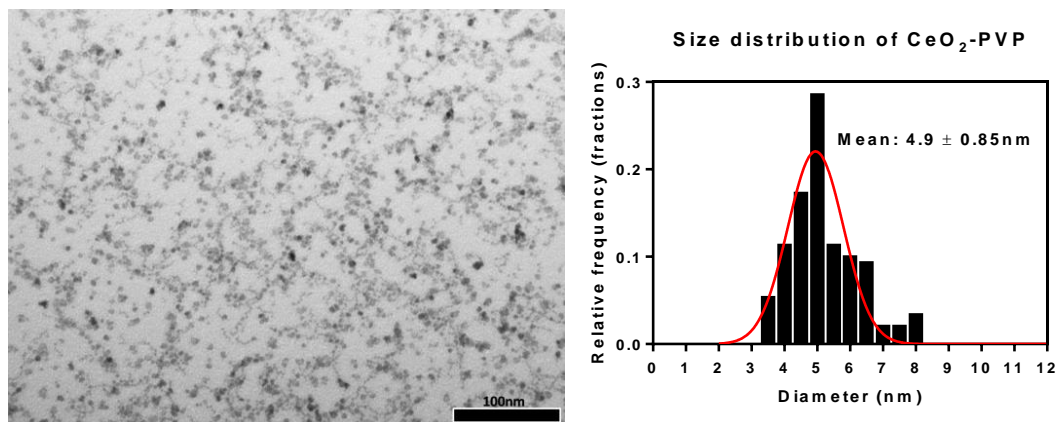
Figure 18: *Image TEM of CeO$_2$-PVP taken from Jeol 1010 80KV. Size distribution is calculated by ImageJ software.*

3.2.2.4 COLOUR EVOLUTION

Colours initially coincide with synthesis without surfactant but at long times, it is not viewed white colour previously described because of absence of aggregates.
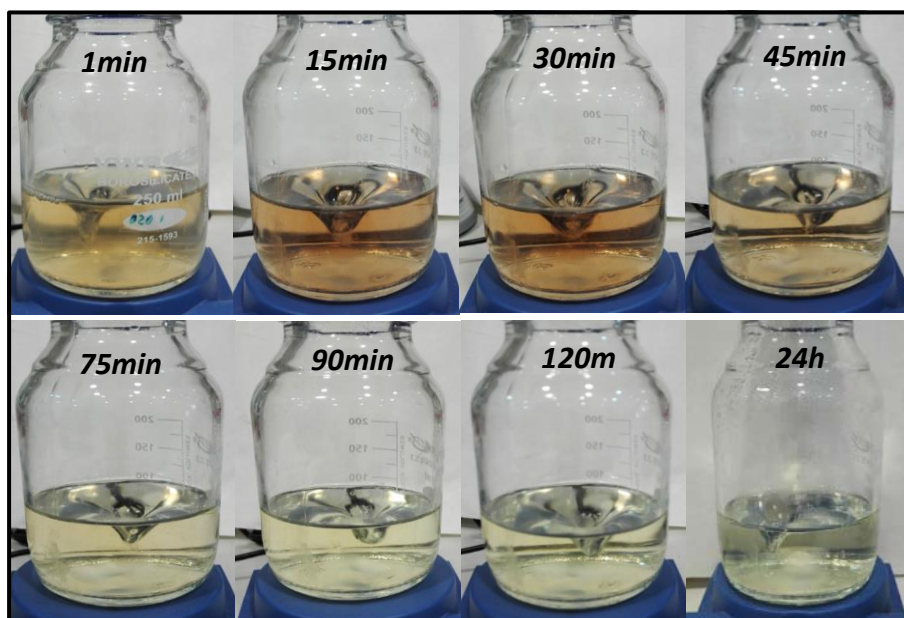
Figure 19: *Colour evolution of CeO$_2$-PVP synthesis over time.*

3.3 SYNTHESIS CeO₂ WITH CITRATE

3.3.1 INTRODUCTION

Citrate is a substance which acts as surfactant of nanoparticles but it also is able to interact with precursor. Bobtelsky et al[61] reported capacity of citrate to form complex with cerium (III), producing a white solid easily capable of being dissolved in excess of ligand or base. This effect is viewed in this work and it is related with stoichiometry of reaction (table 5, figure 20).

Due to capacity of white solid formation of Ce^{3+} with citrate, it is desirable the 100% conversion with the aim of avoiding presence of this solid in the reaction.

Utilization of citrate as surfactant presents notable differences in comparison with the use of PVP. Reaction is slower than the others previously described. Colours generated are different and, in addition, there is a modification in size of nanoparticles being 3 nanometers, smaller than original synthesis. Thus, the use of citrate not only has consequences synthesizing stable monodispersed CeO_2 NPs but it is generated a new different type of nanoparticle.
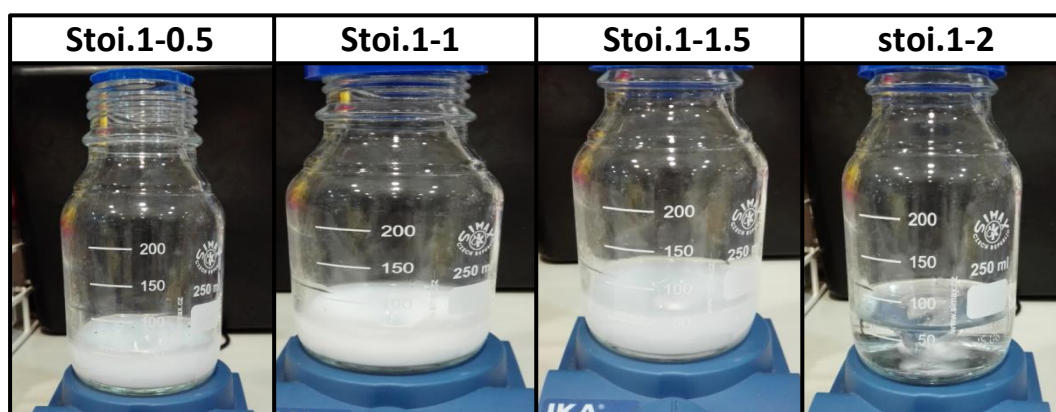
Figure 20: *Visualization reactions of Ce^{3+} with citrate according to stoichiometry (considering 1 for Ce^{3+}).*

	Species in solution	Color
Stoichiometry 1-0.5	Ce^{3+}; $Ce[Cecit_2]_{(s)}$	Partially white
Stoichiometry 1-1	$Ce[Cecit_2]_{(s)}$	Totally white intense
Stoichiometry 1-1.5	$Ce[Cecit_2]_{(s)}$; $(Ce_2cit_3)^{3-}$	Partially white
Stoichiometry 1-2	$(Ce_2cit_3)^{3-}$	colorless

Table 5: Probable species which are in solution when cerium (III) is mixed with citrate.

Method of synthesis with citrate as surfactant is described in section 8.6 Annex of this thesis work. It is obtained nanoparticles with negative charge in their surface as consequence of citrate molecules interaction at basic pH.

In addition, red pellet centrifuged in synthesis CeO₂ NPs naked (see 2.4 point) can be also resuspended with citrate solution (2.2mM) instead of water. But in this case there is no modification in size (5nm) although negative charges in nanoparticle surface are obtained equally as it has been described previously (Samples done by this way are called CeO₂ resuspended in citrate in this thesis).

3.3.2 STUDIES OF REACTION

3.3.2.1 UV SPECTROSCOPY MONITORING

There is no decrease of peak ~290nm, indicating absence of aggregation and stabilization with citrate. Also it is viewed that peak 24h is higher than peak 120min, showing reaction still works after that time.
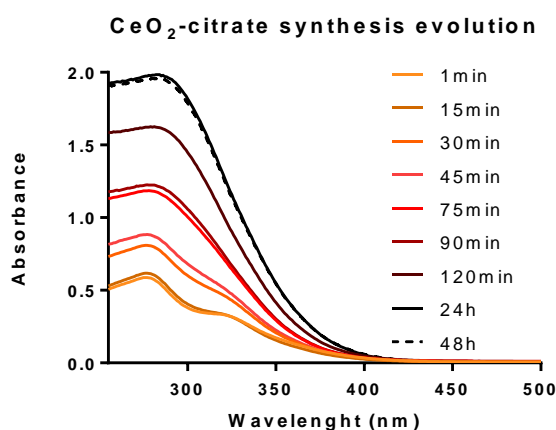
Figure 21: UV monitoring of formation CeO₂ NPs with citrate during synthesis. There is no influence of citrate concentration in analyzed peaks.

3.3.2.2 DLS MONITORING

Following table shows small hydrodynamic size of CeO_2-citrate in comparison with other reactions described in earlier sections. This small diameter detected is remarkable because it is not common obtain such small sizes of any metal oxide nanoparticles with DLS technique. Also, x-ray analysis is done obtaining oxide specie as nature of new material synthesized.

	Hydrodynamic ratio (diameter)
1min	2.43±0.05nm
15min	2.70±0.15nm
30min	2.78±0.35nm
45min	3.18±0.13nm
75min	3.12±0.06nm
90min	3.00±0.05nm
120min	3.02±0.07nm
24h	8±0.37nm

Tables 6: *It is shown values of hydrodynamic size over time in this kind of synthesis by Number distribution.*
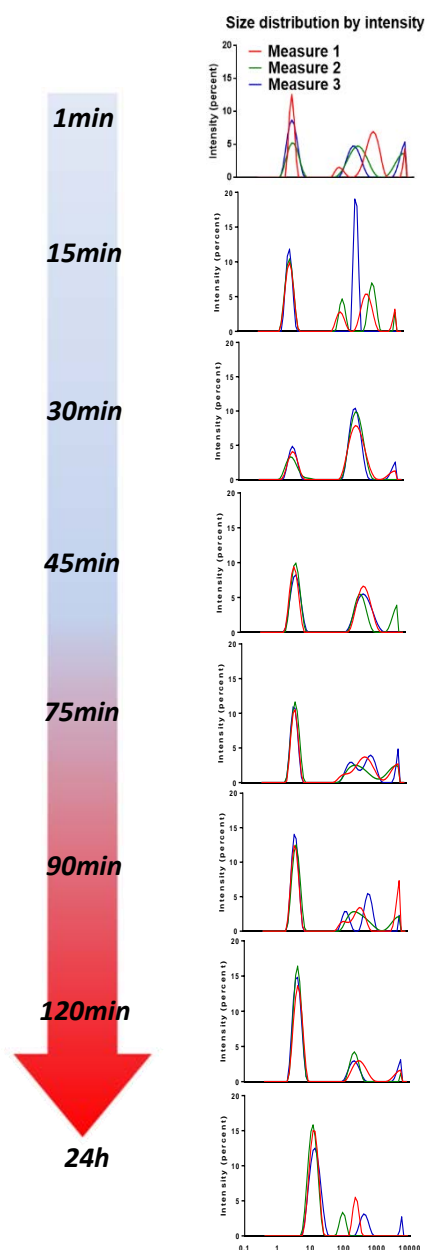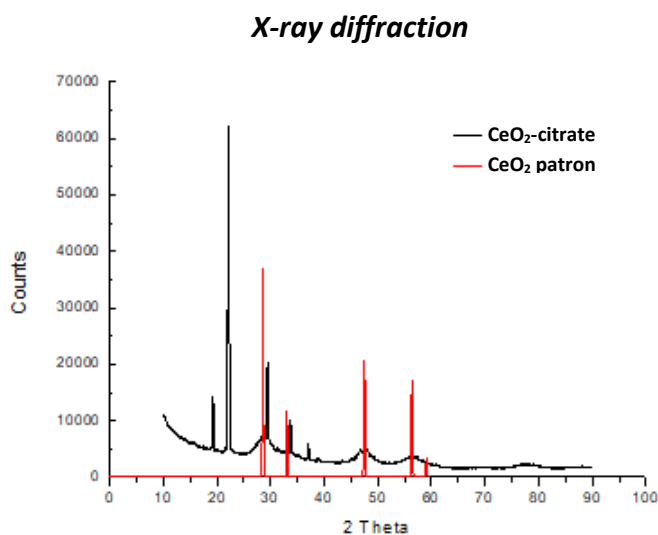
Figure 22: *In the right, scheme presenting evolution of hydrodynamic size of nanoparticle by intensity distribution. In the left, X-ray diffraction showing product synthesized is really CeO₂.*

3.3.2.3 IMAGES TEM

It is viewed a smaller size of nanoparticle than rest of syntheses made in this work, around 3nm. Due to their size and low contrast which present this type of nanoparticles, it is recommendable utilization of ultrafine carbon grids in order to improve visualization and detection. It is curiously checked presence of two different kinds of nanoparticles in reaction Ce-citrate stoichiometry 1-0.5 (figure 23), ones with 5nm and others with 3nm. This fact may be explained viewing table 5, in which Ce^{3+} free in solution produces size nanoparticles of 5nm while cerium in combination with citrate generates size nanoparticles around 3nm.
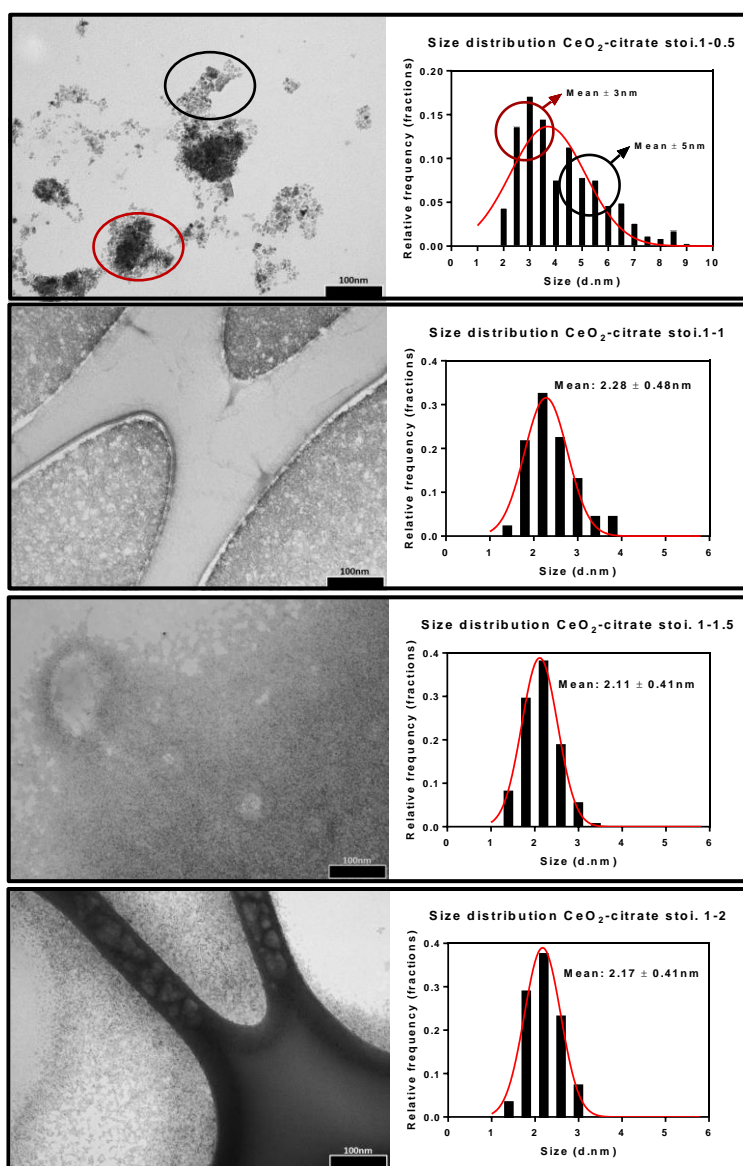
Figure 23: *Images TEM taken from Jeol1010 80KV of synthesis CeO₂-citrate at different stoichiometry. Size distribution is calculated by ImageJ software.*

3.3.2.4 COLOUR EVOLUTION

White colour of initial compound deriving from combination between cerium (III) and citrate (see figure 20) is rapidly dissolved in the moment of base addition. Red colour commonly viewed in this synthesis persists more time and finally a transparent yellow solution is obtained.
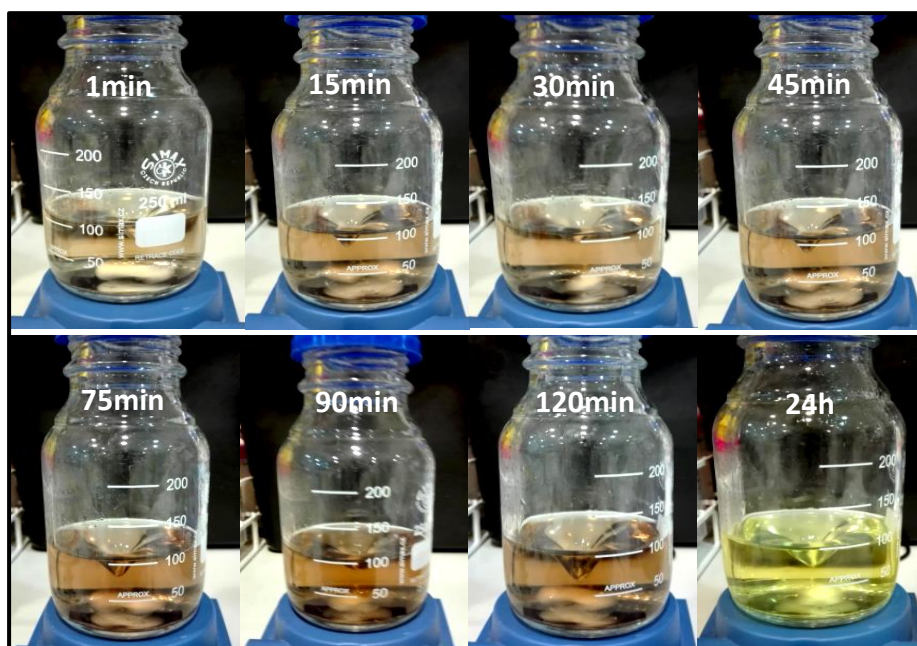
Figure 24: *Colour evolution of CeO₂-citrate synthesis over time.*

3.3.2.5 EVOLUTION pH REACTION

Due to activity of buffering pH of citrate, reaction is kept at basic pH over time. It is viewed an acidification during reaction but at the end there is no acidic pH.
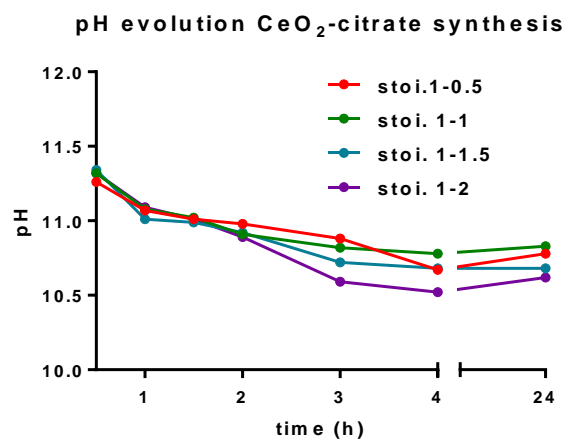
Figure 25: *Evolution of pH in reaction of synthesis CeO₂-citrate at different stoichiometry.*

3.4 DISCUSSION

It is checked surfactants offer an alternative in order to avoid aggregation. This effect is tested both PVP and citrate viewing no decrease in peaks of their UV spectrum while reaction is evolving, hydrodynamic sizes measured by DLS remain practically constant during reaction for both surfactants and there is no visualization of white solid in the process of synthesis. Indeed, there is a transparent colorless solution in the case of PVP and transparent yellow solution in case of citrate.

Monodispersed CeO$_2$ NPs are obtained with both surfactants but there are differences among them. In the case of PVP reaction, evolution of pH is the same that synthesis nanoceria without surfactants, having an acidic pH at the end of reaction. Contrarily, in the case of citrate reaction, pH is kept around 10 because citrate solutions have a buffering capacity at basic pH. Thus, CeO$_2$-citrate NPs have negative charge while CeO$_2$-PVP NPs present neutral charge. That is because PVP molecules are attached on the surface of nanoparticle, evading any outside interaction. Indeed, PVP gives stability owing to steric impediment while citrate gives stability owing to electrostatically impediment.

On the other hand, size of nanoparticle is not affected when PVP is employed as surfactant whereas in case of use citrate varies. Images taken from electronic microscopy are shown diameter of 5nm for CeO$_2$-PVP and around 3nm diameter for CeO$_2$-citrate.

Consequently, another type of nanoparticle is generated and subsequent catalytic and biological assays needs to be done with the aim of being able to distinguish what kind of nanoparticle can be more suitable for medical applications.

CHAPTER 4:

DISPERSION OF CeO$_2$ NANOPARTICLES

IN BIOLOGICAL SYSTEMS

4.1 INTRODUCTION

Polidispersity produced in some synthesis of cerium oxide nanoparticles happens because interactions among nanoparticles are stronger than rest of interactions present in solution. This polydispersity affects drastically biodistribution and conjugation with biological materials. Any aspect which affects the surface, it will have implications in biological media because interaction between cerium oxide nanoparticles and biological entities are produced at nanoparticle surface. For that reason, monodispersity of nanomaterial is the key to understand interactions of biological components. On the other hand, surface charge plays an important role in the kinetic of interactions so, the study and control of this parameter could be greatly useful for predicting behavior of nanomaterials in presence of proteins or their internalization in cells[62,63]. Proteins have the ability to join nanoparticles avoiding their aggregation, very common effect in physiological media. Adsorption of proteins onto nanoparticle surface can be defined as Protein-Corona. Protein-corona can provide the biological entity of nanoparticles. Hünh et al[64] viewed that there was no much difference in protein-corona formation when negative and positive nanoparticles are used but charge surface of protein-corona influenced in cellular interaction. According to Verma et al[63], nanoparticles with neutral charge do not interact to cells while nanoparticles with negative or positive charge do it with different grade of affinity, being the positives more efficient than the negatives.

Normally, physiological media has a wide variety of components which interacts with cerium oxide nanoparticles. At the beginning, proteins with high mobility are the first to be adsorbed onto the inorganic surface, forming Soft-Corona at short times. But at longer times, these same proteins tend to be exchanged for others with more affinity owing to equilibrium process forming Hard-Corona (figure 26) an irreversible permanent structure[65–67]. This fact is well described by the Vroman effect[68]. Some factors such as media composition, proteins concentration, pH, temperature, exposure time, size and curvature of nanoparticle affects to protein-corona formation[69,70].

Nanoparticles interact with living cells through protein-corona so, it is important investigate this phenomenon to understand how nanomaterials can be beneficial for future medical applications or, on the contrary, how they can be harmful from nanotoxicology point of view. According to Lynch et al[71], adsorption of proteins is caused mainly by electrostatic interactions although hydrophobic and specific chemical interactions have importance too.
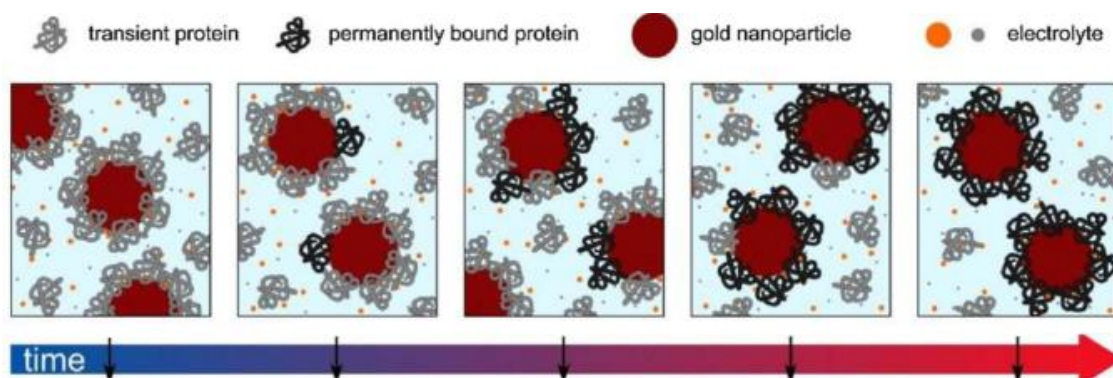
Figure 26: Evolution and formation of hard protein-corona over time using gold nanoparticles as example. Figure taken from Barbero et al, "Formation of protein corona: The interface between nanoparticles and the immune system", Seminars in immunology, 34, 52-60, 2017.

It was viewed that aggregation can influence notably in protein-corona formation. A high grade of aggregation offers different kinds of protein binding. Besides, Protein-corona also influences biodistribution, making cerium oxide nanoparticles more selective to different tissues in the body. Protein coating will be responsible for fate inside the body.

4.2 CONJUGATION CeO$_2$ NPs WITH ALBUMIN

Cerium oxide nanoparticles need to be recovered with biological components for medical applications because all kind of nanoparticles tends to be unstable in physiological conditions. This instability is due to ionic conditions and pH, altering surface charge of nanoparticles leading to aggregation and consequently affecting negatively to systems in-vivo.

It is important highlight the fact that conditions in which biological components are stable nanoparticles are not while conditions in which nanoparticles tend to be stable biological components are not. Thus, to find good conditions for suitable conjugation is required.

Conjugation with albumin (BSA) will be done because is the most abundant protein in blood stream (35mg/ml). CeO$_2$ naked (viewed chapter 2) already synthesized will be used to conjugate because of their positive charge, which will interact fast with negative charge of protein. Nanoparticles with negative charge are also capable of being conjugated with proteins but conjugation with nanoparticles positively charged is electrostatically more favorable.

It can be detected an increase of hydrodynamic size of CeO$_2$-BSA NPs by DLS but it is highlighted monodispersity during conjugation. Besides, negative charge is presented in this type of sample as consequence of hard-corona formation and excess of protein used during synthesis. Procedure of synthesis is explained in section 8.7 Annex of this thesis work.
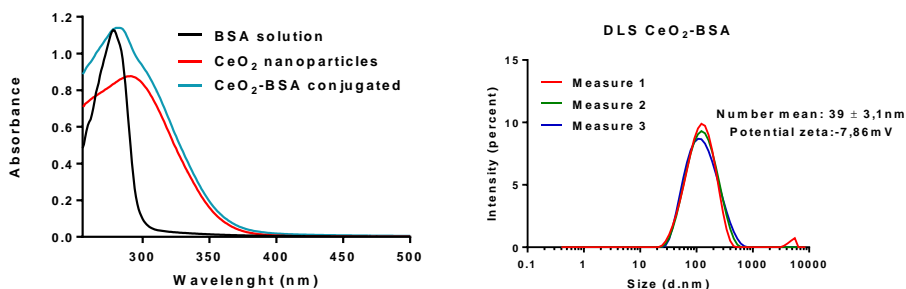
Figure 27: In the left, *UV spectrum of CeO₂ conjugated with albumin. In the right, DLS of CeO₂-BSA.*

4.3 STUDIES OF CeO₂-PROTEIN-CORONA

4.3.1 INTRODUCTION

Nanoparticles interact with living organisms through their protein-corona structure. Consequently, to study this phenomenon allows getting interesting information about behavior of nanoparticles in physiological media. Casals et al[72] checked protein-corona formation of several metal oxide nanoparticles in cell culture media supplemented with FBS, monitoring it with combination of hydrodynamic sizes and surface charges studies. Thus, they were able to distinguish experimentally between soft-corona and hard-corona. Finally, Casals et al could conclude that once values surface charge of nanoparticles and serum coincide, a hard-corona is generated.

This method of work will be taken in order to study effect protein-corona formation in nanoceria (see Annex section 8.8 of this thesis). In this thesis work, CeO_2 naked resuspended with water (5nm, positive charge), CeO_2 naked resuspended with citrate (5nm, negative charge) and CeO_2 synthesized with citrate (3nm, negative charge) will be used as samples in order to check effect of surface charge and size to protein-corona formation.

Studies of formation protein-corona will be done in both phosphate buffer (PB) pH 7.2 10mM and cell culture Dulbecco modified eagle media (DMEM, without phenol red) supplemented with fetal bovine serum (FBS) or BSA solution. PB has proper conditions of salinity and pH to see formation of protein-corona and cell culture media is employed to study evolution of nanoparticles in physiological media where cells are incubated and in-vitro assays are done in biological experiments.

4.3.2 CeO$_2$ IN PB SUPPLEMENTED WITH BSA

Physiological media are composed by 90% volume of cell culture media and 10% supplemented material. This proportion will be kept in all experiments of protein-corona made in this thesis. Concretely this experiment will be done in the following way: 350mg BSA is dissolved in 9ml PB 10mM. Later, 1ml of CeO$_2$ NPs 1mg/ml is added slowly on the PB solution with protein. Then, procedure explained in section 8.8 in Annex is applied at different times of incubation, making measures of DLS and zeta potential of purified sample.

CeO$_2$ naked		
Time	**Hydrodynamic Size**	**Potential zeta; conductivity**
Control	11,5±0,6nm	-44,8mV; 1,91mS/cm
0 days	53±6,5nm	-25mV; 1,92mS/cm
1 day	55,5±3,5nm	-7,1mV; 1,98mS/cm
2 days	72,3±1,5nm	-8,5mV; 1,94mS/cm
5 days	84,6±9,2nm	-11mV; 1,97S/cm

CeO$_2$ resuspended citrate		
Time	**Hydrodynamic Size**	**Potential zeta; conductivity**
Control	29,5±7nm	-52,7mV; 1,85mS/cm
0 days	71,3±9,3nm	-26,8mV; 1,78mS/cm
1 day	78,3 ±5,8nm	-16,2mV; 1,84mS/cm
2 days	102,8±7,7nm	-12,7mV; 1,81mS/cm
7 days	108,4±7,13nm	-10,2mV; 1,77mS/cm

CeO$_2$-citrate		
Time	**Hydrodynamic Size**	**Potential zeta; conductivity**
Control	7,5±0,3nm	-27mV; 2,22mS/cm
0 days	3.3±0,4nm	-16,4mV; 2,17mS/cm
1 day	3.2±0,07nm	-13,5mV; 2,12mS/cm
2 days	3,7±0,14nm	-7,95mV; 2,12mS/cm
7 days	4 ±0,36nm	-7,82mV; 2,15mS/cm

Table 7: *Values of hydrodynamic size and surface charge of different CeO$_2$ samples obtained after purification to measure protein-corona in PB supplemented with BSA. Each data is done by triplicate.*
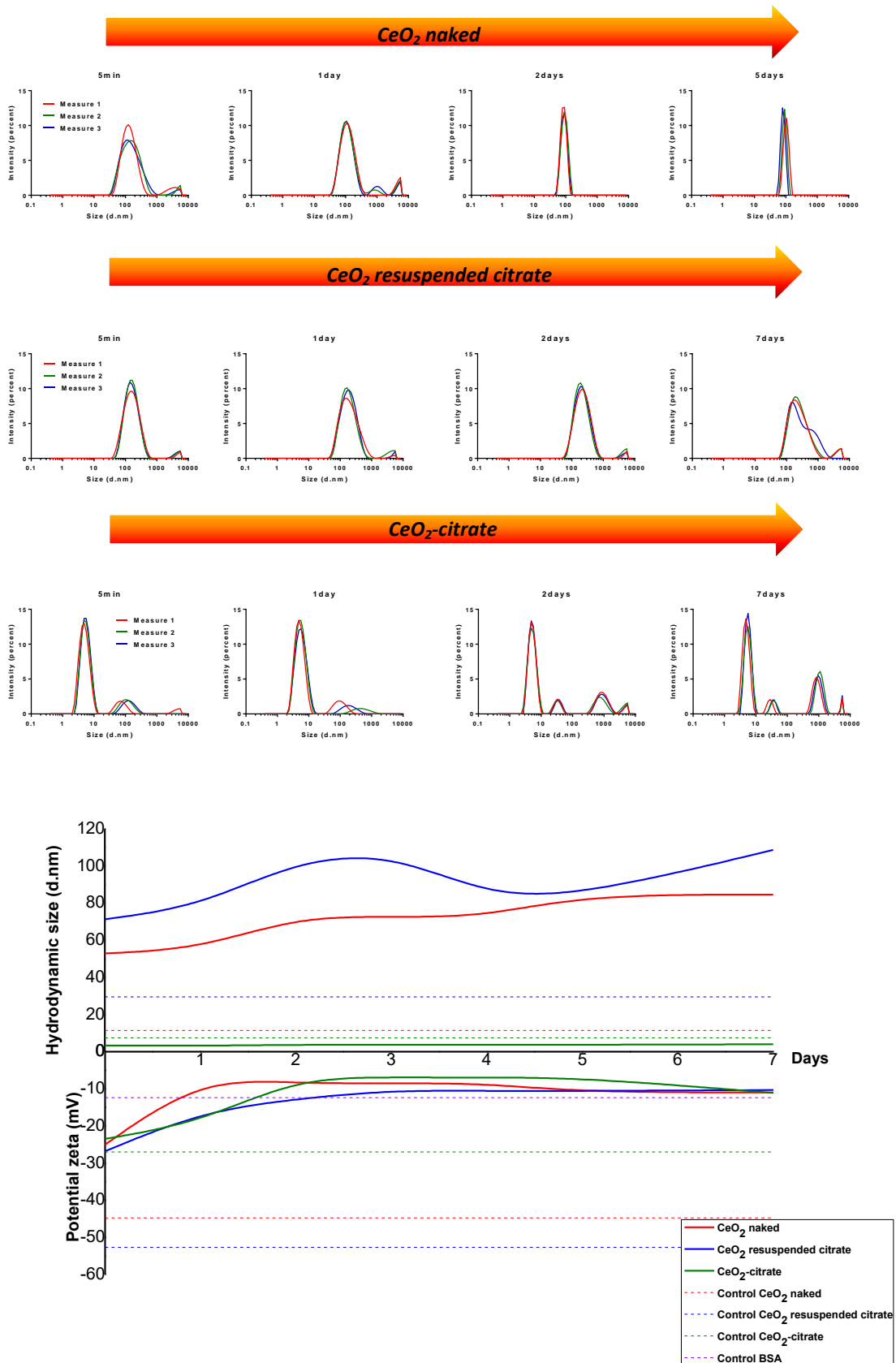
Figure 28: *In the top, graphic representation of evolution protein-corona by DLS owing to intensity distribution for CeO$_2$ samples over time in PB supplemented with BSA. On the bottom, graphic representation of values corresponding to table 7 showing evolution of surface charge and hydrodynamic size of protein-corona.*

4.3.3 CeO_2 IN PB SUPPLEMENTED WITH FBS

Normally, cell culture media is composed by 90% volume of cell culture and 10% volume of protein. In case of employing FBS as protein media, this proportion will be maintained. So, this experiment will be done in the following manner: 0.9ml of FBS solution is mixed in 8.1ml of PB 10mM. Then, 1ml of CeO_2 NPs 1mg/ml is added slowly on the mix and after that, protocol described previously is done.

CeO_2 naked		
Time	**Hydrodynamic Size**	**Potential zeta; conductivity**
Control	11,5±0,6nm	-44,8mV; 1,91mS/cm
0 days	97,5±19nm	-31,1mV; 1,81mS/cm
1 day	104,1±9,2nm	-30,9mV; 1,79mS/cm
2 days	75,4±4,8nm	-25,6mV; 1,80mS/cm
7 days	100,6±6,9nm	-23,4mV; 1,79mS/cm

CeO_2 resuspended citrate		
Time	**Hydrodynamic Size**	**Potential zeta; conductivity**
Control	29,5±7nm	-52,7mV; 1,85mS/cm
0 days	82,3 ±26nm	-28,8mV; 1,80mS/cm
1 day	76 ±4,8nm	-16,2mV; 1,83mS/cm
2 days	130,8 ±5,8nm	-12,4mV; 1,83mS/cm
7 days	109,2 ±13,1nm	-13,4mV; 1,76mS/cm

CeO_2-citrate		
Time	**Hydrodynamic Size**	**Potential zeta; conductivity**
Control	7,5±0,3nm	-27mV; 2,22mS/cm
0 days	74,4 ±1nm	-30,1mV; 1,78mS/cm
1 day	60,3 ±17,5nm	-26mV; 1,81mS/cm
2 days	107,2 ±12,8nm	-15,4mV; 1,82mS/cm
7 days	67,7 ±21,1nm	-17,4mV; 1,76mS/cm

Table 8: *Values of hydrodynamic size and surface charge of different CeO₂ samples obtained after purification to measure protein-corona in PB supplemented with FBS. Each data is done by triplicate.*
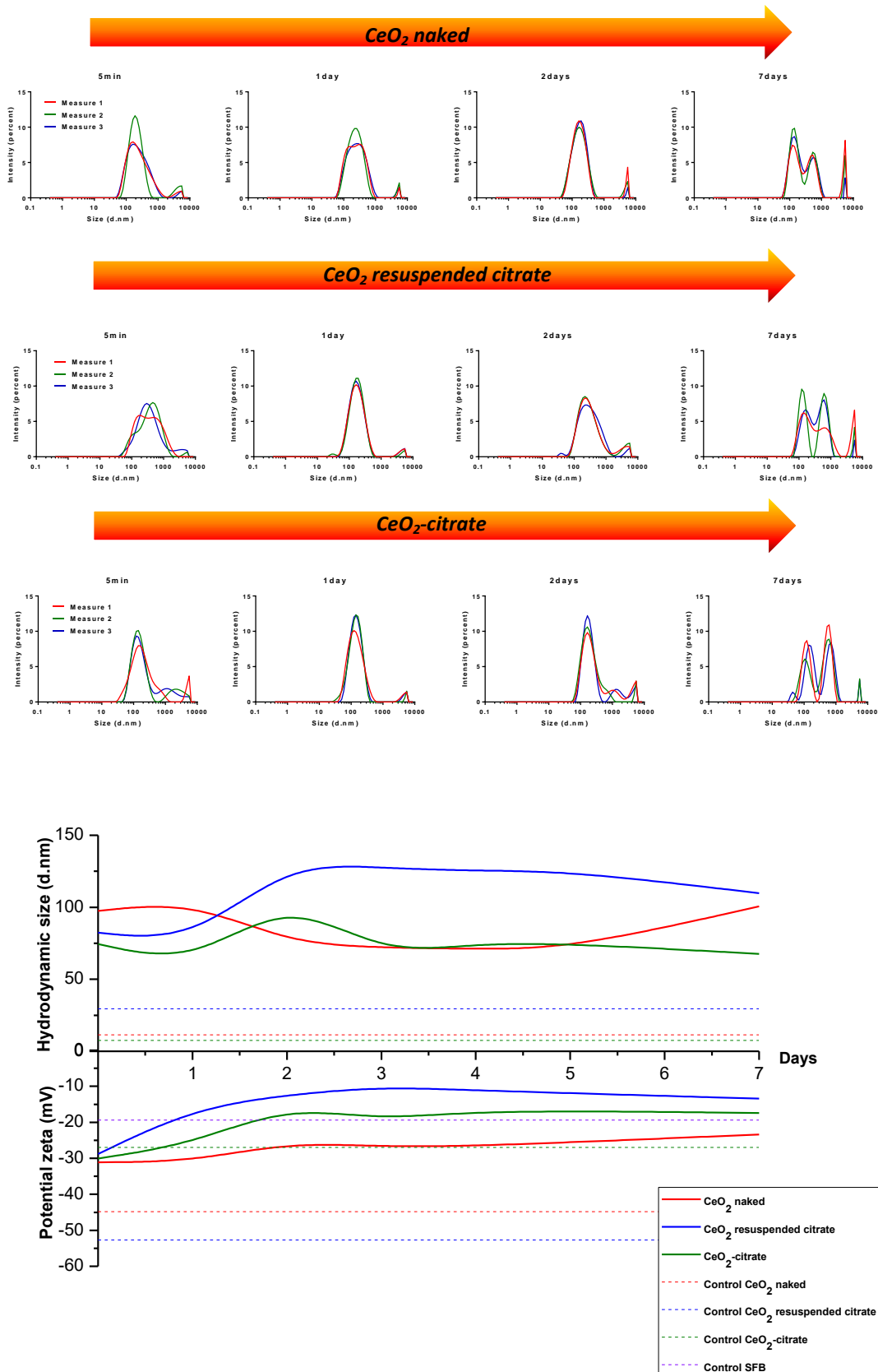
Figure 29: *In the top, graphic representation of evolution protein-corona by DLS owing to intensity distribution for CeO₂ samples over time in PB supplemented with FBS. On the bottom, graphic representation of values corresponding to table 8 showing evolution of surface charge and hydrodynamic size of protein-corona.*

4.3.4 CeO$_2$ IN DMEM SUPPLEMENTED WITH FBS

In this experiment, procedure will be the same as explained in the earlier point but employing DMEM instead of PB buffer 10mM. Volume of 8.1ml DMEM is mixed with 0.9ml FBS. Then, 1ml of CeO$_2$ NPs 1mg/ml is added slowly in cell culture media and after that, method previously explained in section 8.8 in Annex is done.

CeO$_2$ naked		
Time	**Hydrodynamic Size**	**Potential zeta; conductivity**
Control	11,5±0,6nm	-44,8mV; 1,91mS/cm
0 days	57±5,6nm	-29,8mV; 2,03mS/cm
1 day	76,9±3,6nm	-25,7mV; 2,17mS/cm
2 days	95,3±3,4nm	-20,2mV; 2,30mS/cm
4 days	145,3±3,8nm	-21,9mV; 2,03mS/cm

CeO$_2$ resuspended citrate		
Time	**Hydrodynamic Size**	**Potential zeta; conductivity**
Control	29,5±7nm	-52,7mV; 1,85mS/cm
0 days	159,5±23,2nm	-30,5mV; 1,86mS/cm
1 day	134,5±33,7nm	-30,2mV; 1,88mS/cm
2 days	96,5±3,6nm	-25,4mV; 1,88mS/cm
7 days	148,9±7,5nm	-26,3mV; 1,91mS/cm

CeO$_2$-citrate		
Time	**Hydrodynamic Size**	**Potential zeta; conductivity**
Control	7,5±0,3nm	-27mV; 2,22mS/cm
0 days	207,9±115,2nm	-32,3mV; 1,88mS/cm
1 day	182,1±42nm	-32,4mV; 1,91mS/cm
2 days	172,3±13,3nm	-32,6mV; 1,89mS/cm
7 days	113,5±7,3nm	-29,8mV; 1,81mS/cm

Table 9: *Values of hydrodynamic size and surface charge of different CeO$_2$ samples obtained after purification to measure protein-corona in DMEM supplemented with FBS. Each data is done by triplicate.*

Figure 30: *In the top, graphic representation of evolution protein-corona by DLS owing to intensity distribution for CeO₂ samples over time in DMEM supplemented with FBS. On the bottom, graphic representation of values corresponding to table 9 showing evolution of surface charge and hydrodynamic size of protein-corona.*

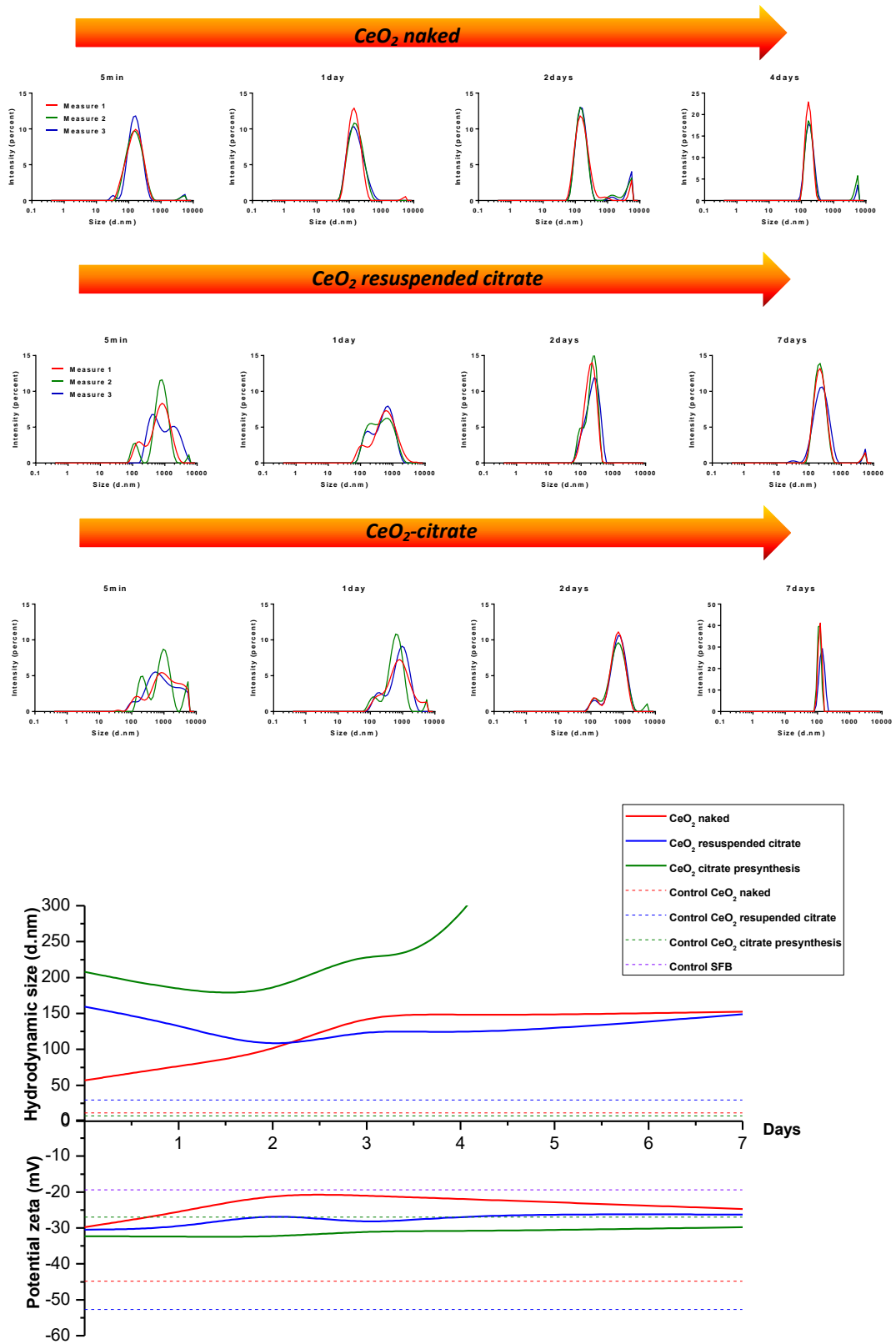## 4.3.5 CeO$_2$ IN DMEM SUPPLEMENTED WITH BSA

In this experiment, BSA will be dissolved previously in PB before being added in cell culture DMEM. 350mg BSA is dissolved in 0.9ml PB 10mM and this volume is added on 8.1ml DMEM. After that, 1ml of CeO$_2$ NPs 1mg/ml is added slowly and method of work described previously is done.

CeO$_2$ naked		
Time	**Hydrodynamic Size**	**Potential zeta; conductivity**
Control	11,5±0,6nm	-44,8mV; 1,91mS/cm
0 days	98,6±18,1nm	-28,5mV; 1,88mS/cm
1 day	118,7±44,7nm	-28mV; 1,95mS/cm
2 days	116,7±21,2nm	-14,7mV; 1,96mS/cm
7 days	107,3±14,5nm	-16,4mV; 1,84mS/cm

CeO$_2$ resuspended citrate		
Time	**Hydrodynamic Size**	**Potential zeta; conductivity**
Control	29,5±7nm	-52,7mV; 1,85mS/cm
0 days	127±28,6nm	-31,2mV; 1,89mS/cm
1 day	312±23,8nm	-28,2mV; 1,87mS/cm
2 days	168±11,2nm	-22,8mV; 1,86mS/cm
7 days	256,8±25,6nm	-16,8mV; 1,86mS/cm

CeO$_2$-citrate		
Time	**Hydrodynamic Size**	**Potential zeta; conductivity**
Control	7,5±0,3nm	-27mV; 2,22mS/cm
0 days	aggregated	-30,9mV; 1,90mS/cm
1 day	aggregated	-31,8mV; 1,94mS/cm
2 days	aggregated	-29,2mV; 1,95mS/cm
7 days	aggregated	-24.4mV; 1,86mS/cm

Table 10: *Values of hydrodynamic size and surface charge of different CeO$_2$ samples obtained after purification to measure protein-corona in DMEM supplemented with BSA. Each data is done by triplicate.*
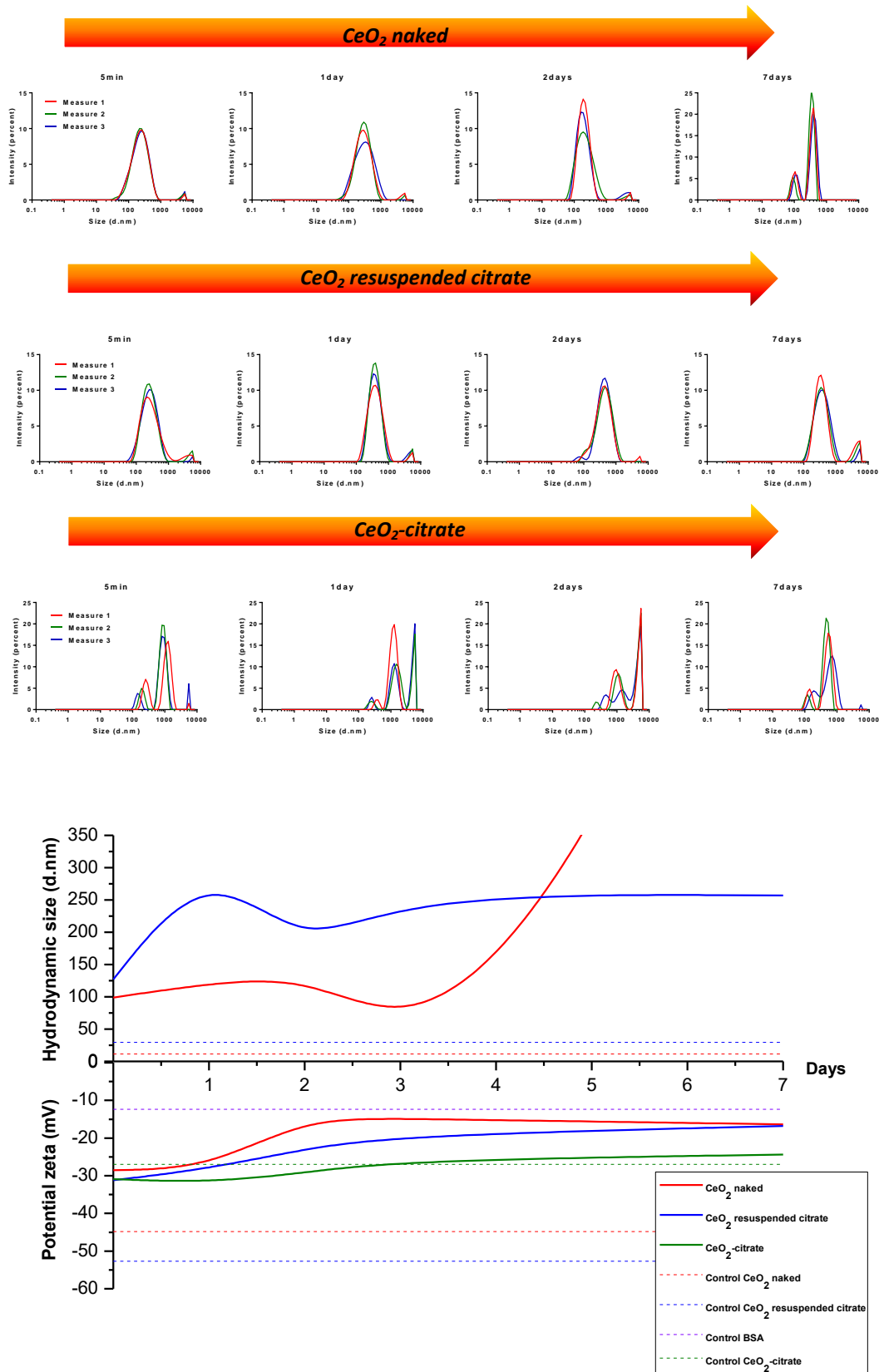
Figure 31: *In the top, graphic representation of evolution protein-corona by DLS owing to intensity distribution for CeO₂ samples over time in DMEM supplemented with BSA. On the bottom, graphic representation of values corresponding to table 10 showing evolution of surface charge and hydrodynamic size with exception of CeO₂-citrate because of his aggregated state.*

57

4.4 DISCUSSION

Studies of protein-corona have proportionated useful information to understand behavior of CeO$_2$ NPs in physiological media. Due to measures of surface charge and hydrodynamic sizes by DLS, hard-corona formation has been monitored. When surface charge of nanoparticle reaches the same value of surface charge of protein, then hard-corona is formed.

CeO$_2$-PVP is not employed in this experiment because PVP attached on their surface avoid interaction of this material with other molecules so, it is useless study protein-corona formation in this type of nanoparticle if it is previously known proteins will not interact.

It is checked formation of protein-corona both BSA and FBS in phosphate buffer is better than cell culture DMEM. Possibly, DMEM may have some substances such as aminoacids or antibiotic which difficult formation of hard-corona in those conditions. Nevertheless, it is checked evolution of protein-corona in DMEM is better in nanoparticles with positive charge than negative.

In the case of BSA, it is viewed in PB hard-corona is formed during 1 day for CeO$_2$ naked and 2 days for CeO$_2$ resuspended in citrate and CeO$_2$-citrate, keeping practically the same hydrodynamic size. On the opposite, it is viewed in DMEM formation of hard-corona during 2 days for CeO$_2$ naked and 3 days at least for CeO$_2$ resuspended in citrate, viewing a slowdown in DMEM media in comparison with PB. CeO$_2$-citrate is not considered in this situation because it tends to aggregate in those conditions for unknown reasons.

In the case of FBS, It is viewed in PB that CeO$_2$ naked requires 7 days and CeO$_2$-citrate requires 2 days to form hard-corona while CeO$_2$ resuspended in citrate requires only 1 day. However, in DMEM media it is detected formation of hard-corona for CeO$_2$ naked at 2 days, CeO$_2$ resuspended in citrate does not reach value of surface charge of serum and protein-corona of CeO$_2$-citrate is not viewed (no variation in his surface charge). Formation of protein-corona with FBS instead of BSA is slower because of wide variety of proteins present in serum.

In conclusion, if it is required conjugation of CeO$_2$ NPs with protein to make it biocompatible in order to employ it for future systems in-vivo, utilization of buffer instead of cell culture media is the best option and use BSA is much better than FBS in spite of serum is composed by albumin mostly. In addition, CeO$_2$ naked generally tends to interact with proteins in greater degree than coated nanoparticles.

On the other hand, cell lines are incubated in cell culture media supplemented with serum so, to study the different kind of CeO$_2$ NPs in DMEM supplemented with FBS offer additional information about their behavior in physiological media where in-vitro assays with cells are done.

As it has been described before, CeO$_2$-citrate (3nm) apparently do not form protein-corona in those conditions and, in fact, it tends to aggregate at few days of incubation so, apparently it is viewed that this sample is not proper for applications in cellular studies. Additionally, CeO$_2$ resuspended in citrate do not shown clear results in these conditions but CeO$_2$ naked present more promising results. In case of CeO$_2$ naked, it is viewed a good evolution with a homogeneous peak in size distribution by intensity (figure 30, corresponding to hardening of protein-corona). Probably, molecules of citrate are responsible of slow adhesion of proteins onto nanoparticle surface in cell culture conditions.

As consequence, CeO$_2$ naked looks like suitable sample for cell culture media for being able to form hard-corona apart from the fact that present better distribution and homogeneity in these conditions, due to their positive surface charge possibly.

CHAPTER 5:

CATALYTIC ACTIVITY OF CeO$_2$

NANOPARTICLES

5.1 INTRODUCTION

It is well known the role of catalyzer of cerium oxide nanoparticles in petrochemical industry. Cerium in combination with oxygen adopts a fluorite structure which allows behaving as "oxygen storage". CeO$_2$ NPs work as a catalytic supplier of oxygen for combustion of hydrocarbons, apart from becoming CO and NO$_x$ into non-toxic forms for the environment[73]. Application of nanoceria in automotive pollution control has been one of the most common in the last years[74] although catalytic capacity of CeO$_2$ NPs is also taken advantage of water treatment[75]. According to Recillas et al[76,77] and Zhong et al[78], nanoceria are effective sorbent for the removal of lead, arsenic(V) and Chromium(VI) from water, apart from oxidizing carbon monoxide into CO$_2$. Catalytic activity of nanoceria is related with oxygen vacancies of their surface. The formation of lattice oxygen vacancies plays an important role in oxidation and reduction activity in nanoceria. Recently, it has been tried to apply this property of CeO$_2$ NPs to biotechnological fields but with especial interest in medicine, as alternative to treat free radicals.

Normally there is an intracellular balance between generation and elimination of reactive oxygen species (ROS) regulated by enzymes superoxide dismutase, peroxidase, catalase or glutathione. Nevertheless, some alterations in cellular metabolism origin a major increase of free radicals such as superoxide (O_2^-), peroxide (O_2^{2-}) and hydroxyl radical (OH$^.$). This effect is called oxidative stress and it can cause cell death. As consequence of this deregulation, some illnesses have emerged and adverse effects are caused in the organism. Some examples of these diseases derived from oxidative stress can be seen in figure 1. But increase of these free radicals may not be only related with a failure in cellular activity but it can be also derived from microbial infection as defense mechanism[79]. Indeed, the high concentration of ROS promotes inflammation which is triggered by immune system. Hence, necessity of controlling and regulating this kind of response is great importance in medicine in order to avoid serious consequences in the body. Additionally, it is really important inhibition of causers which trigger immune response because otherwise, same immune system can damage the organism.
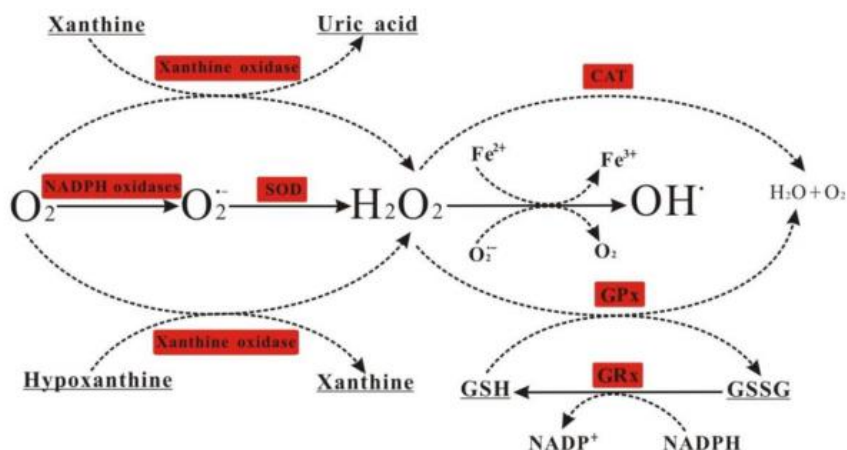
Figure 32: *Schematic diagram showing the generation of free radicals, taken from Li et al, "Natural plant polyphenols for alleviating oxidative damage in man: Current status and future perspectives", Topical Journal of pharmaceutical research, 15(5), 1089-1098, **2016**[80].*

For those reasons CeO$_2$ NPs have emerged with great attention in medicine in order to control population of ROS in biological systems, not only scavenging free radicals (antioxidant) but also reversing inflammatory response (anti-inflammatory). CeO$_2$ NPs have special interest in neurodegenerative diseases[81], in cardiovascular problems[82], in liver cirrhosis[25], retinal ilnesses[83] and many others. Besides, it has been reported cerium oxide nanoparticles as useful radioprotective agents in radiotherapy treatment against cancer, protecting healthy tissues from ROS generated by radiation[84,85].

Catalytic capacity of nanoceria comes from their ability to be oxidized or reduced according to environment, behaving as natural electron buffer. CeO$_2$ NPs can act as superoxide dismutase (Eq. 9-10) and catalase (Eq.11) behaving as a multienzymatic catalyzer according to Nelson et al[86]:

$$O_2^- + Ce^{3+} + 2H^+ \leftrightarrow H_2O_2 + Ce^{4+} \text{ (Eq. 9)}$$

$$O_2^- + Ce^{4+} \leftrightarrow O_2 + Ce^{3+} \text{ (Eq.10)}$$

$$H_2O_2 + 2Ce^{4+} + 2OH^- \leftrightarrow 2H_2O + O_2 + 2Ce^{3+} \text{ (Eq. 11)}$$
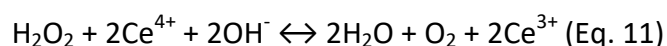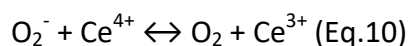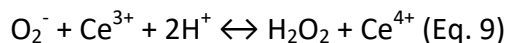
However, properties of nanomaterials are conditioned by their process of synthesis. So, once optimized a protocol of synthesis in this thesis work, it is necessary to evaluate catalytic activity of synthesized product in order to meet desired expectations for being applied in medical field.

5.2 AMPLEX RED ASSAY

Hydrogen peroxide (H$_2$O$_2$) is one of the most common free radicals which are responsible of oxidative stress. Hence, utilization of a technique which is capable of measure and quantify this concrete substance will be essential to check antioxidant capacity of synthesized CeO$_2$ NPs. So, from all techniques described in literature for this purpose, Amplex Red is chosen. In fact, Pirmohamed et al[87] used this technique to evaluate catalase activity of nanoceria. Amplex Red offers high sensitivity being able to detect concentration of H$_2$O$_2$ in nanomolar, range of concentrations in which this metabolite is normally found in biological systems. In addition, fluorescence is the signal analyzed in Amplex Red instead of absorbance. The advantage of measuring fluorescence consists in this type of signal is less susceptible of interferences in comparison with absorbance. Besides, other factor to be considered consists in limitations of equipment. Fluorimeter from our laboratory works with filters instead of scanner so, it has to be adapted in area of work that present the device. Fortunately, there is no inconvenience for Amplex Red because its range of excitation and emission coincides with our filters of fluorimeter.

Amplex Red forms a complex 1:1 with H$_2$O$_2$ and, in presence of a peroxidase emits a red fluorescent signal (Resorufin). Resorufin has excitation and emission maxima of approximately 571nm and 585nm (see figure 33). This compound is sensitive to light so, work in dark conditions is recommendable. Protocol of work made by Invitrogen will be taken as reference[88] and procedure can be seen in section 8.9 Annex.
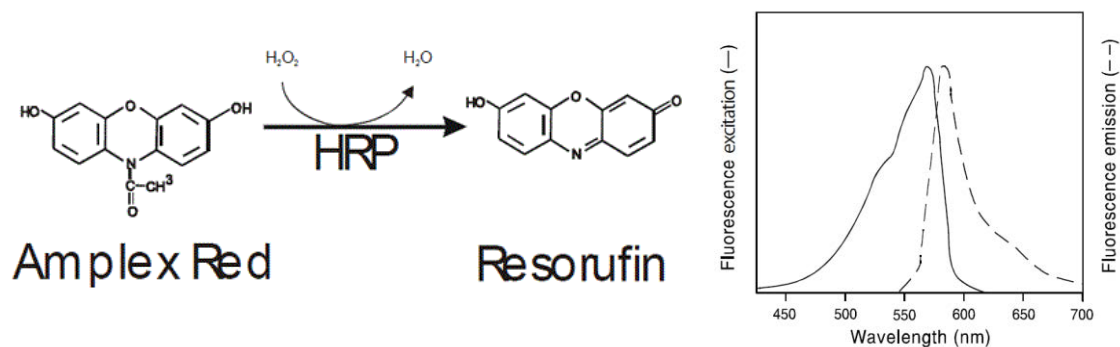
Figure 33: *In the left, reaction of Amplex Red during assay. In the right, normalized excitation and emission spectra of resorufin, the product of the Amplex Red reaction. Images taken from Invitrogen protocol.*

5.3 STUDIES OF ANTIOXIDANT CAPACITY

5.3.1 CATALYTIC CAPACITY OF NANOCERIA

It is check efficacy of Amplex Red technique using a negative control which does not react with H_2O_2, gold nanoparticles. At the same time, CeO$_2$ NPs are used to see their catalytic capacity. It is viewed no reaction by Au NPs whereas uptake of hydrogen peroxide both CeO$_2$ aggregated and CeO$_2$ well dispersed is detected. Suitable dispersion of NPs improves their antioxidant characteristics.
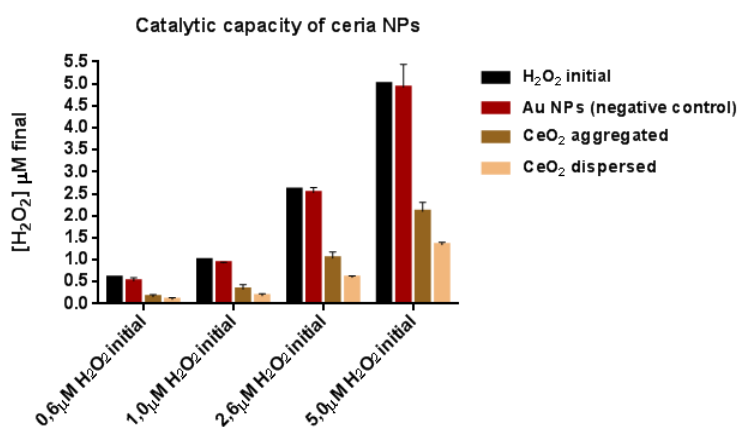
Figure 34: *Antioxidant assay of Au NPs, CeO$_2$ aggregated and CeO$_2$ well dispersed.*

5.3.2 CATALYTIC ACTIVITY ACCORDING TO CONCENTRATION

CeO$_2$ naked is used to do this assay at different concentrations (0,1mg/ml, 0,05mg/ml and 0,01mg/ml). It is viewed that at same concentration of hydrogen peroxide, the more concentration of CeO$_2$ is used, more H_2O_2 is degraded (or the less H_2O_2 free is detected). At the same time, at constant concentration of CeO$_2$ NPs, the more initial concentration H_2O_2 is employed, the more H_2O_2 is reacted. In other words, the higher concentration of H_2O_2, the higher is catalytic activity of CeO$_2$ in those conditions. This effect is tremendously useful for medicine, because not only nanoceria are able to scavenge ROS but they are also able to reduce their catalytic activity when free radicals are at low concentrations (as healthy conditions).
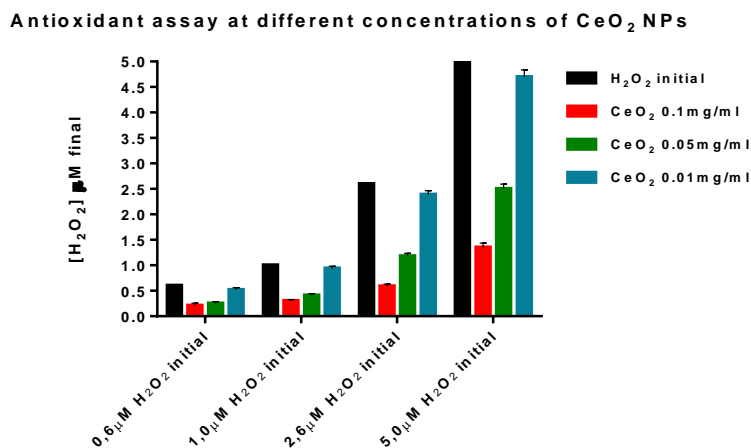
Figure 35: *Antioxidant assay at different concentrations of CeO$_2$ NPs.*

5.3.3 EFFECT OF SONICATION IN CATALYSIS

Sonication is a technique to disperse aggregates in solution. It is viewed sonication will not affect to catalysis if synthesis CeO$_2$ NPs is already good dispersed initially. However, if CeO$_2$ NPs are initially aggregated and sonication is used in order to disperse, this fact can reduce their catalytic capacity. In spite of good dispersion by sonication, it is clearly viewed a great difference in the catalysis in comparison with CeO$_2$ naked. Consequently, sonication is not recommendable during synthesis of CeO$_2$ NPs.
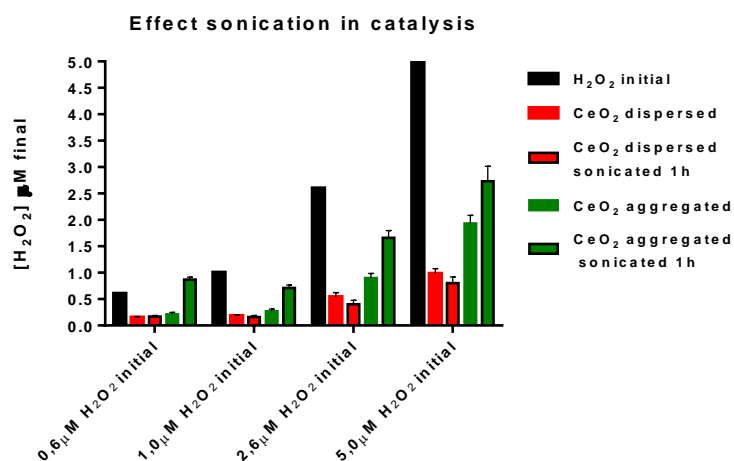
Figure 36: *Antioxidant assay in which effect of sonication in CeO$_2$ NPs is checked.*

5.3.4 CATALYTIC CAPACITY OF CeO$_2$-PVP AND CeO$_2$-CITRATE

It is viewed that surfactants, independently of their concentration, does not affect catalytic properties of CeO$_2$ NPs. Once it is checked effect of surfactants in catalysis, it is decided to work with least concentration as possible of them during synthesis: 0,5mM PVP and 10mM citrate (see section 8.5 and 8.6 in Annex of this thesis work) In the case of CeO$_2$-citrate, it can be highlight a decreased activity when 5mM citrate is used in comparison with rest of the samples. Probably, this effect is done as consequence of polydispersity of the sample (see section 3.3.2.3 images TEM in chapter 3).
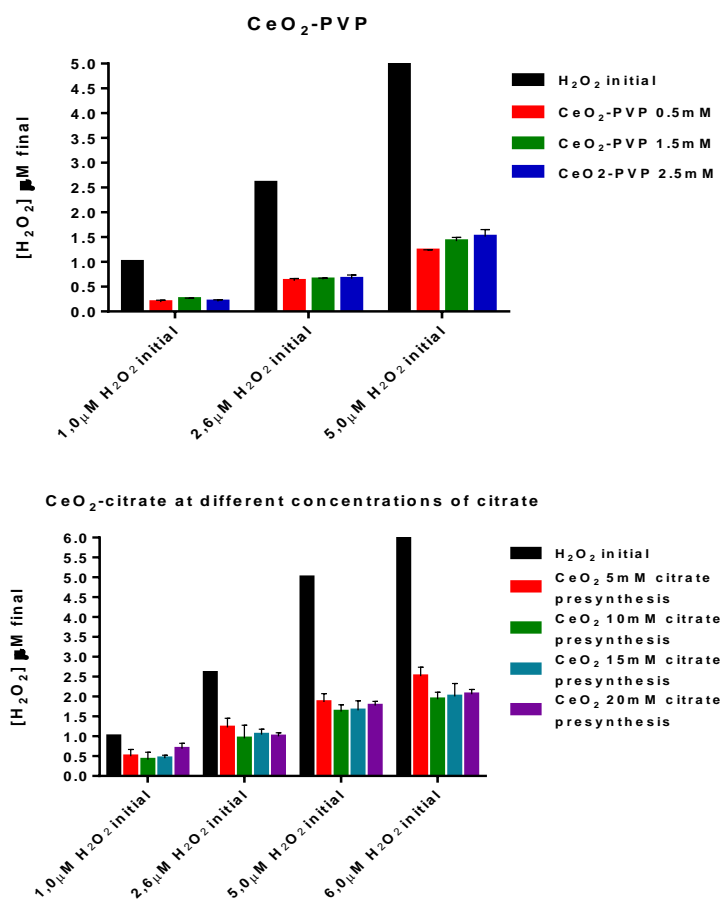
Figure 37: *Antioxidant assay of CeO$_2$-PVP and CeO$_2$-citrate at different concentration of surfactant.*

5.3.5 ANTIOXIDANT ASSAY RESUSPENSIONS OF CeO$_2$ NAKED

It is viewed once CeO$_2$ is well dispersed, subsequent stabilization with some surfactants (PVP, BSA, citrate) does not affect their catalytic properties. This information is important to know because from this way, if it is desired to employ interesting characteristics of CeO$_2$ NPs in conditions in which this nanomaterial is not stable (physiological media, for instance), can be stabilize subsequently without altering their initial properties.

Comparison among CeO$_2$ naked/PVP/citrate/BSA
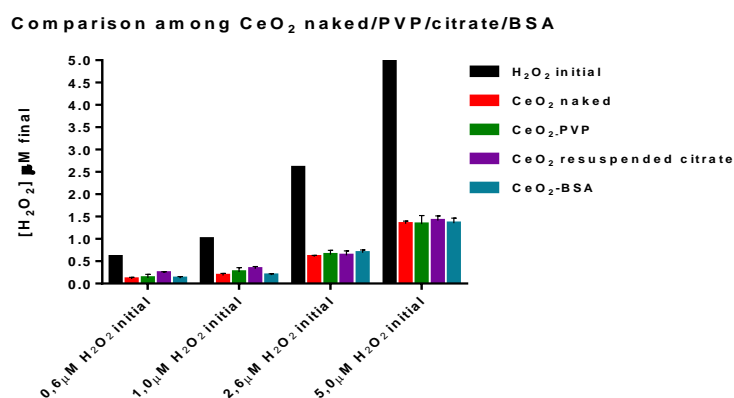
Figure 38: *Antioxidant assay of subsequent resuspensions of CeO$_2$ naked in different stabilizers.*

5.3.6 COMPARATIVE WITH OTHER REDUCERS

It is viewed lower antioxidant activity of nanoceria in comparison with tannic or ascorbic acid but higher activity than citrate. However, the effect of CeO$_2$ NPs presents longer durability while rest of antioxidants is consumed in the moment of reaction.

Antioxidant assay with others antioxidants
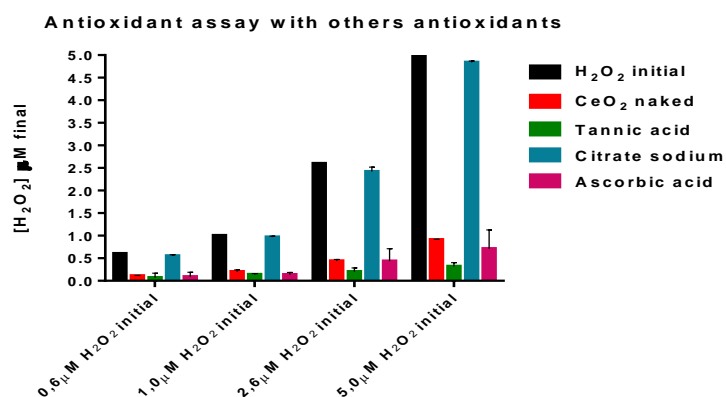
Figure 39: *Antioxidant assay of CeO$_2$ NPs compared with other antioxidants.*

5.3.7 INCUBATION CeO₂ NPs IN PBS MEDIA

Phosphate buffer saline (PBS) is a buffer mostly employed in biological and biochemical research, with osmolality and concentration of ions quiet similar to extracellular fluid. So, in this experiment, PBS is used as model of physiological media conditions instead of cell culture media because it is required no compounds (aminoacids, colorants or antibiotics) in order to avoid interferences. Hence, different types of CeO₂ NPs are incubated in PBS and their catalytic activity is measured at different times. It is viewed practically the same catalytic activity for all kind of CeO₂ NPs at initial times but differences start to be appreciated after 24 hours. These variations are derived from aggregation of the samples in physiological media with exception of CeO₂-BSA, the only capable of keeping their stability in those conditions. Effect of aggregation promotes reduction of catalytic property as it can be seen in figure 41. The same effect is checked in CeO₂ NPs with 7 days of incubation in PBS. Stabilization of samples is also studied by UV spectrophotometer viewing decrease of peak over time as consequence of aggregation in PBS conditions. Decrease of peak in the case of CeO₂-BSA is related with sedimentation (see figure 40).
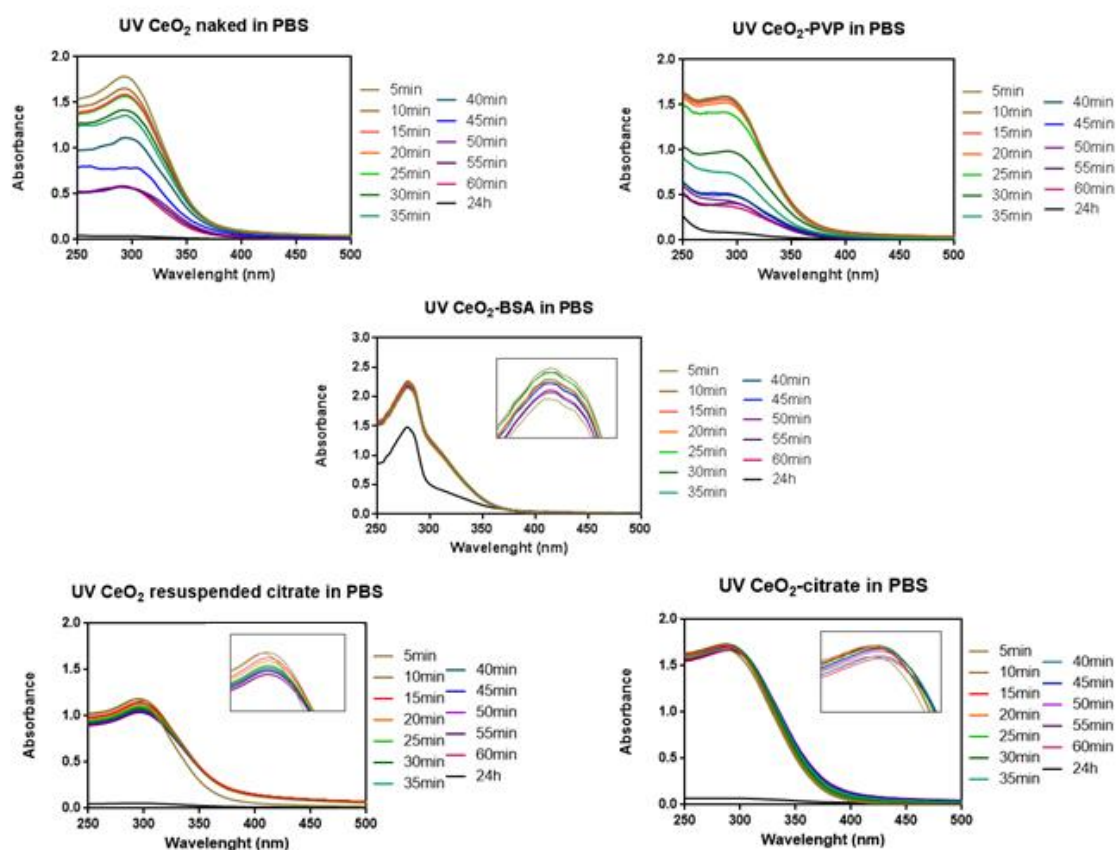
Figure 40: *UV evolution of different CeO₂ NPs incubated in PBS over time during 24 hours.*
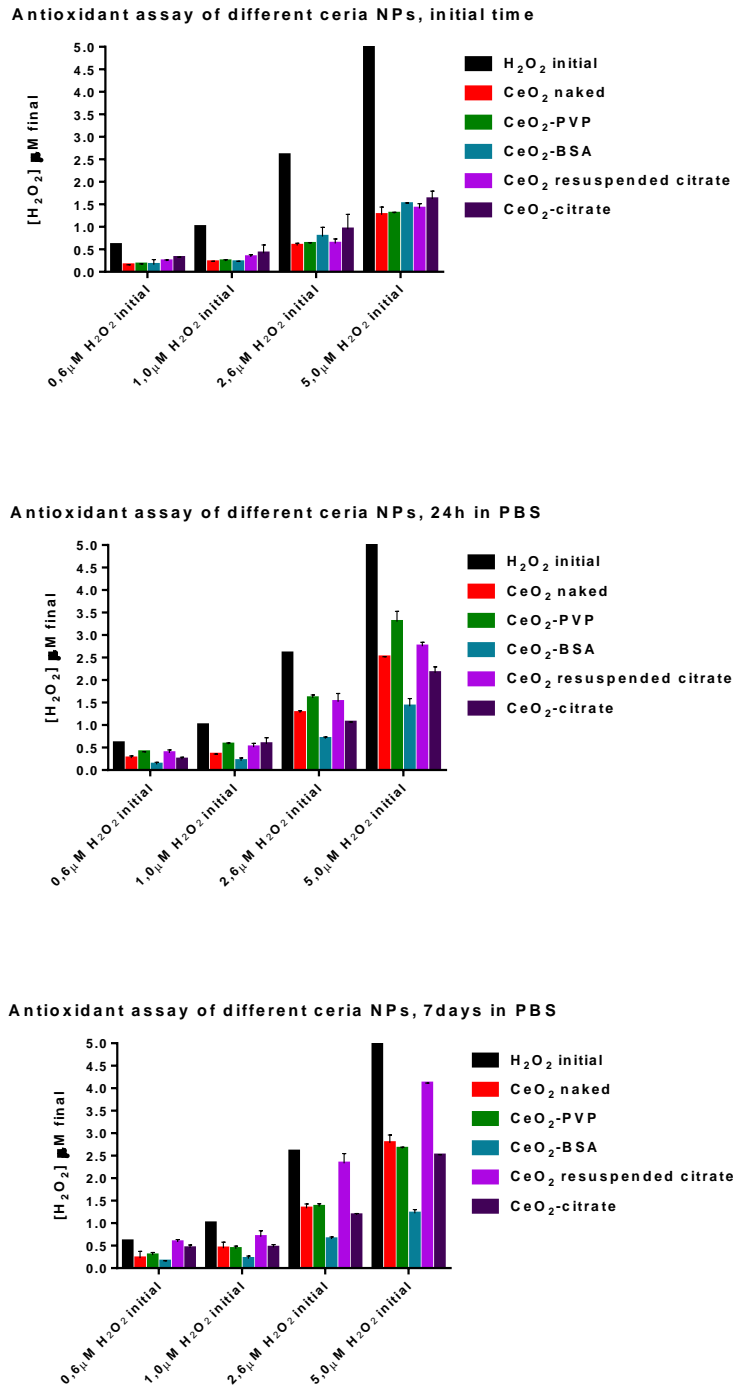
Figure 41: *Antioxidant assay of different CeO₂ NPs incubated in PBS at different times.*

5.4 DISCUSSION

It is important to evaluate catalytic capacity of synthesized CeO$_2$ NPs before being applied in cellular assays or in-vivo systems. In addition, it has been check good efficacy of Amplex Red technique as tool for this purpose. Amplex Red is a suitable method in order to measure antioxidant activity because it offers the next advantages:

- It is highly sensitive. This technique can detect H$_2$O$_2$ in the order of nanomolar.
- Amplex Red assay works in range of concentration of H$_2$O$_2$ similar to found in biological systems.
- As an enzyme is used in this experiment, conditions of physiological media (salinity and pH) are required in order to be functional. Therefore, every measure done is like measuring it in biological conditions.

All kind of cerium oxide nanoparticle synthesized in this thesis work is analyzed with positive results. It is viewed collection of good dispersion of CeO$_2$ NPs during synthesis offer great quality product for medical applications. In contrast, it is checked aggregation affects negatively to their catalytic properties but curiously aggregates still present high antioxidant activity. Indeed, if aggregated material is dispersed by sonication, they are still less effective than before. Moreover, it is also viewed a major activity of nanoceria in presence of high concentration of H$_2$O$_2$ while a minor activity is detected at low concentrations of H$_2$O$_2$. This fact shows the therapeutic effect of nanoceria in medicine, being more active in stress oxidative conditions and getting inactive in no presence of free radicals. Additionally, it is tested subsequent stabilization of CeO$_2$ NPs owing to surfactants such as PVP, citrate or biomolecules like BSA do not affect their initial characteristics. At the same time, it is viewed that use of PVP and citrate during synthesis do not altered antioxidant properties of final product.

Finally, it can be concluded that conjugation with biomolecules in CeO$_2$ NPs is mandatory if it is wished their subsequent application in biological systems in spite of being previously stabilized with surfactants because they present the best stability in biological media. Indeed, only surfactants are not good enough to protect any kind of nanoparticle in physiological conditions.

CHAPTER 6:

BIOLOGICAL RESULTS OF CeO$_2$ NANOPARTICLES

6.1 INTRODUCTION

Once it is checked good quality of CeO$_2$ NPs in this process of synthesis, this material is led to cell-lines. It is desired to see if previous antioxidant capacity analyzed is also detected in systems in-vivo. This task is done in collaboration with the *Ophthalmology Group in Vall d´Hebron Institut Recerca (VHIR)* with the aim of treating age-related macular disease (AMD). AMD is the main cause of blindness in elderly worldwide[89]. AMD can be classified in two forms: "dry" and "wet". The first is related with alteration in retinal photoreceptors and the second is related with degeneration of photoreceptors in retina with an abnormal growth of blood vessels[26]. This disease is a neurodegenerative pathology in which oxidative stress is involved. Due to the large amount of light crossing the eye, great production of ROS is done in comparison with the rest of tissues. But a major activity of antioxidant enzymes compensates this effect. When deregulation of these enzymes happened, then, ROS are overproduced and they damage the eye internally. Actually, there is no cure or treatment that returns vision lost. For that reason, properties of nanoceria offer an alternative to deal with this illness.

In addition, if CeO$_2$ NPs are utilized in systems in-vivo, toxicity assays are indispensable both cell and animals. Moreover, if animals are used, it will be interesting to make biodistribution experiment before start to deal them in order to know if nanomaterial persists in the area of interest.

Therefore, CeO$_2$ NPs will be incubated with ARPE-19 retinal cells in cell culture media DMEM supplemented with FBS for in-vitro assays and additionally, experiments in-vivo with mice will be done.

6.2 IN-VITRO EXPERIMENTS WITH CELLS

6.2.1 TOXICITY ASSAYS

It is important to know if cerium oxide nanoparticles synthesized by the methods explained in this thesis work can be toxic for cells. For that reason, MTT assay was done with retinal ARPE-19 cells. CeO$_2$ naked was chosen because of positive results shown in protein-corona studies in cell culture media. Therefore, it is viewed no toxicity as shown in figures 42. Method of work is described in section 8.10.1 of Annex.
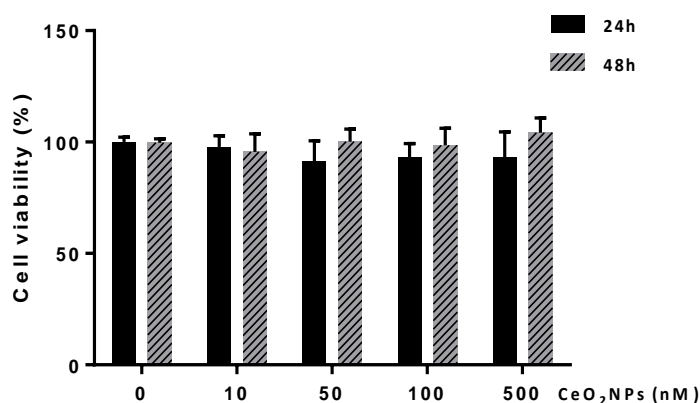
Figure 42: MTT toxicity assay of CeO$_2$ NPs with retinal cells ARPE-19.

Also it was done toxicity assay for CeO$_2$ naked with MCF-7 breast cancer cells owing to PrestoBlue assay indicating the same result, no toxicity of these nanomaterials in spite of using another cell line. Method of work is also described in point 8.10.2 of Annex.
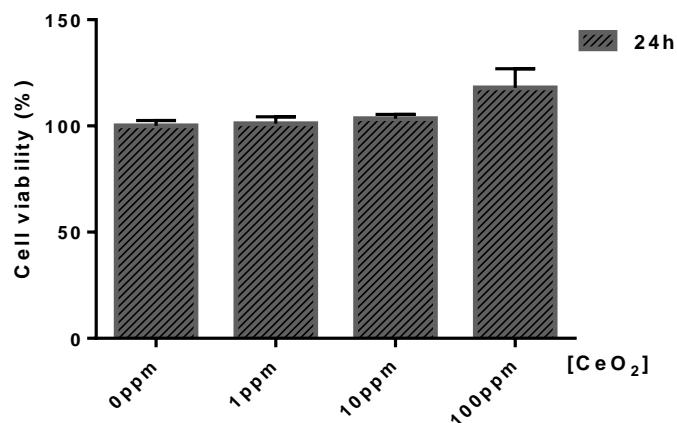
Figure 43: Prestoblue toxicity assay of CeO$_2$ NPs with MCF-7 cells at 24h.

6.2.2 ANTIOXIDANT ASSAYS

Firstly, it is necessary to know ideal conditions to generate oxidative stress to cells owing to H$_2$O$_2$ without producing too much cell death. Once those conditions are found, then stressed cells can be treated with CeO$_2$ NPs in order to check any improvement in cell proliferation and efficacy of nanoparticles. CeO$_2$ naked is chosen for these experiments due to good results offered during protein-corona studies. It is viewed incubation with 300µM H$_2$O$_2$ is enough to produce high concentrations of free radicals without decreasing viability cell (figure 44), although there are other options in order to produce ROS owing to different substances such as antimycin A or tBH. These molecules are capable of generate intracellular ROS and they will be also employed for antioxidant assays. Protocol of this experiment is described in section 8.11.1 of Annex.
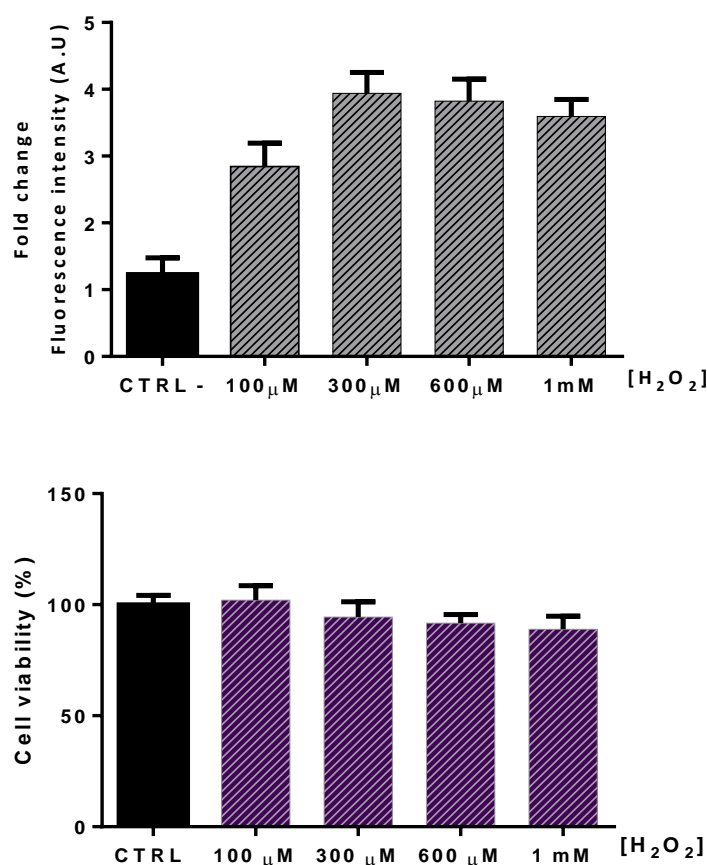
Figure 44: *In the top, DCF-DA assay in order to detect ROS generated by ARPE-19 cells at different concentrations of H$_2$O$_2$ during 1 hour. The highest fluorescence analyzed, the highest concentration of free radicals produced. On the bottom, MTT assay of ARPE-19 cells incubated at different concentrations of H$_2$O$_2$ during 1 hour in order to see cell viability in those oxidative stress conditions.*

After that, ARPE-19 cells are supplemented with CeO_2 NPs in those conditions. It is viewed promising results detecting decrease in ROS at cellular level owing to DCF-DA technique (explained in 8.11.1 point). This effect is viewed in all tests employing H_2O_2, antimycin A and tBH as causers of oxidative stress (Antimycin A and tBH produce intracellular ROS). Description of these experiments is located in 8.11.2 section.
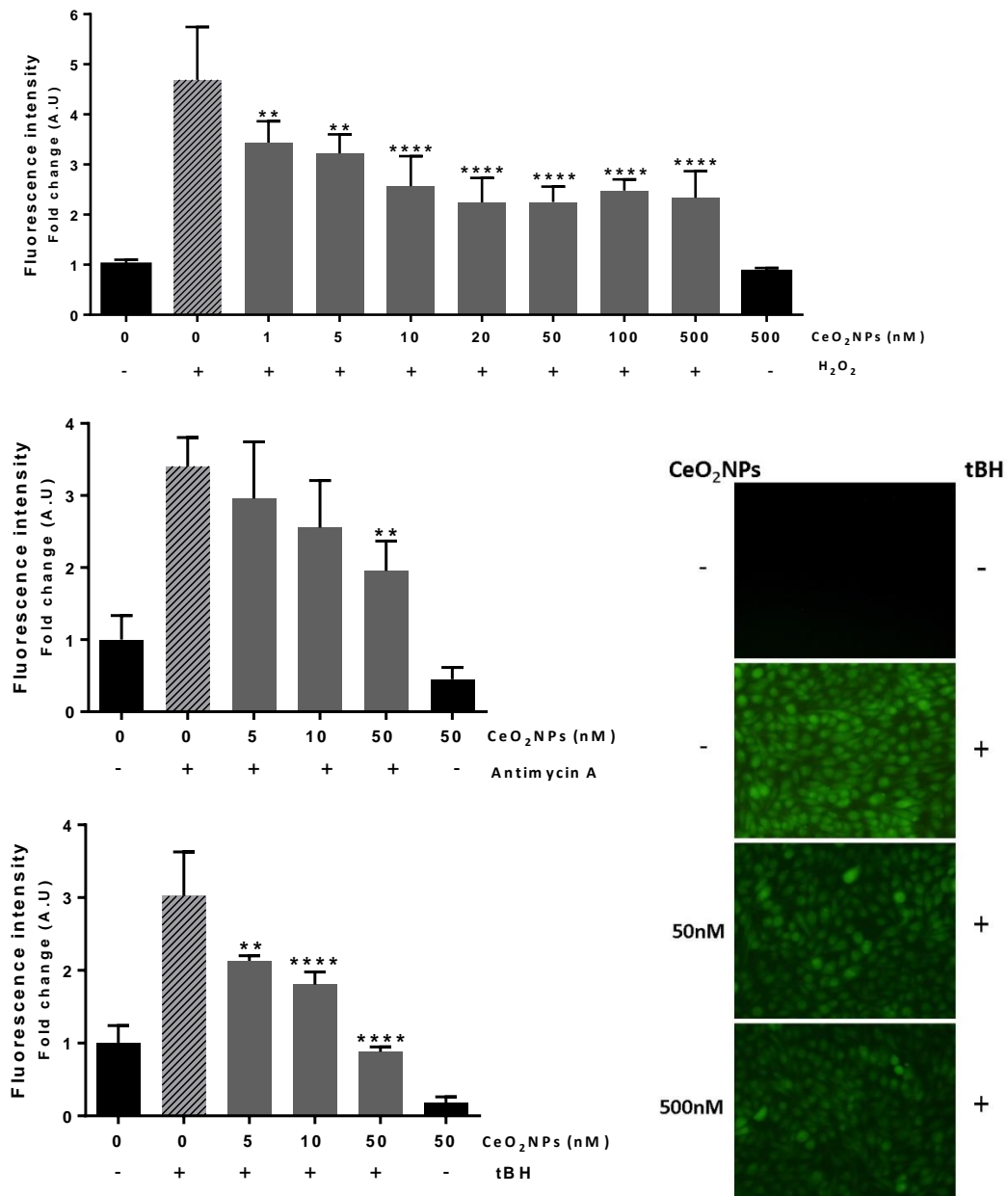
Figure 45: *In the top, DCF-DA assay in order to detect ROS generated by H_2O_2 in ARPE-19 cells supplemented with different concentrations of CeO_2 NPs. In the middle, DCF-DA assay of ROS generated by antimycin A in ARPE-19 cells supplemented with different concentrations of CeO_2 NPs On the bottom, DCF-DA assay of ROS generated by tBH in ARPE-19 cells supplemented with different concentrations of CeO_2 NPs. Each antioxidant assay is done by triplicate (**p<0.01; ****p<0.0001). In the left, there is visualization of fluorescence microscope when tBH is used at different concentrations of nanoceria.*

75

6.3 IN-VIVO EXPERIMENTS

When it is viewed positive results obtained in in-vitro assays, experiments with animals were the following step. Firstly, biodistribution of the eye was done in mice with the aim of finding out if CeO$_2$ NPs are retained inside the eye and, in case of positive results, in which area was more abundant. Liver and brain was also analyzed in order to check if cerium oxide nanoparticles can go to other organs once they are stablished in eye. It is highlighted no presence of toxic effects produced by CeO$_2$ NPs in mice during their application.

For this task, two methods of administration were done: intraocular injection and with eyewash (topical treatment). Therefore, sample which will be injected requires conjugation with mouse albumin while conjugation in sample for eyewash is not necessary. This fact is because most of eye drops have hydroxypropyl methylcellulose (HPMC), a compound responsible for viscosity of material which can behave as surfactant for nanoparticles, similar to dextrane. Consequently, previous analysis of CeO$_2$ NPs is done in order to choose proper sample for biodistribution experiment. Finally, it can be concluding CeO$_2$-resuspended in citrate is apparently the most suitable because of their better antioxidant behavior in those conditions (figure 46).
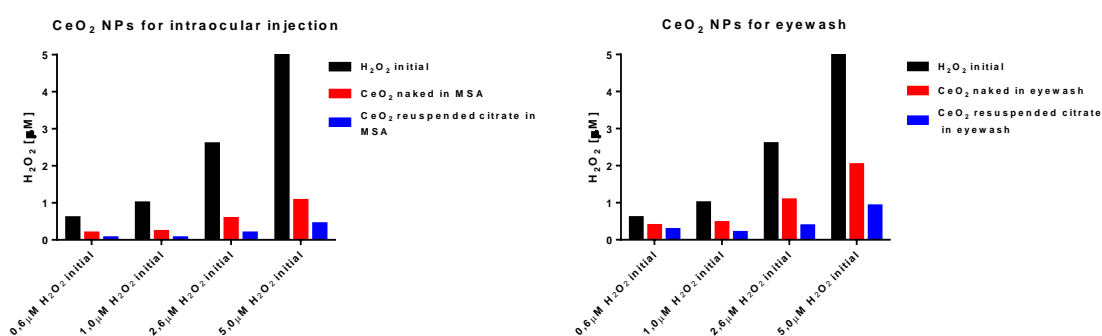
Figure 46: *Antioxidant assay with Amplex Red in which is detected a major activity of CeO$_2$ resuspended citrate for intraocular sample and eyewash.*

Then, samples of CeO$_2$ NPs 2mg/ml were administrated both via topical and via intraocular to mice: 2µl by injection and 5µl by topical treatment for each eye. After 24 hours animals were euthanized and biological samples were extracted. Liver and brain were aliquoted and each eye was divided in different parts: anterior pole, retina, lens, posterior pole and optic nerve. Process of digestion of biological samples was prepared in order to quantify concentration of Ce by ICP-MS (inductively coupled plasma mass spectroscopy). This analysis was done by external service and digestion procedure is explained in section 8.12 of Annex. Results obtained are shown in figure 47 and it could be concluded that there is a higher concentration of cerium by intraocular administration than topical treatment, with exception of optic nerve. Liver and brain hardly had shown presence of cerium in their tissues. However, the differences of concentration between topical and intraocular administration were not so large. This effect was quite interesting because it means cerium can be administrated owing to eyewash, much comfortable and easier to deal than injection.
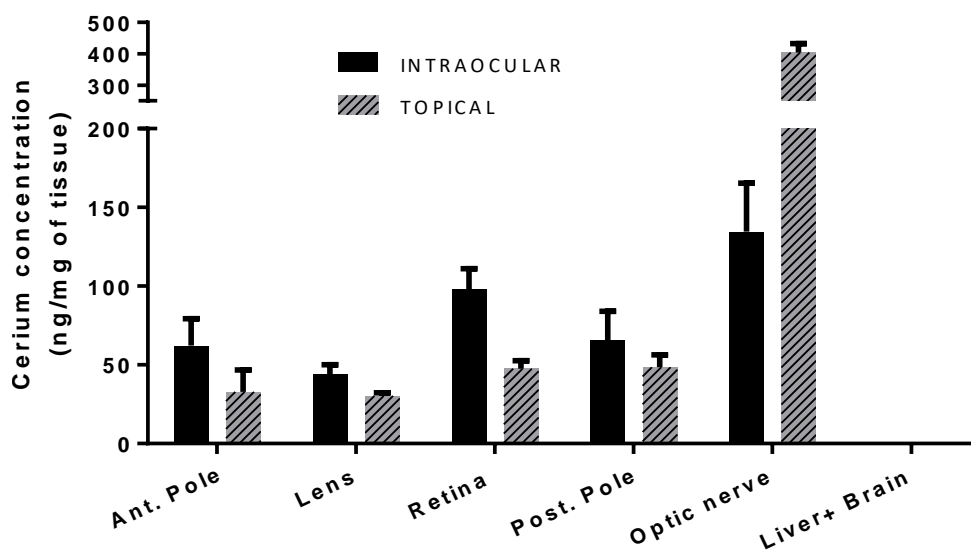
Figure 47: *Initial results of biodistribution both via intraocular and topical of cerium concentration in different tissues.*

Consequently, a second biodistribution is done but only employing eyewash containing nanoceria. In this experiment, it is tried to check if there is accumulation of CeO$_2$ NPs in eye. For that, mice are treated with that eyewash each day during a week and euthanized at 7 days. There are also mice with only one administration of eye drop in the first day as control (they are also sacrificed after 7 days). Results are shown in figure 48. Process and analysis of biological samples are treated in the same way of previous experiment. It is confirmed good efficacy of eye drops in order to apply nanoceria in the eye but it is viewed no accumulation of CeO$_2$ NPs in the eye during treatment for 7 days. Indeed, a decrease of cerium concentration is detected over time, indicating elimination of this nanomaterial. Probably, it is removed through membrane of cornea.
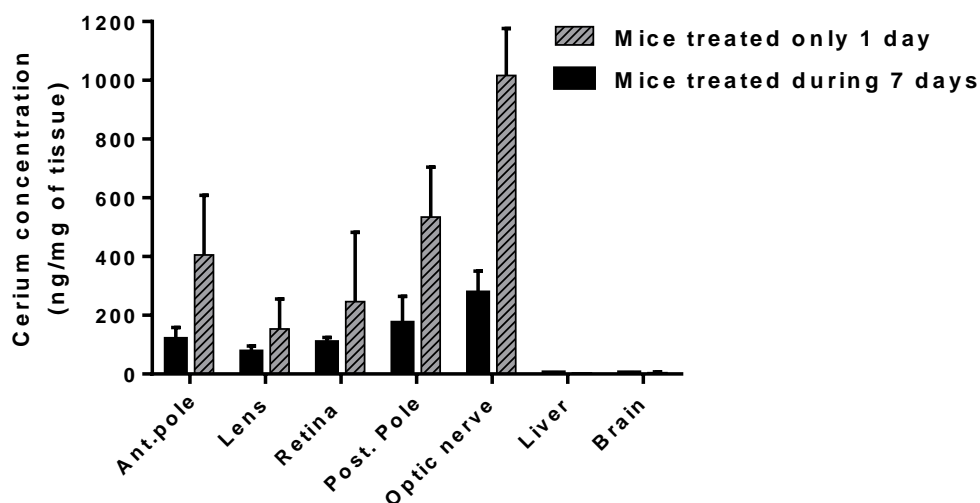
Figure 48: *Results of biodistribution experiment of CeO$_2$ NPs in different tissues after via topical treatment during 7 days.*

Currently, these CeO$_2$ NPs are being applied in DKOrd8 mouse (animal model of age-related macular degeneration) and biological studies are still working with positive expectations.

6.4 DISCUSSION

Application of CeO$_2$ NPs made by this process of synthesis in biological systems has offered good and promising results because not only there is no toxicity related with this kind of synthesized nanoceria but their antioxidant properties have been seen in cellular experiments. It is detected reduction of free radicals by DCF-DA assay in cells incubated with CeO$_2$ NPs owing to application of different substances generators of ROS such as antimycin A, tBH or even H$_2$O$_2$.

At the same time, in-vivo experiments are also done. Inoculation of CeO$_2$ NPs in eye is made both via intraocular injection and topical treatment. Results of biodistribution show better retention of nanoceria via injection than via topical but the difference of concentrations between two methods is not so vast. Indeed, it is really surprising detect cerium inside the eye owing to administration of eye drops. A second analysis of biodistribution confirms this fact. More biological experiments such as genetic studies or evaluation of VEGF levels (protein related with angiogenesis) as consequence of CeO$_2$ NPs treatment are still in process.

Consequently, it can conclude that CeO$_2$ NPs offer positive effects in biological systems both in cell-lines and mice. Besides, it is really interesting the possibility to apply nanoceria owing to eyewash because it is much more comfortable and easier this type of treatment than the use of needles in injections although their effect is minor.

CHAPTER 7:

CONCLUSIONS

7.1 CONCLUSIONS

In general, metal oxide nanoparticles have interesting properties which applied in medicine can improve analysis, detection and some treatments, where CeO_2 NPs have been the most promising in the last years. It is important to emphasize not all nanoparticles synthesized by different processes are equal so, evaluate synthesis method and study characteristics of prepared product should be of great importance. According to desired destination of nanoparticle, type of synthesis has to be assessed and their obtained product should be revised. Aggregation, polydispersity, cell viability and ROS generation of synthesized cerium oxide nanoparticle are some parameters to control before their subsequent applications for in-vivo systems. In fact, conditions of nanoparticles intended for medical applications must be more restrictive. Aggregation is recommended to avoid in any clinical application and apparently, monodisperse homogeneous soluble samples would be more qualified for these cases.

For medical applications, aqueous synthesis seems to be more suitable in comparison with non-aqueous synthesis due to obliged phase change. In this necessary step, water normally deteriorates nanoparticles synthesized from this route by dissolution, modifying their shape and in the most cases produce aggregation. Besides, the possibility of having traces of organic compounds can cause a major toxicity in nanoparticles elaborated by non-aqueous synthesis. Indeed, in this thesis work it has been viewed that method of alkali precipitation in aqueous phase in soft conditions (room temperature and non-toxic reactants) has probed being excellent for this purpose. In fact, studying the reaction of synthesis have allow understanding better the formation of nanoceria, comprehend evolution of CeO_2 NPs during reaction and consequently, a correct optimization in order to synthesize monodispersed non-aggregated suitable nanomaterial for medical applications.

At the same time, synthesis of cerium oxide nanoparticles with PVP and citrate as surfactants has also been made in this thesis, showing good results from these substances avoiding aggregation and obtaining monodispersed solutions. Particularly, the case of citrate is quite peculiar because their use allows obtaining CeO_2 NPs

smaller than usual in aqueous phase, around 3nm in monodisperse distribution without employing hard conditions such as high temperature, high pressures or toxic compounds. However, more cellular and in-vivo studies should do with this new nanomaterial in order to know their behavior in biological conditions.

On the other hand, a better knowledge of interaction of cerium oxide nanoparticles with biological materials such as proteins or cells will help to understand how these nanomaterials work in physiological media. CeO_2 NPs interact with living organisms through protein-corona structure so, study of formation nanoparticle-protein-corona can be crucial for understanding their interactions. In this thesis it has been tested that conjugation of any kind of nanoceria with albumin can be done for systems in-vivo, except for CeO_2-PVP whose surfactant evades all type of external interaction. Additionally, studies of formation of protein-corona probe effectivity of CeO_2 NPs with positive surface charge in cell culture media, keeping their catalytic capacity in that media without being altered by aggregation in cellular assays thanks to formation of hard-protein corona.

Moreover, in this thesis work it is checked catalytic capacity of different CeO_2 NPs synthesized by Amplex Red technique. Optimized protocol has allowed detecting antioxidant activity both qualitative and quantitatively in physiological media conditions, showing good efficacy of this technique in order to measure catalysis of nanoceria without employing cells. It is remarkable viewed aggregated CeO_2 NPs still present antioxidant activity in comparison with dispersed nanomaterial. Probably because of this fact it is reported in literature efficacy of nanoceria synthesized in any way as antioxidant catalyzer but without considering their state in solution. Cerium oxide nanoparticles aggregated are also functional but they cannot be applied in medical application due to negative consequences involved by the own phenomenon of aggregation which can produce in in-vivo systems (immune response, obstruction in some blood vessel). In addition, in this thesis work it is also viewed that only CeO_2 NPs conjugated with albumin are capable of resisting physiological conditions without being aggregated and keeping their initial properties, concluding that any kind of nanoceria which is going to be inoculated inside the body has to be previously bioconjugated.

Also, CeO$_2$ NPs synthesized are led both cell lines and animals, showing no toxicity in any case. This fact is probably because of good dispersion presented of these nanomaterials as consequence of their process of synthesis. Besides, in vitro-cells experiments clearly show antioxidant capacity of nanoceria, reducing free radicals generated (also ROS intracellular) measured by DCF-DA technique. This ability of CeO$_2$ NPs to scavenge free radicals intracellularly is quite attractive because most neurodegenerative diseases derived from oxidative stress are related with this effect. Interesting properties of nanoceria made by this method of synthesis has been tested in cell culture media successfully.

In addition, CeO$_2$ NPs synthesized in this thesis work have been supplied in mice with the aim of dealing and reduce symptoms of AMD disease. Administration of cerium oxide nanoparticles in eyes of animals is made by two different methods: one by intraocular injection and the other by topical treatment with eyewash. Biodistribution assays show presence of nanoceria in both cases, with slight increase in the case of intraocular injection. However, it is remarkable the fact that owing to eyewash administration CeO$_2$ NPs can be internalized into eyes. This effect is quite interesting because in this way treatment is much more comfortable and easier than injection although dose is minor. Currently, effect of CeO$_2$ NPs application in knockout mouse model of AMD is still doing. More biological studies such as genetic analysis or detection of determined proteins like VEGF which influence in evolution of AMD are being analyzed in this moment. First impressions are positive because it is detected a decrease of angiogenic activity, one indicator of this disease.

In conclusion, in this work it has been possible synthesized good monodispersed CeO$_2$ NPs without using hard conditions or toxic reactants, with the catalytic properties desired for medicine, being functional and non-toxic in biological conditions and, in addition, presenting positive expectations in one particular case of disease derived from oxidative stress. Consequently, it is expected nanoceria prepared by method of synthesis described in this thesis can be perfectly applied in other treatments of different illnesses generated as consequence of oxidative stress.

ANNEX: SYNTHESES AND METHODS

8.1 UV-VISIBLE EQUIPMENT

The *Cary 60* of Agilent is used as spectrophotometer in order to measure Ultraviolet spectrums of the samples. Polystyrene cuvettes of 1,5ml are also used. All samples measured and represented in this thesis work by this technique are diluted 1:20 with miliQ water.

8.2 DLS EQUIPMENT

All measurements of DLS is analyzed by Zetasizer Nano-ZS (from Malvern instruments) equipment. Polystyrene cuvettes of 1,5ml are used to measure hydrodynamic sizes of the samples doing dilution 1:20 with miliQ water. Zeta potential measures are done with specific zeta potential cuvettes (from Malvern instruments) without diluting samples. Each sample is measured by triplicate and values shown in tables are an average of them, obtained by Number distribution. Graphic representations are obtained by Intensity distribution.

8.3 XYLENOL-ORANGE ASSAY

This procedure is based on Tonosaki[51] work. Hence, it is proceed in the following way. In each vial, is mixed 3ml of acetate buffer pH 6.2 with 0,7ml of xylenol-orange 1mM (xylenol orange disodium salt from Sigma Aldrich). Then, different volumes of solution Ce^{3+} are added in different vials with the aim of having final concentrations of 0,2,4,6 and 8µg/ml (more concentration implies saturation of signal) and after that, solution are made up with water to 5ml. An aliquot of 1ml of each vial/sample is measured by UV spectrophotometer at 576nm. Thus, a calibration curve of Ce^{3+} is done and subsequently, samples have to be diluted in that range to be measured.
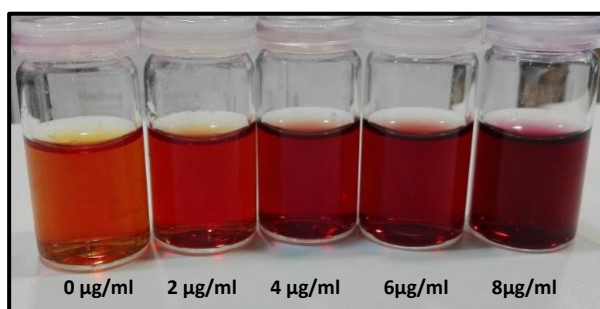
Figure 49: *Visualization of xylenol-orange solutions with different concentrations of Ce^{3+}.*

8.4 SYNTHESIS CeO$_2$ NAKED

Solution of 37,5mM cerium (III) nitrate hexahydrate (Sigma Aldrich) in 50mL and solution of 44mM TMAOH (Sigma Aldrich) in 50mL are mixed. The basic solution is added above the solution of cerium under vigorous stirring at room temperature. After 30 minutes of reaction, solution is centrifuged at 20000g for 50min and red pellet is resuspended in miliQ water. Finally, after 48 hours, when solution becomes colorless, CeO$_2$ NPs are ready and good dispersed. CeO$_2$ NPs are obtained at 1mg/ml.
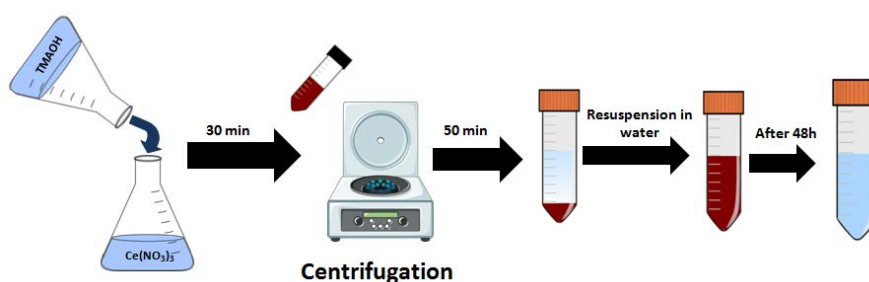
Figure 50: *Schematic representation of synthesis CeO$_2$ naked.*

8.5 SYNTHESIS CeO$_2$-PVP

In 97.8ml miliQ water is dissolved 0.5g of PVP (10KDa Sigma Aldrich) with stirring, having 0.5mM final concentration. Then, 0.43422g of cerium (III) nitrate hexahydrate is added, having 10mM in solution. Later, 2.2ml TMAOH 1M (Sigma Aldrich) is added, having 22mM in solution at room temperature. After that, it is expected 24h until reaction finishes, producing final concentration of 1mg/ml CeO$_2$ NPs.

It is viewed no surface charge in this type of sample. That is because molecules of PVP are attached on the nanoparticle surface, avoiding all kind of interaction, including among them.

	Potential zeta	**Conductivity**
CeO$_2$-PVP	0.347mV	3.88mS/cm

Table 11: *Values of potential zeta and their conductivity of CeO$_2$-PVP samples.*

8.6 SYNTHESIS CeO₂-CITRATE

40mM cerium (III) nitrate hexahydrate (Sigma Aldrich) are prepared in 25ml miliQ water. Then, 25ml of 40mM sodium citrate tribasic (Sigma Aldrich) is added on solution of cerium. After 5 minutes stirring, 50ml solution 60mM TMAOH (Sigma Aldrich) is added with vigorous stirring on the mix (final concentrations: 10mM Ce^{3+}, 10mM citrate and 30mM OH^-). Then, soft stirring is kept until 24 hours at room temperature, when reaction is finished. In this way, 1,4mg/ml CeO_2 NPs are obtained.

This kind of CeO_2 NPs has negative charge as consequence of presence of citrate molecules in their surface, causing electrostatic repulsion and finally stability.

	Potential zeta	Conductivity
CeO₂-citrate	-36.8mV	8.84mS/cm

Table 12: *Values of potential zeta and their conductivity of CeO₂-citrate samples.*

8.7 SYNTHESIS CeO₂-BSA

A quantity of Bovine Serum Albumin (BSA, Sigma Aldrich) is dissolved in Phosphate Buffer Saline 1x (20% volume) to obtain a final concentration of 35mg/ml. Then, 80% volume CeO_2 naked NPs (1mg/ml) is added drop by drop on protein solution with soft stirring during 1 hour. After that, stirring is stopped and solution is kept in fridge at 4ºC for 24 hours. Finally, hard protein-corona structure is done and solution CeO_2-BSA 0,8mg/ml is ready for their utilization.
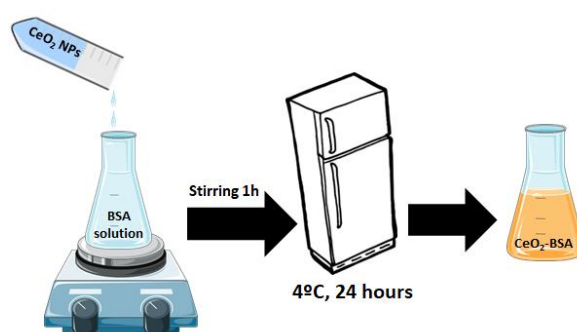
Figure 51: *Schematic representation of synthesis CeO₂-BSA.*

8.8 METHOD OF WORK IN PROTEIN-CORONA STUDIES

To study formation of protein-corona, method of work described by Casals et al[72] is used. 1ml aliquot of any kind of media supplemented with protein and corresponding CeO_2 NPs is purified by centrifugation. This step is tremendously important and it has to be optimized earlier. Soft conditions of centrifugation do not allow obtaining pellet to resuspend, doing a bad purification and hard conditions of centrifugation tends to form aggregated samples difficult to disperse. Each sample has their purification conditions in each different media. After process of centrifugation, supernatant is removed and pellet obtained (CeO_2 recovered with protein) is resuspended with phosphate buffer 10mM. All samples have to be resuspended in the same buffer in order to have same pH and salinity conditions. From this way, all measures done can be compared.

	PB+BSA	PB+SFB	DMEM+SFB	DMEM+BSA
CeO_2 naked	15000g; 20min	14000g; 20min	15000g; 20min	8000g; 15min
CeO_2 resuspended citrate	12500g; 20min	10000g; 15min	12500g; 15min	5000g; 15min
CeO_2-citrate	10000g; 30min*	14500g; 20min	10000g; 15min	3000g; 5min

Table 13: *Conditions of purification of different CeO_2 samples in different media.* Due to small size of nanoparticle in those conditions, centrifugal filter 3KDa is used for this particular case and manufacturer recommendations are employed.*
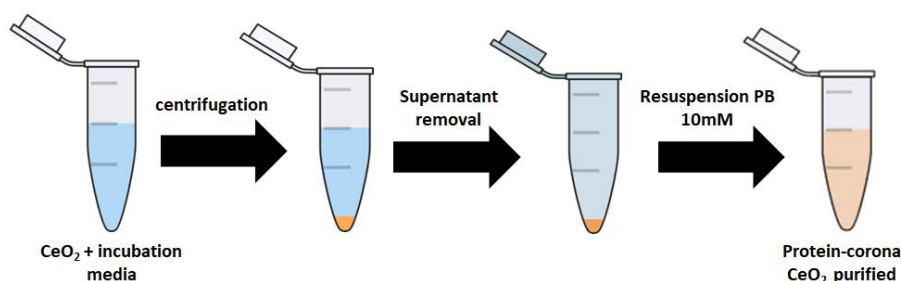
Figure 52: *Process of work in order to study protein-corona formation. 1ml CeO_2 once incubated in any kind of media supplemented with protein is purified by centrifugation. Later, supernatant is removed and pellet is resuspended in buffer PB 10mM.*

8.9 AMPLEX RED PROTOCOL

This work is based on Invitrogen protocol with some modifications[88]. Amplex Red signal will be measured in solutions of 5µM, 2.6µM, 1µM, 0.6µM H_2O_2 with and without CeO_2 NPs in dark microplate. The measures without NPs are employed to do a calibration curve of H_2O_2 and the measures with CeO_2 are used to calculate concentration of H_2O_2 free (no reacted). Thus, concentration of H_2O_2 reacted by CeO_2 NPs is calculated by difference between initial concentration (calibration curve) and free concentration of H_2O_2.

Combination of reactants is done in 96-wells dark microplates in a maximum volume of 100µl. Controls are considered in the assay (view table 14). First, PBS is added and later stock H_2O_2 is mixed in wells. Once it is mixed, CeO_2 NPs media (control solution of citrate, PVP, BSA, for instance) is added in case which is necessary and then, CeO_2 NPs at 1mg/ml are added, subsequently it is waited 15 minutes and addition of Amplex Red stock in darkness is done. After this step, rapidly stock HRP is added. After complete addition of all reactants, microplate is covered with aluminium foil and kept in dark conditions during 30 minutes. Then, fluorescence is measured at 530/25nm excitation and 590/20nm emission.

Results obtained are analyzed and represented in chapter 5 using GraphPad software.

 Preparation of reactants and elaboration of method are explained below.

-Amplex Red 375µM: 5mg Ampliflu Red (Sigma Aldrich) is completely dissolved in 1ml of dimethyl sulfoxide (DMSO, Sigma Aldrich). Then, 20µl of this solution is mixed with 980µl PBS 1x. This new solution will be Stock.

-H_2O_2 20µM: 41µl hydrogen peroxide (Sigma Aldrich, 30% wt) is diluted in 20ml water making solution 20mM. Then, this solution is diluted 1:1000 to obtain new stock 20µM.

-HRP 15U/ml: 1mg horseradish peroxidase (Sigma Aldrich, 150U/mg) is dissolved in 1ml PBS 1x. Then, this solution is diluted 1:10 with PBS 1x to obtain stock 15U/ml.

H$_2$O$_2$ calibration	PBS 1x	Stock H$_2$O$_2$	Media CeO$_2$ NPs (BSA, PVP)	CeO$_2$ NPs (1mg/ml)	Stock Amplex Red	Stock HRP
0µM	60µl	-	10µl	-	20µl	10µl
0µM with NPs	60µl	-	-	10µl	20µl	10µl
5µM	35µl	25µl	10µl	-	20µl	10µl
5µM with NPs	35µl	25µl	-	10µl	20µl	10µl
2.6µM	47µl	13µl	10µl	-	20µl	10µl
2.6µM with NPs	47µl	13µl	-	10µl	20µl	10µl
1µM	55µl	5µl	10µl	-	20µl	10µl
1µM with NPs	55µl	5µl	-	10µl	20µl	10µl
0.6µM	57µl	3µl	10µl	-	20µl	10µl
0.6µM with NPs	57µl	3µl	-	10µl	20µl	10µl

Table 14: *Combination of reactants mixed in 96-wells microplate for each sample. Each sample is measured by duplicate in the same microplate.*

8.10 TOXICITY ASSAYS IN CELLULAR LINES

8.10.1 MTT EXPERIMENT

MTT is a colorimetric assay for assessing cell metabolic activity. Enzymes of metabolism are able to react with MTT compound in insoluble formazan crystals, which have purple colour easily detectable for spectrophotometer. Intensity of signal is related with cellular viability. So, procedure of work is done in the following manner:

First, in 24-well plate, ARPE-19 cells at 80000cell/ml are seeded in 500µl of cell culture media (DMEM supplemented with FBS and ampicillin) and incubated at 37ºC for 24 hours. In the next day, medium is removed and cells are washed with PBS 1x. Then, new cell culture media supplemented with corresponding concentrations of CeO$_2$ naked NPs is supplied to ARPE-19 cells and it is incubated again at 37ºC during 24 or 48 hours (of course there is also cells incubated with medium without CeO$_2$ NPs which will act as control). After that, 100µl of MTT (Sigma Aldrich) solution is added in each well and it is incubated during 4 hours at 37ºC. Subsequently, cell culture media is eliminated and 300µl of DMSO is added. In these conditions, formazan crystals are formed so, they are dissolved by pipetting and reading is proceed in spectrophotometer at 590nm. Results obtained are represented by GraphPad.

8.10.2 PRESTOBLUE EXPERIMENT

Prestoblue is a reagent which is reduced to a fluorescence compound by components belonged to cellular respiration. So, signal analyzed is related with mitochondrial activity and, thus, with cellular viability. Indeed, prestoblue is more sensitive than MTT[90]. The procedure of work is the following way:

First, MCF-7 breast cancer cells which were previously incubated in cell culture media (MEM supplemented with FBS) are transferred to wells at 5000cell/ml and they are incubated 24 hours at 37ºC. After that incubation, volume of CeO_2 naked NPs is added in that wells in order to have desired concentrations in the assay and it is also incubated again during 24 hours at 37ºC. After that time, addition of 10µl prestoblue (Termofisher) reagent in each well is done, it is waited 2 hours and then, samples are measured by fluorimeter, reading fluorescence at 535/25nm excitation and 590/10nm emission. Results obtained are represented by GraphPad software.

8.11 ANTIOXIDANT ASSAYS IN CELLULAR LINES

8.11.1 CONDITIONS FOR GENERATION OF OXIDATIVE STRESS: DCF-DA PROBE

This experiment is done in order to evaluate the levels of intracellular ROS after the induction of oxidative stress with H_2O_2 in ARPE-19 cells. Conditions for generation of oxidative stress are analyzed by DCF-DA probe. In those same conditions MTT assay is also done with the aim of detecting cell viability (this technique has already explained previously). So, to optimize concentration required of H_2O_2 in order to generate enough ROS to alter cells but without killing them is done in the following way:

First, in 24-well plate, ARPE-19 cells at 50000cell/ml are seeded in 500µl of cell culture media (DMEM supplemented with FBS and ampicillin) and incubated at 37ºC for 24 hours. The next day, cell culture media is changed and the following day, medium is removed, it is washed with PBS 1x and then, cell culture media with different concentrations of H_2O_2 are added to cells and it is incubated for 1 hour.

After that time, new medium is also eliminated, it is washed again with PBS 1x and 500µl solution 10µM of DCF-DA[*] in medium is added and incubated at 37ºC for 30 minutes. Then, another washed with PBS 1x is done and 200µl cell lysis buffer[**] is added and incubated during 10-15 minutes with shacking at 4ºC. Subsequently, 50µl of each lysate obtained is transferred to 96-wells black microplate and it is read immediately by fluorimeter at 485/20nm excitation and 528/20nm emission (Fluorescence values will be corrected with protein content and results will be expressed as percentage to controls (untreated cells)). Results obtained are represented by GraphPad software.

[*] It is dissolved 1mg DCF-DA (Sigma Aldrich) in 400µl of DMSO forming solution 5mM DCF-DA. Then, 20µl of previous solution is added in 10ml of cell culture media. Thus, 10µM DCF-DA is prepared.

[**] Cell lysis buffer is composed by 20mM Tris-HCL; 150mM NaCl; 1mM EDTA and 1 % Triton, all dissolved in miliQ water.

8.11.2 EFFECT OF CeO₂ NPs IN OXIDATIVE STRESS CONDITIONS

Procedure of these experiments is quiet similar to explained before, but in this case concentration of causers of oxidative stress are known and incubation with nanoceria is done.

First, in 24-well plate, ARPE-19 cells at 50000cell/ml are seeded in 500µl of cell culture media (DMEM supplemented with FBS and ampicillin) and incubated at 37ºC for 36 hours. The following day cell culture media is removed, it is washed with PBS 1x and new cell culture media supplemented with different concentrations of CeO_2 naked NPs is supplied to cells and it is incubated at 37ºC for 24 hours. The next day medium is eliminated, it is washed with PBS 1x and now it is incubated at 37ºC during 1 hour with cell culture media supplemented with 300µM H_2O_2 or 50µM antimycin A or 250µM tBH in order to generate free radicals. After that time, medium is eliminated, it is washed with PBS 1x and 500µl solution 10µM of DCF-DA in medium is added and

incubated at 37ºC for 30 minutes. Then, DCF-DA solution is removed, it is washed again with PBS 1x and 200µl cell lysis buffer is added and incubated during 10-15 minutes with shacking at 4ºC. Subsequently, 50µl of each lysate obtained is transferred to 96-well black microplate and it is read immediately by fluorimeter at 485/20nm excitation and 528/20nm emission. Results obtained are represented by GraphPad software.

8.12 DIGESTION OF CeO$_2$ IN BIOLOGICAL SAMPLES FOR ICP-MS ANALYSIS

Once biological samples are extracted, they have to suffer process of digestion in order to be analyzed by ICP-MS. ICP-MS is a precise technique with high sensitivity which is able to detect concentration of analyte in ppb. CeO$_2$ NPs present in samples needs to be ionized in order to be measured. For that purpose, samples are subjected to strong acidic and oxidant conditions.

In first place, samples are weighted and transferred to 12ml vials. Then, 1ml of piranha solution (H$_2$SO$_4$/ H$_2$O$_2$ 3:1, reactants from Sigma Aldrich) is added on the biological samples. The next step consists in heating solution by microwaves under fume hood because of vapors generated. So, vial is closed with septum-cap crossed by crystal tube in order to let fumes to go and they do not make so much pressure inside vials. Later, several cycles of heating at different powers are done in the following way:

-3 cycles of 1 minute at 180W. After each cycle, door of microwave is opened 30 seconds in order to ventilate microwaves. Initially, low power is used due to formation of foam by denatured proteins.

-3 cycles of 1 minute at 250W. After each cycle, door of microwave is opened 30 seconds in order to ventilate microwaves. Once proteins are degraded, power is increased.

-3 cycles of 1 minute at 350W. After each cycle, door of microwave is opened 30 seconds in order to ventilate microwaves. Power is increased to dissolve biological samples.

-3 cycles of 1 minute at 550W. After each cycle, door of microwave is opened 30 seconds in order to ventilate microwaves. Power is also increased to make sure everything is dissolved.

After heating treatment, vials are cooled and 1ml of aqua regia (HCl/HNO$_3$ 3:1, reactants from Sigma Aldrich) is added on the digested samples under fume hood and it is waited at least 2 days before doing ICP-MS analysis.

Then, 10ml of solution 5% acid is done from volume of digestion (which is 100% acid) and this is analyzed by ICP-MS technique. Results obtained are represented by GraphPad software.

REFERENCES

1.   Andreescu, S., Njagi, J., Ispas, C. & Ravalli, M. T. JEM Spotlight: Applications of advanced nanomaterials for environmental monitoring. *Journal of environmental monitoring : JEM* **11,** 27–40 (2009).

2.   Silvana Andreescu, Maryna Ornatska, Joseph S. Erlichman, A. E. and J. C. L. & Abstract. *Fine particles in medicine and pharmacy*. *Fine Particles in Medicine and Pharmacy* (2011). doi:10.1007/978-1-4614-0379-1

3.   Franke, M. E., Koplin, T. J. & Simon, U. Metal and metal oxide nanoparticles in chemiresistors: Does the nanoscale matter? *Small* **2,** 36–50 (2006).

4.   Cao, S. *et al.* Size- and shape-dependent catalytic performances of oxidation and reduction reactions on nanocatalysts. *Chem. Soc. Rev.* **100,** 201–215 (2016).

5.   Gupta, A. K. & Gupta, M. Synthesis and surface engineering of iron oxide nanoparticles for biomedical applications. *Biomaterials* **26,** 3995–4021 (2005).

6.   Shim, K., Abdellatif, M., Choi, E. & Kim, D. Nanostructured ZnO films on stainless steel are highly safe and effective for antimicrobial applications. *Appl. Microbiol. Biotechnol.* (2017). doi:10.1007/s00253-017-8099-6

7.   Esparza-González, S. C. *et al.* Effects of different surface modifying agents on the cytotoxic and antimicrobial properties of ZnO nanoparticles. *Toxicol. Vitr.* **37,** 134–141 (2016).

8.   Hirst, S. M. *et al.* Anti-inflammatory properties of cerium oxide nanoparticles. *Small* **5,** 2848–2856 (2009).

9.   Slowing, I. I., Trewyn, B. G., Giri, S. & Lin, V. S.-Y. Mesoporous Silica Nanoparticles for Drug Delivery and Biosensing Applications. *Adv. Funct. Mater* **17,** 1225–1236 (2007).

10.   Wason, M. S. & Zhao, J. Cerium oxide nanoparticles: Potential applications for cancer and other diseases. *Am. J. Transl. Res.* **5,** 126–131 (2013).

11.   Laurent, S., Bridot, J.-L., Elst, L. Vander & Muller, R. N. Magnetic iron oxide nanoparticles for biomedical applications. *Future Med. Chem.* **2,** 427–49 (2010).

12.   Laurent, S., Dutz, S., Häfeli, U. O. & Mahmoudi, M. Magnetic fluid hyperthermia: Focus on superparamagnetic iron oxide nanoparticles. *Adv. Colloid Interface Sci.* **166,** 8–23 (2011).

13.   Schwenk, M. H. Ferumoxytol: a new intravenous iron preparation for the treatment of iron deficiency anemia in patients with chronic kidney disease. *Pharmacotherapy* **30,** 70–79 (2010).

14. Ford, D. C. *et al.* Ferumoxytol versus placebo in iron deficiency anemia: Efficacy, safety, and quality of life in patients with gastrointestinal disorders. *Clin. Exp. Gastroenterol.* **9,** 151–162 (2016).

15. Fei Yin, Z., Wu, L., Gui Yang, H. & Hua Su, Y. Recent progress in biomedical applications of titanium dioxide. *Phys. Chem. Chem. Phys.* **15,** 4844 (2013).

16. Sirelkhatim, A. *et al.* Review on zinc oxide nanoparticles: Antibacterial activity and toxicity mechanism. *Nano-Micro Lett.* **7,** 219–242 (2015).

17. Lu, J., Liong, M., Zink, J. I. & Tamanoi, F. Mesoporous silica nanoparticles as a delivery system for hydrophobic anticancer drugs. *Small* **3,** 1341–1346 (2007).

18. Weitzmann, M. N. *et al.* Bioactive silica nanoparticles reverse age-associated bone loss in mice. *Nanomedicine Nanotechnology, Biol. Med.* **11,** 959–967 (2015).

19. Celardo, I., Pedersen, J. Z., Traversa, E. & Ghibelli, L. Pharmacological potential of cerium oxide nanoparticles. *Nanoscale* **3,** 1411–20 (2011).

20. Hussain, S. *et al.* Cerium Dioxide Nanoparticles Induce Apoptosis and Autophagy in Human Peripheral Blood Monocytes. *ACS Nano* 5820–5829 (2012).

21. De Marzi, L. *et al.* Cytotoxicity and genotoxicity of ceria nanoparticles on different cell lines in vitro. *Int. J. Mol. Sci.* **14,** 3065–3077 (2013).

22. Tseng, M. T. *et al.* Alteration of hepatic structure and oxidative stress induced by intravenous nanoceria. *Toxicol. Appl. Pharmacol.* **260,** 173–182 (2012).

23. Zeyons, O. *et al.* Direct and indirect CeO2 nanoparticles toxicity for Escherichia coli and Synechocystis. *Nanotoxicology* **3,** 284–295 (2009).

24. Cafun, J.-D., Kvashnina, K. O., Casals, E., Puntes, V. F. & Glatzel, P. Absence of Ce^{3+} Sites in Chemically Active Colloidal Ceria Nanoparticles. *ACS Nano* **7,** 10726–10732 (2013).

25. Oro, D. *et al.* Cerium oxide nanoparticles reduce steatosis, portal hypertension and display anti-inflammatory properties in rats with liver fibrosis. *J. Hepatol.* **64,** 691–698 (2016).

26. Kyosseva, S. V., Chen, L., Seal, S. & McGinnis, J. F. Nanoceria inhibit expression of genes associated with inflammation and angiogenesis in the retina of Vldlr null mice. *Exp. Eye Res.* **116,** 63–74 (2013).

27. Zhang, Y., Chen, Y., Westerhoff, P., Hristovski, K. & Crittenden, J. C. Stability of commercial metal oxide nanoparticles in water. *Water Res.* **42,** 2204–2212 (2008).

28. Niederberger, M. *et al.* Nonaqueous synthesis of metal oxide nanoparticles:Review and indium oxide as case study for the dependence of particle morphology on precursors and solvents. *J. Sol-Gel Sci. Technol.* **40,** 259–266 (2006).

29. Niederberger, M. & Garnweitner, G. Organic reaction pathways in the nonaqueous synthesis of metal oxide nanoparticles. *Chem. - A Eur. J.* **12,** 7282–7302 (2006).

30. Niederberger, M. Nonaqueous Sol – Gel Routes to Metal Oxide Nanoparticles. *Acc. Chem. Res.* **40,** 793–800 (2007).

31. Vijaya Kumar, R., Diamant, Y. & Gedanken, A. Sonochemical synthesis and characterization of nanometer-size transition metal oxides from metal acetates. *Chem. Mater.* **12,** 2301–2305 (2000).

32. Hayashi, H. & Hakuta, Y. Hydrothermal Synthesis of metal oxide nanoparticles in supercritical water. *Materials (Basel).* **3,** 3794–3817 (2010).

33. Stankic, S., Suman, S., Haque, F. & Vidic, J. Pure and multi metal oxide nanoparticles: synthesis, antibacterial and cytotoxic properties. *J. Nanobiotechnology* **14,** 73 (2016).

34. Schwarzer, H. C., Schwertfirm, F., Manhart, M., Schmid, H. J. & Peukert, W. Predictive simulation of nanoparticle precipitation based on the population balance equation. *Chem. Eng. Sci.* **61,** 167–181 (2006).

35. Hirano, M., Fukuda, Y., Iwata, H., Hotta, Y. & Inagaki, M. Preparation and Spherical Agglomeration of Crystalline Cerium(IV) Oxide Nanoparticles by Thermal Hydrolysis. *J. Am. Ceram. Soc.* **83,** 1287–1289 (2000).

36. Yin, L., Wang, Y., Pang, G., Koltypin, Y. & Gedanken, A. Sonochemical synthesis of cerium oxide nanoparticles - Effect of additives and quantum size effect. *J. Colloid Interface Sci.* **246,** 78–84 (2002).

37. Zhang, F. *et al.* Cerium oxide nanoparticles: Size-selective formation and structure analysis. *Appl. Phys. Lett.* **80,** 127–129 (2002).

38. Chen, H. I. & Chang, H. Y. Homogeneous precipitation of cerium dioxide nanoparticles in alcohol/water mixed solvents. *Colloids Surfaces A Physicochem. Eng. Asp.* **242,** 61–69 (2004).

39. Tsai, Y.-Y. *et al.* Novel synthesis of cerium oxide nanoparticles for free radical scavenging. *Nanomedicine* **2,** 325–332 (2007).

40. Patil, S., Sandberg, A., Heckert, E., Self, W. & Seal, S. Protein adsorption and cellular uptake of cerium oxide nanoparticles as a function of zeta potential. *Biomaterials* **28,** 4600–4607 (2007).

41. Asati, A., Santra, S., Kaittanis, C. & Perez, J. M. Surface-charge-dependent cell localization and cytotoxicity of cerium oxide nanoparticles. *ACS Nano* **4,** 5321–5331 (2010).

42. Periyat, P., Laffir, F., Tofail, S. A. M. & Magner, E. A facile aqueous sol–gel method for high surface area nanocrystalline CeO2. *RSC Adv.* **1,** 1794 (2011).

43. Walton, R. I. Solvothermal synthesis of cerium oxides. *Prog. Cryst. Growth Charact. Mater.* **57,** 93–108 (2011).

44. Xue, Y., Luan, Q., Yang, D., Yao, X. & Zhou, K. Direct Evidence for Hydroxyl Radical Scavenging Activity of Cerium Oxide Nanoparticles. *J. Phys. Chem. C* **115,** 4433–4438 (2011).

45. Renuka, N. K. Structural characteristics of quantum-size ceria nano particles synthesized via simple ammonia precipitation. *J. Alloys Compd.* **513,** 230–235 (2012).

46. Chaudhury, K. *et al.* Mitigation of endometriosis using regenerative cerium oxide nanoparticles. *Nanomedicine Nanotechnology, Biol. Med.* **9,** 439–448 (2013).

47. Balavi, H., Samadanian-isfahani, S., Mehrabani-zeinabad, M. & Edrissi, M. Preparation and optimization of CeO2 nanoparticles and its application in photocatalytic degradation of Reactive Orange 16 dye. *Powder Technol.* **249,** 549–555 (2013).

48. Khadse, V. R., Thakur, S., Patil, K. R. & Patil, P. Humidity-sensing studies of cerium oxide nanoparticles synthesized by non-isothermal precipitation. *Sensors Actuators, B Chem.* **203,** 229–238 (2014).

49. Kargar, H., Ghasemi, F. & Darroudi, M. Bioorganic polymer-based synthesis of cerium oxide nanoparticles and their cell viability assays. *Ceram. Int.* **41,** 1589–1594 (2015).

50. Karakoti, A. S. *et al.* Preparation and characterization challenges to understanding environmental and biological impacts of ceria nanoparticles. *Surf. Interface Anal.* **44,** 882–889 (2012).

51. Tonosaki, K. & Otomo, M. Spectrophotometric Determination of Cerium(III) and Some Rare Earths with Xylenol Orange. *Bull. Chem. Soc. Jpn.* **35,** 1683–1686 (1962).

52. Zhou, X., Wong, L. L., Karakoti, A. S., Seal, S. & McGinnis, J. F. Nanoceria inhibit the development and promote the regression of pathologic retinal neovascularization in the Vldlr knockout mouse. *PLoS One* **6,** (2011).

53. Damatov, D. & Mayer, J. M. (Hydro)peroxide ligands on colloidal cerium oxide nanoparticles. *Chem. Commun. Chem. Commun* **52,** 10281–10284 (2016).

54. Chen, P. & Chen, I. Reactive Cerium(IV) Oxide Powders. *J. Am. Ceram. Soc.* **76,** 2–8 (1993).

55. Tang, C., Bando, Y., Liu, B. & Golberg, D. Cerium oxide nanotubes prepared from cerium hydroxide nanotubes. *Adv. Mater.* **17,** 3005–3009 (2005).

56. Chen, H. I. & Chang, H. Y. Synthesis of nanocrystalline cerium oxide particles by the precipitation method. *Ceram. Int.* **31,** 795–802 (2005).

57. Hirano, M. & Kato, E. Hydrothermal synthesis of Cerium(IV) oxide. *J. Am. Ceram. Soc.* **82,** 786–788 (1999).

58. Ravin, H. A., Seligman, A. M. & Fine, J. Polyvinyl pyrrolidone as a plasma expander. *N. Engl. J. Med.* **247,** 921–929 (1952).

59. Koczkur, K. M., Mourdikoudis, S., Polavarapu, L. & Skrabalak, S. E. Polyvinylpyrrolidone (PVP) in nanoparticle synthesis. *Dalt. Trans.* **44,** 17883–17905 (2015).

60. Bastús, N.; Merkoçi, F; Piella, J.; Puntes, V. Synthesis of Highly Monodisperse Citrate- Stabilized Silver Nanoparticles of up to 200 nm: Kinetic Control and Catalytic Properties. *Chem. Mater.* **26,** 2836–2846 (2014).

61. Bobtelsky, M. & Graus, B. Cerous Citrate Complexes, their Composition, Structure and Behavior. *J. Am. Chem. Soc.* **77,** 1990–1993 (1955).

62. Cho, E. C., Xie, J., Wurm, P. A. & Xia, Y. Understanding the role of surface charges in cellular adsorption versus internalization by selectively removing gold nanoparticles on the cell surface with a I 2/KI etchant. *Nano Lett.* **9,** 1080–1084 (2009).

63. Verma, A. & Stellacci, F. Effect of surface properties on nanoparticle-cell interactions. *Small* **6,** 12–21 (2010).

64. Hühn, D. *et al.* Polymer-coated nanoparticles interacting with proteins and cells: Focusing on the sign of the net charge. *ACS Nano* **7,** 3253–3263 (2013).

65. Casals, E. & Puntes, V. F. Inorganic nanoparticle biomolecular corona: formation, evolution and biological impact. *Nanomedicine* **7,** 1917–1930 (2012).

66. Casals, E., Pfaller, T., Duschl, A., Oostingh, G. J. & Puntes, V. Time evolution of the nanoparticle protein corona. *ACS Nano* **4,** 3623–3632 (2010).

67. Barbero, F. *et al.* Formation of the Protein Corona: The Interface between Nanoparticles and the Immune System. *Semin. Immunol.* **34,** 52–60 (2017).

68. Vroman, L. Effect of adsorbed proteins on the wettability of hydrophilic and hydrophobic solids. *Nature* **196,** 476–477 (1962).

69. Nguyen, V. H. & Lee, B. Protein corona : a new approach for nanomedicine design. *Int. J. Nanomedicine* **12,** 3137–3151 (2017).

70. Lundqvist, M., Sethson, I. & Jonsson, B. H. Protein adsorption onto silica nanoparticles: Conformational changes depend on the particles' curvature and the protein stability. *Langmuir* **20,** 10639–10647 (2004).

71. Lynch, I. & Dawson, K. A. Proteins-nanoparticle interactions. *nanotoday* **3,** 40–47 (2008).

72. Casals, E., Pfaller, T., Duschl, A., Oostingh, G. J. & Puntes, V. F. Hardening of the nanoparticle-protein corona in metal (Au, Ag) and oxide (Fe 3O 4, CoO, and CeO 2) nanoparticles. *Small* **7,** 3479–3486 (2011).

73. Sayle, T. X. T. X. T., Parker, S. C. S. C. & Catlow, C. R. a. R. a. The role of oxygen vacancies on ceria surfaces in the oxidation of carbon monoxide. *Surf. Sci.* **316,** 329–336 (1994).

74. Kašpar, J., Fornasiero, P. & Graziani, M. Use of CeO2-based oxides in the three-way catalysis. *Catal. Today* **50,** 285–298 (1999).

75. Garcia, A. *et al.* Effect of cerium dioxide, titanium dioxide, silver, and gold nanoparticles on the activity of microbial communities intended in wastewater treatment. *J. Hazard. Mater.* **199–200,** 64–72 (2012).

76. Recillas, S. *et al.* Chromium VI adsorption on cerium oxide nanoparticles and morphology changes during the process. *J. Hazard. Mater.* **184,** 425–431 (2010).

77. Recillas, S. *et al.* Use of CeO2 , TiO2 and Fe3O4 nanoparticles for the removal of lead from water: Toxicity of nanoparticles and derived compounds. *Desalination* **277,** 213–220 (2011).

78. Zhong, L. S. *et al.* 3D Flowerlike Ceria Micro/ Nanocomposite Structure and Its Application for Water Treatment and CO Removal. *Chem. Mater.* **19,** 1648–1655 (2007).

79. Fang, F. C., Actions, A., Species, R. O., Feeds, R. S. S. & Journal, a S. M. Antimicrobial Actions of Reactive Oxygen Species Antimicrobial Actions of Reactive Oxygen Species. *MBio* **2,** 1–6 (2011).

80. Li, J.-K., Liu, X.-D., Shen, L., Zeng, W.-M. & Qiu, G.-Z. Natural plant polyphenols for alleviating oxidative damage in man: Current status and future perspectives. *Trop. J. Pharm. Res.* **15,** 1089–1098 (2016).

81. Das, M. *et al.* Auto-catalytic ceria nanoparticles offer neuroprotection to adult rat spinal cord neurons. *Biomaterials* **28,** 1918–1925 (2007).

82. Niu, J., Azfer, A., Rogers, L. M., Wang, X. & Kolattukudy, P. E. Cardioprotective effects of cerium oxide nanoparticles in a transgenic murine model of cardiomyopathy. *Cardiovasc. Res.* **73,** 549–559 (2007).

83. Kyosseva, S. V & McGinnis, J. F. Cerium oxide nanoparticles as promising ophthalmic therapeutics for the treatment of retinal diseases. *World J. Ophthalmol.* **5,** 23–30 (2015).

84. Ouyanga, Z. *et al.* Potential of using cerium oxide nanoparticles for protecting healthy tissue during accelerated partial breast irradiation (APBI). *Phys Med* **150,** 137–143 (2016).

85. Tarnuzzer, R. W. *et al.* Vacancy Engineered Ceria Nanostructures for Protection from Radiation-Induced Cellular Damage. *Nano Lett.* **5,** 2573–2577 (2005).

86. Nelson, B., Johnson, M., Walker, M., Riley, K. & Sims, C. Antioxidant Cerium Oxide Nanoparticles in Biology and Medicine. *Antioxidants* **5,** 15 (2016).

87. Pirmohamed, T. *et al.* Nanoceria exhibit redox state-dependent catalase mimetic activity. *Chem. Commun. (Camb).* **46,** 2736–8 (2010).

88. Invitrogen. Amplex® Red Hydrogen Peroxide/Peroxidase Assay Kit. 1–7 (2009).

89. Gehrs, K. M., Anderson, D. H., Johnson, L. V. & Hageman, G. S. Age-related macular degeneration - Emerging pathogenetic and therapeutic concepts. *Ann. Med.* **38,** 450–471 (2006).

90. Xu, M., McCanna, D. J. & Sivak, J. G. Use of the viability reagent PrestoBlue in comparison with alamarBlue and MTT to assess the viability of human corneal epithelial cells. *J. Pharmacol. Toxicol. Methods* **71,** 1–7 (2015).

NOMENCLATURE

CeO$_2$ NPs: Cerium oxide nanoparticles/nanoceria.

ROS: Reactive oxygen species.

H$_2$O$_2$: Hydrogen peroxide.

OH$^.$: Hydroxil radical.

O$_2^-$: Superoxide radical.

SOD: Superoxide dismutase.

GSH: Glutathione.

AMD: Age-related macular degeneration.

HERFD-XAS: High-energy resolution fluorescence detected X-ray absorption spectroscopy.

Eq: Equation.

Fe$_3$O$_4$: Iron oxide nanoparticles.

AZO: Azodicarbonamide.

DEAO: Diethanolamine oleate.

TEA: Triethanolamine.

AOT: Dioctyl sulfosuccinate sodium salt.

PAA: Poly (acrylic) acid.

HMT: Hexamethylenetetramine.

TMAOH: Tetramethylammonium hydroxide.

DLS: Dynamic Light scattering.

TEM: Transmission electron microscopy.

HR-TEM: High resolution- transmission electron microscopy.

UV: Ultraviolet.

PZC: Point zero charge.

PVP: Polyvinylpyrrolidone.

Cit: citrate.

BSA: Bovine serum albumin.

DMEM: Dulbecco modified eagle media.

DMSO: Dimethyl sulfoxide.

FBS: Fetal Bovine serum.

PB: Phosphate buffer.

PBS: Phosphate buffer saline.

HRP: Horseradish peroxidase.

tBH: tert-Butyl Hydroperoxide

HPMC: Hydroxypropyl methylcellulose.

ICP-MS: Inductively coupled plasma mass spectroscopy.

VEGF: Vascular endothelial growth factor.

MTT: 3-(4,5-dimethylthiazol-2-yl)-2,5-diphenyltetrazolium bromide.

DCF-DA: 2',7' –dichlorofluorescin diacetate.

LIST OF CONTRIBUTIONS

CONFERENCE CONTRIBUTIONS

- NanoBio&Med 2016, Barcelona, with poster exhibition: "Control synthesis of metal oxide nanoparticles for medical application".

- NanoSpain 2018, Bilbao, with poster exhibition: "Synthesis of cerium oxide nanoparticles for medical applications".

ARTICLES

- Formation of the Protein Corona: The Interface between Nanoparticles and the Immune System. Seminars in immunology, **34**, 72-80, (2017).

- Metal oxide nanoparticles for nanomedicine: Synthesis, applications, toxicity and biological interactions (manuscript in writing).

- Synthesis of monodisperse colloidally stable water dispersed CeO_2 NPs designed for medical use (manuscript in writing).

- Studies of catalysis of good quality CeO_2 NPs dispersed in water for medical application use (manuscript in writing).

ACKNOWLEDGEMENTS